ROTARY ULTRASONIC MACHINING OF HARD-TO-MACHINE MATERIALS

by

NIKHIL CHURI

B. S., University of Mumbai, India, 2002

AN ABSTRACT OF A DISSERTATION

Submitted in partial fulfillment of the requirements for the degree

DOCTOR OF PHILOSOPHY

Department of Industrial and Manufacturing Systems Engineering
College of Engineering

KANSAS STATE UNIVERSITY
Manhattan, Kansas

2010

ABSTRACT

Titanium alloy is one of the most important materials used in major segments of industries such as aerospace, automobile, sporting goods, medical and chemical. Market survey has stated that the titanium shipment in the USA has increased significantly in last two decades, indicating its increased usage. Industries are always under tremendous pressure to meet the ever-increasing demand to lower cost and improve quality of the products manufactured from titanium alloy. Similar to titanium alloys, silicon carbide and dental ceramics are two important materials used in many applications.

Rotary ultrasonic machining (RUM) is a non-traditional machining process that combines the material removal mechanisms of diamond grinding and ultrasonic machining. It comprises of a tool mounted on a rotary spindle attached to a piezo-electric transducer to produce the rotary and ultrasonic motion. No study has been reported on RUM of titanium alloy, silicon carbide and dental ceramics.

The goal of this research was to provide new knowledge of machining these hard-to-machine materials with RUM for further improvements in the machining cost and surface quality. A thorough research has been conducted based on the feasibility study, effects of tool variables, effects of machining variables and wheel wear mechanisms while RUM of titanium alloy. The effects of machining variables (such as spindle speed, feedrate, ultrasonic vibration power) and tool variables (grit size, diamond grain concentration, bond type) have been studied on the output variables (such as cutting force, material

removal rate, surface roughness, chipping size) and the wheel wear mechanisms for titanium alloy. Feasibility of machining silicon carbide and dental ceramics is also conducted along with a designed experimental study.

ROTARY ULTRASONIC MACHINING OF HARD-TO-MACHINE MATERIALS

by

NIKHIL CHURI

B. S., University of Mumbai, India, 2002

A DISSERTATION

Submitted in partial fulfillment of the requirements for the degree

DOCTOR OF PHILOSOPHY

Department of Industrial and Manufacturing Systems Engineering
College of Engineering

KANSAS STATE UNIVERSITY
Manhattan, Kansas

2010

Approved by:

_____

Major Professor
Dr. Zhijian Pei

ABSTRACT

Titanium alloy is one of the most important materials used in major segments of industries such as aerospace, automobile, sporting goods, medical and chemical. Market survey has stated that the titanium shipment in the USA has increased significantly in last two decades, indicating its increased usage. Industries are always under tremendous pressure to meet the ever-increasing demand to lower cost and improve quality of the products manufactured from titanium alloy. Similar to titanium alloys, silicon carbide and dental ceramics are two important materials used in many applications.

Rotary ultrasonic machining (RUM) is a non-traditional machining process that combines the material removal mechanisms of diamond grinding and ultrasonic machining. It comprises of a tool mounted on a rotary spindle attached to a piezo-electric transducer to produce the rotary and ultrasonic motion. No study has been reported on RUM of titanium alloy, silicon carbide and dental ceramics.

The goal of this research was to provide new knowledge of machining these hard-to-machine materials with RUM for further improvements in the machining cost and surface quality. A thorough research has been conducted based on the feasibility study, effects of tool variables, effects of machining variables and wheel wear mechanisms while RUM of titanium alloy. The effects of machining variables (such as spindle speed, feedrate, ultrasonic vibration power) and tool variables (grit size, diamond grain concentration, bond type) have been studied on the output variables (such as cutting force, material

removal rate, surface roughness, chipping size) and the wheel wear mechanisms for titanium alloy. Feasibility of machining silicon carbide and dental ceramics is also conducted along with a designed experimental study.

TABLE OF CONTENTS **Page**

ACKNOWLEDGEMENTS xiv

1. INTRODUCTION **1**

1.1 TITANIUM ALLOY 1

1.2 SILICON CARBIDE 7

1.3 DENTAL CERAMICS 8

2. LITERATURE REVIEW **11**

2.1 BACKGROUND OF RUM PROCESS 11

2.2 HISTORICAL REVIEW OF RUM PROCESS 14

2.2.1 REVIEW OF USM HISTORY 14

2.2.2 REVIEW OF RUM HISTORY 15

2.3 EXPERIMENTAL STUDY ON RUM PROCESS 18

2.3.1 MACHINABILITY OF HARD-TO-MACHINE MATERIALS USING RUM 18

2.3.2 EFFECTS OF CONTROL VARIABLES ON RUM PERFORMANCE 19

2.3.2.1 EFFECTS OF STATIC PRESSURE 20

2.3.2.2 EFFECTS OF ULTRASONIC VIBRATION AMPLITUDE 21

2.3.2.3 EFFECTS OF ULTRASONIC VIBRATION FREQUENCY 22

2.3.2.4 EFFECTS OF ROTATIONAL SPEED 22

2.3.2.5 EFFECTS OF ABRASIVE (CONCENTRATION, SIZE, TYPE AND BOND TYPE) 22

2.3.2.6 EFFECTS OF COOLANT 23

2.4 REVIEW OF THEORETICAL STUDY 24

2.5 REVIEW OF WHEEL WEAR MECHANISMS 25

2.6 SUMMARY 28

3. ROTARY ULTRASONIC MACHINING OF TITANIUM ALLOY: A FEASIBILITY STUDY **29**

3.1 SETUP AND CONDITIONS 29

3.2 MEASUREMENT PROCEDURES 32

3.3 EXPERIMENTAL RESULTS 35

3.3.1 TOOL WEAR 35

3.3.2 CUTTING FORCE 37

3.3.3 MRR 37

3.3.4 SURFACE ROUGHNESS 40

3.3.4.1 SURFACE ROUGHNESS ON MACHINED HOLES 40

3.3.4.2 SURFACE ROUGHNESS ON MACHINED RODS 40

3.4 SUMMARY 43

4. ROTARY ULTRASONIC MACHINING OF TITANIUM ALLOY: EFFECTS OF TOOL VARIABLES 44

4.1 EXPERIMENTAL CONDITIONS AND PROCEDURES 44

4.2 EXPERIMENTAL RESULTS 45

4.2.1 EFFECTS OF CUTTING FORCE 45

4.2.1.1 GRIT SIZE 47

4.2.1.2 DIAMOND CONCENTRATION 47

4.2.1.3 METAL BOND TYPE 47

4.2.2 EFFECTS ON SURFACE ROUGHNESS OF MACHINED HOLE 47

4.2.2.1 GRIT SIZE 49

4.2.2.2 DIAMOND CONCENTRATION 49

4.2.2.3 METAL BOND TYPE 49

4.2.3 EFFECTS ON SURFACE ROUGHNESS OF MACHINED ROD 50

4.2.3.1 GRIT SIZE 52

4.2.3.2 DIAMOND CONCENTRATION 52

4.2.3.3 METAL BOND TYPE 52

4.2.4 EFFECTS ON TOOL WEAR 53

4.2.4.1 GRIT SIZE 54

4.2.4.2 DIAMOND CONCENTRATION 54

4.2.4.3 METAL BOND TYPE

4.3 SUMMARY 55

5. ROTARY ULTRASONIC MACHINING OF TITANIUM ALLOY: EFFECTS OF MACHINING VARIABLES 56

5.1 EXPERIMENTAL CONDITIONS AND PROCEDURES 56

5.2 EXPERIMENTAL RESULTS 58

5.2.1 EFFECTS ON CUTTING FORCE 61

5.2.1.1 SPINDLE SPEED 61

5.2.1.2 FEEDRATE 62

5.2.1.3 ULTRASONIC VIBRATION POWER 62

5.2.2 EFFECTS ON MATERIAL REMOVAL RATE 64

5.2.2.1 SPINDLE SPEED 64

5.2.2.2 FEEDRATE 65

5.2.2.3 ULTRASONIC VIBRATION POWER 66

5.2.3 EFFECTS ON SURFACE ROUGHNESS 67

5.2.3.1 SPINDLE SPEED 67

5.2.3.2 FEEDRATE 69

5.2.3.3 ULTRASONIC VIBRATION POWER 71

5.4 SUMMARY 73

6. **ROTARY ULTRASONIC MACHINING OF TITANIUM ALLOY: WHEEL WEAR MECHANISMS** 75

6.1 EXPERIMENTAL CONDITIONS AND PROCEDURES 75

6.2 MEASUREMENT PROCEDURES 76

6.3 WEAR MECHANISMS 77

6.3.1 ATTRITIOUS WEAR 77

6.3.2 GRAIN PULLOUT 79

6.3.3 GRAIN FRACTURE 81

6.3.4 BOND FRACTURE 82

6.3.5 CATASTROPHIC FAILURE 83

6.4 SUMMARY 85

7. ROTARY ULTRASONIC MACHINING OF SILICON CARBIDE 86

7.1 EXPERIMENTAL CONDITIONS AND PROCEDURES 86

7.1.1 SETUP AND CONDITIONS 86

7.1.2 DESIGN OF EXPERIMENTS 87

7.2 EXPERIMENTAL RESULTS 89

7.2.1 MAIN EFFECTS 91

7.2.1.1 ON CUTTING FORCE 91

7.2.1.2 ON SURFACE ROUGHNESS 92

7.2.1.3 ON CHIPPING SIZE 93

7.2.2 TWO FACTOR INTERACTIONS 94

7.2.2.1 ON CUTTING FORCE 94

7.2.2.2 ON SURFACE ROUGHNESS 96

7.2.2.3 ON CHIPPING SIZE 97

7.2.3 THREE FACTOR INTERACTIONS 98

7.3 SUMMARY 98

8. ROTARY ULTRASONIC MACHINING OF DENTAL CERAMICS 99

8.1 EXPERIMENTAL CONDITIONS 99

8.2 EXPERIMENTAL RESULTS 102

8.2.1 EFFECTS ON CUTTING FORCE 102

8.2.1.1 SPINDLE SPEED 102

8.2.1.2 FEEDRATE 102

8.2.1.3 ULTRASONIC VIBRATION POWER 104

8.2.2 EFFECTS ON SURFACE ROUGHNESS 105

8.2.2.1 SPINDLE SPEED 105

8.2.2.2 FEEDRATE 105

8.2.2.3 ULTRASONIC VIBRATION POWER 107

8.2.3 EFFECTS ON CHIPPING SIZE 107

8.2.3.1 SPINDLE SPEED 108

8.2.3.2 FEEDRATE 109

8.2.3.3 ULTRASONIC VIBRATION POWER 109

8.3 SUMMARY 111

9. **PREDICTIVE FORCE MODEL IN ROTARY ULTRASONIC MACHINING OF TITANIUM** **112**

9.1 ASSUMPTIONS 112

9.2 INDENTION DEPTH OF A DIAMOND GRIT INTO THE WORKPIECE 113

9.3 ESTIMATION OF CUTTING FORCE 114

9.4 THE INFLUENCE OF DIFFERENT PARAMETERS ON CUTTING FORCE 116

9.4.1 GRIT DIAMETER

9.4.2 AMPLITUDE 116

9.4.3 TOOL DIAMETER 120

9.4.4 NUMBER OF GRAINS 125

9.4.5 SPINDLE SPEED 129

9.4.6 MACHINING TIME 133

9.5 SUMMARY 137

10. CONCLUSIONS **142**

10.1 SUMMARIES AND CONCLUSIONS OF THIS DISSERTATION 142

10.2 CONTRIBUTIONS OF THIS DISSERTATION 145

REFERENCES **146**

APPENDIX: LIST OF PUBLICATIONS FROM THIS RESEARCH **165**

ACKNOWLEDGEMENTS

Foremost, I wish to express my gratitude to my advisor Professor ZJ Pei at Kansas State University for all the guidance, inspiration and financial support during my doctoral study. He not only acted as thesis advisor and a committee member, but also as a mentor who has spent many long hours helping in my development as a student, and person. Without his guidance and support, not only would this dissertation not have been completed, but I would never have had the chance to attempt it. I would also like to thank committee members, Professor Shuting Lei, Professor Jack Xin and Professor Haiyan Wang for their advice and feedback during this work, and Professor Charles L. Cocke for serving as the outside chairperson for my final doctorial examination.

I would like to extend my thanks to Mr. Clyde Treadwell from Sonic-Mill Corporation, Albuquerque, New Mexico and Mr. Bruno Renzi from N.B.R. Diamond Tool Corporation, Lagrangeville, New York for providing valuable advice, technology and tools for the research. I would also like to thank Ms. Tanni Sisco and Mr. Antonio Micale from the Boeing Company, Everett, Washington for providing their precious assistance, and funding for the research.

I really appreciate the encouragement and help from Dr. Bradley A. Kramer and all the faculty and staff members in the Department of Industrial and Manufacturing Systems Engineering. My friends and fellow graduate students in the Department of Industrial and Manufacturing Systems Engineering also deserve special thanks.

Finally, I will never forget my beloved parents & my fiancé, Anjali for their incredible encouragements and support to me throughout my graduate studies.

CHAPTER 1

INTRODUCTION

1.1 TITANIUM ALLOY (Ti-6Al-4V)

The unique properties of titanium alloys (such as high strength-weight ratio at elevated temperatures, exceptional corrosion resistance at elevated temperatures [Froes et al. 1998], creep strength, stability, and superior fatigue strength) make them attractive materials in industries. Another advantage of titanium alloys is the ease of their recycling [Anonymous 2005a]. It is the fourth most abundant metal element in the earth's crust after aluminum, iron and magnesium [Orr et al. 1982] and the ninth most used metal in industry [Froes et al. 1998].

In 1990, the total market of titanium alloy in the USA and Europe, who consume about 66% of the world's titanium [Allen 1997], was 25,000 tons and 9,500 tons respectively. Figure 1.1 shows the proportion of titanium alloy used in 1990 for jet engines, airframes, and industrial purposes in the USA and Europe respectively. Figure 1.2 shows that there was a gradual increase in the titanium mill product shipment in the USA for four different market segments from 1990 to 2000 [Seddon 2004]. In 2003, 98,000 tons of titanium alloys were produced worldwide [Seddon 2004]. 60% of the titanium is used in the aerospace industry [Boyer 1996, Peacock 1988] for manufacturing compressor blades, stator blades, rotors, and other parts in turbine engines [Seddon 2004, Huber 1973,

Anonymous 2 2004]. Other applications of titanium alloys include such industries as military [Montgomery et al 2001, Lerner 2004], automotive [Anonymous 3 1989, Yamashita et al. 2002], chemical [Farthing 1979, Orr 1982], medical [Froes 2002, Abdullin et al. 1988], and sporting goods [Anonymous 4 2004, Yang et al. 1999].

Poor machinability of titanium alloys poses considerable problems in fabrication of components from them. Their low thermal conductivity leads to high cutting temperatures, and their high chemical reactivity with many tool materials leads to strong adhesion between the tool and work material. These two factors lead to rapid tool wear during machining of titanium alloys, which in turn increases the manufacturing cost [Anonymous 5 1999].

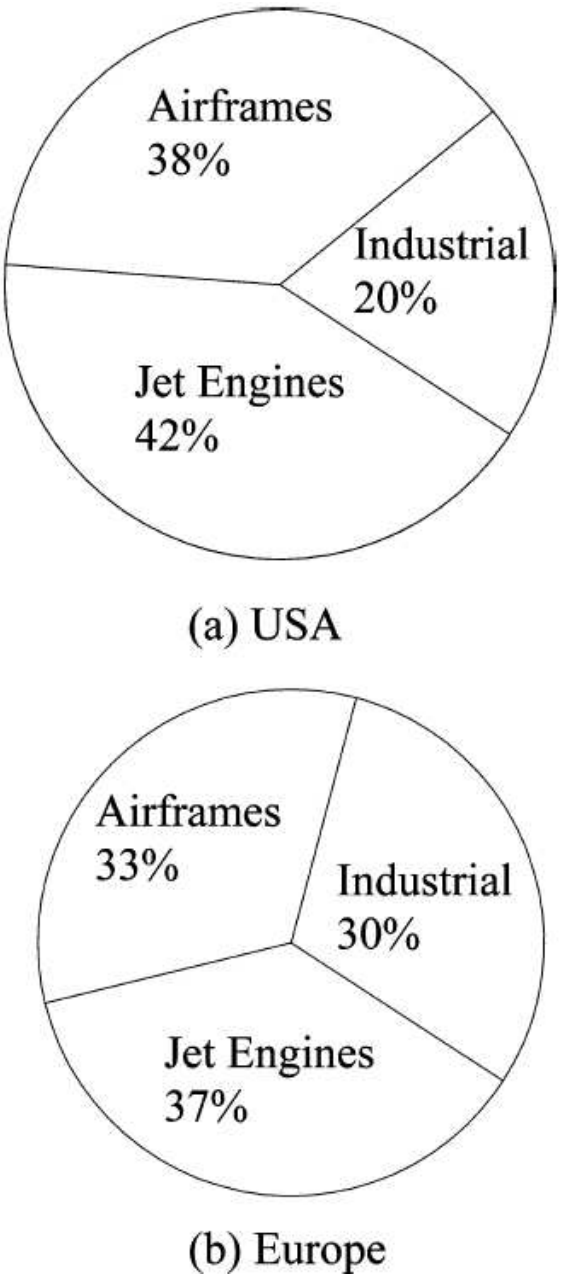

Figure 1.1 Proportion of titanium consumed in 1990 [Anonymous 1 2005]

Availability, increased cost of raw material, and high cost of machining [Anonymous 5 1999] limit their use in industry. With the gradual increasing demand for titanium in various segments of market (Figure 1.2), there is a crucial need to reduce the cost of titanium products. Moreover, composite materials and amorphous alloy are being developed that may replace titanium in many applications [Nelson 1991, Li et al. 1996, Johnson et al. 1993, Jenkins 2003]. Under these conditions, the survival of titanium in the

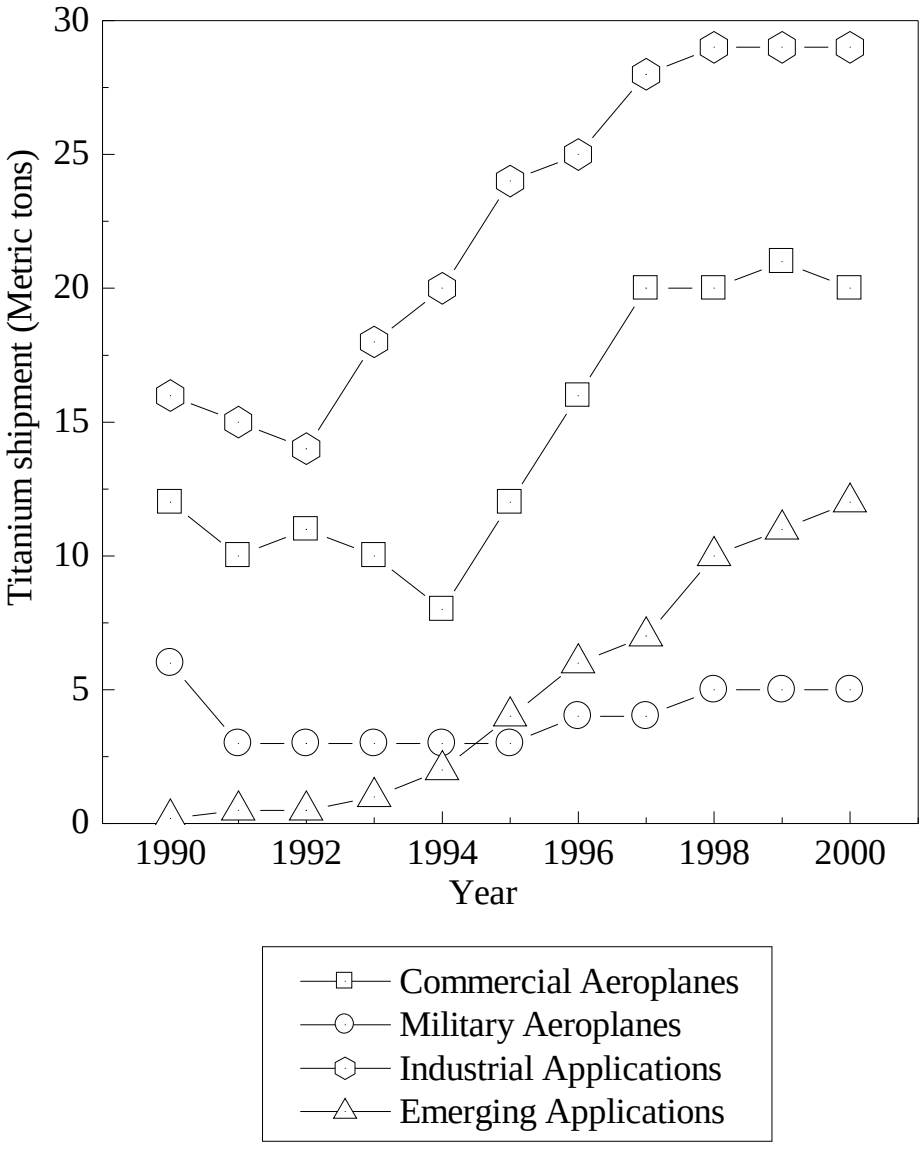

Figure 1.2 Titanium mill product shipments in the USA [after Anonymous 2005a]

market and its expansion will heavily depend on reducing the cost of machining [Kumar 1991]. Therefore, it is critically important to search new manufacturing processes that allow machining of titanium and its alloy more cost effectively.

Many conventional and non-conventional machining processes are used for titanium alloys [Bandopadhyay et al., 2005; Fowler et al., 2005; Huber, 1973; Koenig et al., 1976; Lash and Gilgenbach, 1993; Qin et al., 2003; Tam et al., 1992; Yan and Shieh, 1992]. In addition to conventional machining processes (turning, drilling, milling, etc.), titanium alloys have been machined by many non-conventional machining processes such as abrasive waterjet machining, electro-discharge machining, laser drilling, and ultrasonic vibration assisted drilling. Table 1.1 summarizes reported work about non-conventional machining processes on titanium alloys. Please note the cutting tool is a conventional drill (e.g. a twist drill) in ultrasonic vibration assisted drilling. However, it is still desirable to develop more cost-effective machining processes for titanium alloys.

Table 1.1 Reported processes used to machine titanium and its alloys

Processes	Report
Abrasive water-jet machining	[Fowler et al 2005, Arola et al 2001, Shipway et al 2005]
Electro-chemical machining	[Koenig et al 1976]
Electro-chemical polishing	[Tam et al 1992]
Electro-discharge machining	[Qin et al 2003, Yan and Shieh 1992, Yan and Chen 1994, Lin et al 2000, Zhao et al 2002, Wang et al 2002, Kremer et al 1991, Yishuang 1990]
Laser drilling	Bandopadhyay et al 2005, Yilbas 1997, Beck et al 1997, Kudesia et al 2002, Arzhaou et al 1989, Rodden et al 2001, Lash and Gilgenbach 1993, Yilbas et al 1990, Yilbas and Yilbas 1988, Tam et al 1990, Bandopadhyay et al 2002, Bandopadhyay et al 2001]
Ultrasonic vibration assisted drilling	[Huber 1973]

Rotary ultrasonic machining (RUM) is one such machining process reported in this thesis. Extensive literature search shows that there has been no report about rotary ultrasonic machining of titanium alloys. One of the purposes of this thesis is to investigate the feasibility of machining a titanium alloy with rotary ultrasonic machining.

In the past, rotary ultrasonic machining was used successfully to machine various brittle and hard-to-machine materials

1.2 SILICON CARBIDE (SiC)

Silicon carbide has superior properties such as high strength at elevated temperatures, resistance to chemical degradation, wear resistance, low density, high stiffness, low coefficient of thermal expansion, and superior creep resistance. The combination of these properties makes them attractive in many engineering applications such as high-temperature engines, nuclear fusion reactors, chemical process equipment, and aerospace components [Anonymous 6; Datta and Chaudhari, 2003; Datta et al., 2004; Gopal and Rao, 2003; Yin et al., 2004].

Reported studies on machining of silicon carbide include electrical-discharged machining [Luis et al., 2005; Puertas and Perez, 2003], machining with abrasive paste [Dolotov et al., 1986], grinding with diamond wheels [Gopal and Rao, 2003; Gopal and Rao, 2004; Kibble and Phelps, 1995; Yin et al., 2004], ion beam milling [Hylton et al., 1993], lapping/polishing [Chandler et al., 2000], and micro machining with ultra short laser pulses [Rice et al., 2002]. However, the literature review states that difficulty, high cost and long time associated with machining of silicon carbide limit the use of silicon carbide in industry. Therefore there is a need to develop more cost effective machining methods for silicon carbide.

In this thesis, RUM of silicon carbide will be studied using designed experiments. It presents and discusses the main and interaction effects of process variables (spindle speed, feedrate, and ultrasonic power) on cutting forces, surface roughness, and chipping size.

1.3 DENTAL CERAMICS

It has been predicted that the demand for dental products and materials would rise 5.7% annually in the U.S. and dental ceramics are among the fastest growing biomaterials [Anonymous 7 2004]. Dentals ceramics find applications in aesthetic restorations and prostheses like molar crowns, anterior and posterior bridges, veneers, and onlays. Ceramics are preferred for dental crowns because of their high strength, superior wear resistance, and natural aesthetical appearance. 30 million dental crowns are made per year in the U.S. [Kartz 2000]. The dental crowns have a market of $200-$250 million per year in the U.S. [Anonymous 2004; Kartz 2000]. Most dental ceramics, however, have very low tensile strength and fracture toughness. They are sensitive to surface micro-cracks, as shown in Figure 1.3. Fracture surface analyses [Thompson et al. 1994; Kelly et al. 1990; Noort 2002] have revealed that most clinical failures initiate from the surface micro-cracks. Therefore, it is important to use machining processes that minimize surface micro-cracks.

Currently, high-speed air-driven hand-held diamond tools are used for clinical repair and restoration. Conventional diamond drilling and grinding are employed for producing

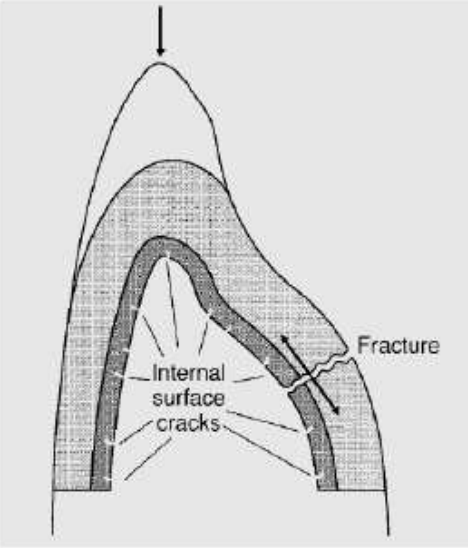

Figure 1.3 Fracture of a ceramic crown initiated from surface micro-cracks [Thompson et al. 1994]

dental tissues such as dental inlays and veneers [Anonymous 2004]. Various machining processes (such as turning, grinding, sawing, drilling, boring, and tapping) have been studied to machine macor (one type of dental ceramics) [Grossman 1977]. Grossman [Grossman 1983] studied the chip formation while turning, Dabnun et al. [Dabnun et al. 2005] developed a surface roughness prediction model for turning, Claus et al. [Claus et al. 1979] studied the tool wear behavior for turning, Weber et al. [Weber et al. 1984] reported cutting force and surface roughness study for turning with ultrasonically vibrated tools, and Marshall et al. [Marshall et al. 1987] presented the microstructural effects in grinding. Preventing and minimizing surface micro-cracks still remain a challenge.

Rotary ultrasonic machining (RUM) produces low force, and hence minimizes surface micro-cracks. Note that no work has ever been reported on RUM of macor. One purpose of this thesis is to test the feasibility of RUM of macor and study the effects of machining parameters (spindle speed, feedrate, and ultrasonic vibration power) on output parameters (cutting force, surface roughness, and chipping size).

CHAPTER 2

LITERATURE REVIEW ON ROTARY ULTRASONIC MACHINING

2.1 BACKGROUND OF RUM

Continuous research and development has resulted in new materials, which are very difficult to machine, for example, super-hard materials, such as tungsten and titanium carbides, diamonds, rubies, hard steels, magnetic alloys. Another group of materials, like germanium, silicon, ferrites, ceramics, glass, quartz, sapphire, corundum and some composites are difficult to machine because of greater brittleness and hardness [Rosenthal et al. 1964]. The need for methods of machining these materials has led to the introduction of special machining techniques like ultrasonic machining (USM).

Figure 2.1 is a schematic illustration of USM. The power supply produces an alternating electric current at ultrasonic frequency (18 to 24 kHz) and supplies to the transducer [Goldman 1962]. This causes the core of the transducer to change in length periodically. Even at the resonance the amplitude of the vibration of the transducer face is about 0.005 to 0.01 mm. This amplitude is increased by using concentrator and tool to a value of 0.03 mm, which is sufficient for practical purposes. The tool thus is made to vibrate at a high frequency (typically 20 kHz) in a direction perpendicular to the surface to be machined. Abrasive particles like aluminum oxide, boron carbide, etc. are mixed with water and this

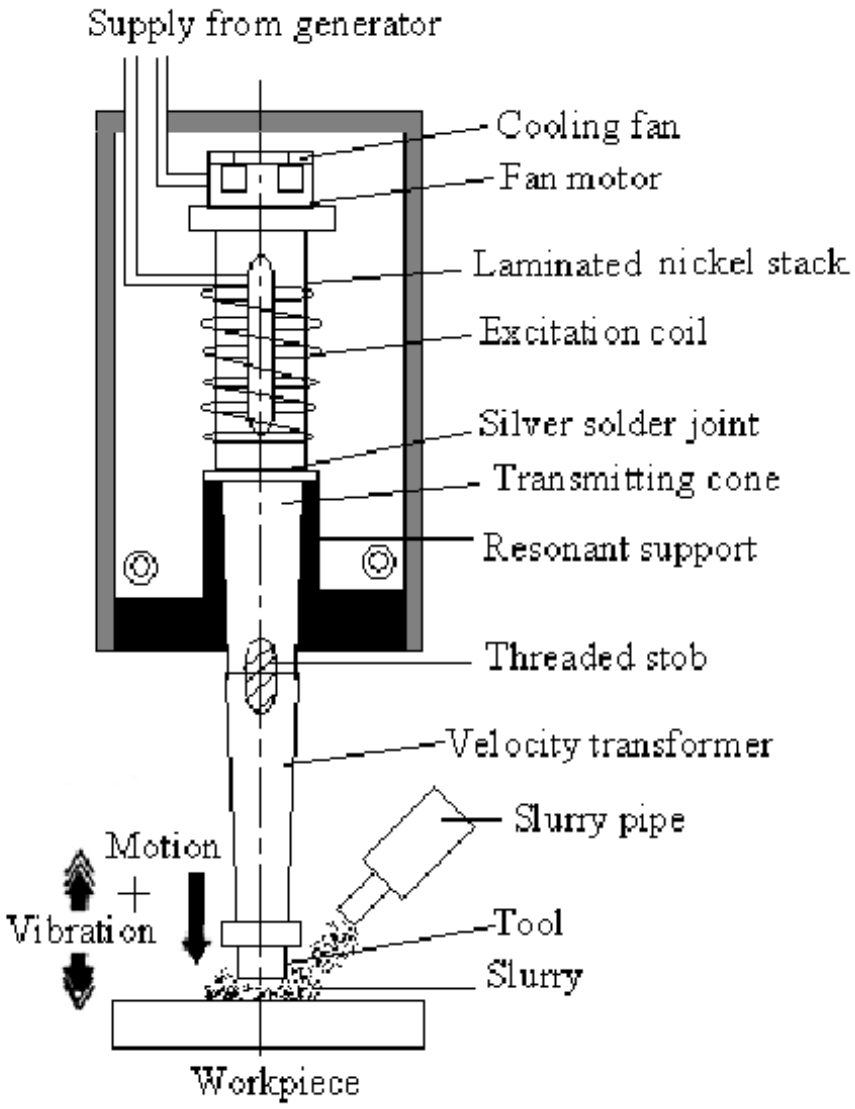

Figure 2.1 Principle of ultrasonic machining [Goldman 1962]

slurry is allowed to enter the gap between the tool and workpiece. Material is removed in the form of tiny particles by the successive impacting action of the abrasive particles into the workpiece [Jana and Satyanarayana 1973].

In order to overcome the shortcomings of USM, rotary ultrasonic machining (RUM) was invented. Rotary ultrasonic machining (RUM) is a hybrid machining process that

combines the material removal mechanisms of diamond grinding and USM, resulting in higher material removal rate (MRR) than that obtained by either diamond grinding or USM [Pei 1995]. In RUM, the slurry is replaced with abrasives bonded to the tool. A rotating core drill with metal-bonded diamond abrasives is ultrasonically vibrated and fed toward to the workpiece at a constant pressure or a constant feedrate. Coolants pumped through the core of the drill wash away the swarf, prevent jamming of the drill, and keep it cool so that the RUM process could be conducted smoothly. The process is illustrated in Figure 2.2.

Experimental results [Prabhakar 1992] have shown that the machining rate obtained from RUM is nearly 6-10 times higher than that from a conventional grinding process under similar conditions. In comparison with USM, RUM is about 10 times faster [Cleave 1976]. Especially, it is much easier to drill deep and small holes with RUM than with USM. Other advantages of improved hole accuracy and low tool pressure are also reported [Graff 1975, Stinson 1979].

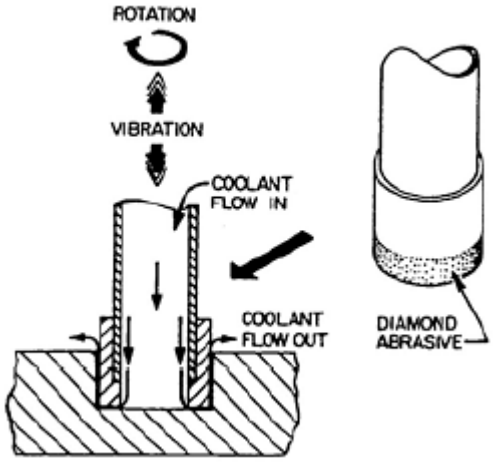

Figure 2.2 Schematic illustration of RUM process [Pei et al. 1995]

2.2 HISTORICAL REVIEW RUM PROCESS

2.2.1 REVIEW OF USM HISTORY

Up to early 1960's, some three to four hundred papers had been published covering the various aspects of ultrasonic machining. Much of this material was covered by two monographs: Ultrasonic machining of intractable materials by A.I. Markov and Ultrasonic cutting by L.D. Rozenberg et al., both originally published in Russian in 1962 and then translated into English [Markov 1966; Rozenberg et al. 1964]. Ultrasonic machining is also referred as ultrasonic impact grinding [Moore 1986; Tyrrell 1970; Kohls 1984; Shaw 1956], ultrasonic grinding [Schwatrz 1992], and ultrasonic abrasive machining [Anonymous 8 1964]. Compared with conventional machining process like grinding and drilling, ultrasonic machining has the following advantages. Firstly, both conductive and nonconductive materials can be machined, and complex three-dimensional contours can be machined as quickly as simple ones. Secondly, the process does not produce a heat-affected zone or cause any chemical/electrical alterations on workpiece surface. Finally, a shallow, compressive residual stress generated on the workpiece surface may also increase the high cycle fatigue strength of the machined part [Markov 1966; Rozenberg et al. 1964].

However, in ultrasonic machining, the slurry has to be fed to and removed from the gap between the tool and the workpiece. Because of this fact, there are some disadvantages to this method: 1) material removal rate slows down considerably and even stops as

penetration depth increases; 2) the slurry may wear the wall of the machined hole as it passes back towards the surface, which limits the accuracy, particularly for small holes; and 3) the action of the abrasive slurry also cuts the tool itself, thus causing considerable tool wear, which in turn makes it very difficult to hold close tolerances. To overcome the shortcomings of ultrasonic machining, rotary ultrasonic machining was invented in 1964 by Mr. Percy Legge, a technical officer at United Kingdom Atomic Energy Authority (UKAEA) [Legge 1964].

2.2.2 REVIEW OF RUM HISTORY

Although Mr. Percy Legge firstly presented rotary ultrasonic machining in 1964, the initial idea of combining drilling with vibration assistance was proposed in G. C. Brown et al's patent (U.S. Patent 2,942,383). In G.C. Brown et al's patent, the drilling process was assisted by some low frequency (lower than 1kHz) vibration. Also, this drilling process is only proposed for machining wood materials.

In Mr. Percy Legge's first RUM device, slurry was abandoned and the combination of abrasive slurry and metal tool in USM was replaced by a diamond impregnated tool and rotating workpiece. But, because the workpiece was held in a rotating four-jaw chuck, this device had the following drawbacks: 1) only circular holes could be machined; and 2) only comparatively small workpiece could be drilled.

Further improvement carried out at United Kingdom Atomic Energy Authority (UKAEA) led to the development of a machine comprising a rotating ultrasonic transducer. The rotating transducer head made it possible to precisely machine stationary workpieces to extremely close tolerances. With different shaped tools, the range of operations could extend to end milling, tee slotting, dovetail cutting, screw threading and internal and external grinding.

The work at UKAEA became almost the only source of English literature on RUM in 1960's [Anonymous 9 1966; Legge 1966; Hards 1966; Dawe Instruments Ltd. 1967; Chechines and Tikhonov 1968]. Several years' later, Russian literature on RUM appeared [Markov 1969; Petruka et al. 1970], with work done at Moscow Aviation Institute. In the 1970s, reports on RUM in USA began to appear [Cleave 1976; Kohls 1984; Anonymous 10 1973]. The work was carried out at Branson Sonic Power Company.

All the above technical articles were devoted to explaining the principle of RUM and describing the equipment and diamond tools. Experimental investigation on the relations between the process input variables (such as vibration amplitude, static force, rotational speed, grit size, etc.) and the output variables (such as MRR, tool wear, surface finish, etc.) were carried out by Russian and Japanese researchers and reported in the literature in the 1970s [Markov and Ustinov 1972; Markov 1977; Kubota 1977].

For a long time, RUM had been viewed merely as an improvement of USM. Another perspective of RUM is to consider RUM as a hybrid process, which combines two

machining process-diamond grinding and USM [Anonymous 8 1964; Prabhakar 1992; Dam 1993; Legge 1964].

RUM is sometimes called Ultrasonic Vibration Grinding [Moore 1986; Kohls 1984], Ultrasonic Drilling [Anonymous 8 1964; Legge 1964], Ultrasonic Twist Drilling [McGeough 1988], and Ultrasonic Grinding [Suzuki et al. 1988]. The term Rotary Ultrasonic Machining also refers to a different process, where the rotation of the workpiece is introduced into USM [Komaraiah and Reddy 1991].

2.3 EXPERIMENTAL STUDY OF RUM

2.3.1 MACHINABILITY OF HARD-TO-MACHINE MATERIALS USING RUM

Table 2.1 Summary of workpiece materials machined by RUM and USM

Workpiece material	Experimental study	Theoretical study
Alumina	[Hu et al 2003, Li et al 2005, Ramu et al 1989, Zeng et al 2004, Jiao et al 2004]	[Zhang et al 2000, Li et al 2004, Jiao et al 2004]
Canasite	[Khanna and Pei, 1995]	
Glass	[Jana 1973, Anonymous 9 1966, Anonymous 10 1973, Treadwell and Pei 2003]	[Luzner 1973]
Polycrystalline Diamond Compacts	[Li et al 2004]	
Silicon Carbide	[Dam et al 1993]	
Silicon Nitride	[Dam et al 1993]	
Stainless Steel	[Dam et al 1993, Deng et al 1993]	[Deng et al 1993]
Titanium Boride	[Dam et al 1993]	
Zirconia	[Prabhakar 1992, Pei 1995, Pei et al, 1995, Ramu et al 1989, Pei et al 1995]	[Pei and Ferreira 1998, Ramu et al 1989, Ya et al 2002, Zhang et al 1998, Deng et al 1993]

Despite the simple geometry of the round hole, few machining operations display more versatility in the type of equipment available than drilling. The development of hard-to-machine materials like advanced ceramics, technical glasses, and some composites possessing enhanced properties is leading to their more widespread consideration for industrial application. However, drilling of small holes was always recognized as one of the most serious challenges in machining difficult-to machine materials. Now, RUM method has been utilized to machine many different types of hard-to-machine materials in industry. Table 2.1 summarizes reported work on RUM (or USM) process since it was invented in 1960's. RUM has been employed to machine many types of materials.

2.3.2 EFFECTS OF CONTROL VARIABLES ON RUM PERFORMANCE

In this section, past research work and experimental investigations about the effects of the RUM process parameters (like applied static pressure, feedrate, rotational speed, ultrasonic vibration amplitude and frequency, diamond type, size, concentration, and bond type, etc.) on the RUM drilling performances (material removal rate, tool wear, surface roughness or hole clearance) for different types of hard-to-machine materials including advanced ceramics [Hocheng et al. 2000; Jana and Satyanarayana 1973; Anonymous 8 1964; Hards 1966; Dawe Instruments Ltd 1967; Petruka et al. 1970; Markov and Ustinov 1972; Markov et al. 1977; Kubota et al. 1977, Legge 1964, Pei et al. 1995; Hu et al. 2003; Li et al. 2005; Ramu et al. 1989; Zhang et al. 1998, Ken-ichi et al. 1998; Adithan and Venkatesh 1976; Jia and Ai 1995; Liu and Chen 1996; Adithan 1983;

Adithan 1974; Hocheng et al. 1999; Keisaku et al. 1988], technical glass [Anonymous 9 1966; Adithan 1976; Diepold and Obermeier 1996; Egashira et al. 2002; Karpov and Stepanov 1986; Saha et al. 1977; Hahin and Schulze 1993; Ya et al. 2001] and some composites [Hocheng et al. 2000, Cusumano et al. 1974] are reviewed and discussed. The major conclusions are summarized.

2.3.2.1 EFFECTS OF STATIC PRESSURE

The static pressure has a great effect on RUM drilling performance. For advanced ceramics (like Al_2O_3, SiC, Si_3N_4, ZrO_2 and B_4C), as the static pressure increases, MRR will increase to a maximum value and then decrease [Hocheng et al. 1999], tool wear will increase [Hocheng et al. 1999], surface roughness (hole clearance) will decrease [Petrukha 1970, Ramu et al. 1989, Adithan and Venkatesh 1976, Jia and Ai 1995, Liu and Chen 1996, Adithan 1983, Adithan 1974, Hocheng et al. 1999].

For the technical glass including regular plate glass, porcelain, and borosilicate glass etc, as the static pressure increases, similar tendency to those of advanced ceramics could be found in some past reports [Adithan and Venkatesh 1976; Diepold and Obermeier 1996; Saha et al. 1977; Hahin and Schulze 1993].

For the hard-to-machine composites (only C/SiC composite was reported until now), as the static pressure increases, MRR will increase; hole clearance and tool wear will decrease [Hocheng et al 2000, Hocheng et al. 1999, Cusumano 1974].

2.3.2.2 EFFECTS OF ULTRASONIC VIBRATION AMPLITUDE

For technical glasses and advanced ceramics, the effects of vibration amplitude are reported by Pei et al. 1998, Hocheng et al. 1999. As the vibration amplitude increases up to some value, MRR increases. A further increase of vibration amplitude above the value will result in a reduction, to some extent, in MRR. The reduction in MRR could be attributed to “an excessive increase in alternation loading on the diamond grits and a weakening of the bond” [Karpov and Stepanov 1986]. There is no significant change of hole clearance (surface roughness) with the change of vibration amplitude.

For the hard-to-machine composites (only C/SiC composite was reported until now), optimal vibration amplitude produces the maximum removal rate and the hole clearance increases with the increase of amplitude [Hocheng et al 2000, Cusumano et al. 1974]. There is no report in detail about tool wear and the edge quality at the hole entrance and exit.

2.3.2.3 EFFECTS OF ULTRASONIC VIBRATION FREQUENCY

The vibration frequency used in the reported experiments [Petruka et al. 1970] ranges from 18 to 24 kHz. For titanium alloy, silicon carbide and dental ceramic, no systematic research work of vibration frequency effects on RUM drilling process was ever conducted.

2.3.2.4 EFFECTS OF ROTATIONAL SPEED

The influence of rotational speed on RUM drilling process is only studied in MRR for some type of advanced ceramic by Pei et al. [1995]. The MRR will increase with the increase of rotational speed. The influences on other outputs (such as tool wear and surface roughness) and other hard-to-machine materials (glass and composites) have not been reported.

2.3.2.5 EFFECTS OF ABRASIVE (CONCENTRATION, SIZE, TYPE AND BOND TYPE)

As for advanced ceramics, many papers have reported the effects of abrasives on RUM drilling process. MRR will increase as the diamond concentration increase up to an optimum value. A further increase in diamond concentration results in lower MRR [86].

According to past research work, it is due to “the considerable reduction in the mechanical strength of the diamond-impregnated layer” [Zhang et al. 1998] that a further increase in diamond concentration results in lower MRR and greatly increased tool wear.

For surface roughness, Petrukha et al. [Petruka et al. 1970] reported that Ra increases to a maximum value and then decrease as the grit size increases. As the bond strength is increased, MRR is reduced and tool wear is particularly reduced. Also, stronger diamond requires stronger binders.

As for glass and composite materials, past research work mainly deals with the effects of abrasive grit size (sometimes cubic boron nitride) on tool wear and hole clearance. For nearly all types of hard-to-machine materials, natural diamond and high-strength synthetic diamond give better performances than weaker synthetic diamond. With natural diamond the MRR is lower but the tool wear is less and surface roughness is lower than that with the strong (high-strength) synthetic diamond. For technical glass, some experimental work was conducted by using cubic boron nitride as abrasives [88]. Systematic work on titanium alloy, silicon carbide and dental ceramic has not been reported.

2.3.2.6 EFFECTS OF COOLANT

Experimental investigations have been conducted on effects of coolant pressure and coolant type on the performance of RUM. Coolant pressure does not have a significant

effect on MRR but the lowest surface roughness can be achieved at an optimal pressure level [Pei et al. 1995]. As for coolant type, the synthetic coolant and tap water show better performances in RUM drilling than the water-based coolant [Hu et al. 2003]. The latest experimental studies present that the air-operated-double-diaphragm pump can be introduced into RUM coolant system to decrease the machined surface roughness [Li et al. 2004, Li et al. 2005]. There are no systematic studies about effects of coolant on RUM machining of titanium alloy, silicon carbide and dental ceramic until now.

2.4 REVIEW OF THEORETICAL STUDY

Since the invention of RUM process, various analytical models were presented. Prabhakar et al. proposed a theoretical MRR model based on brittle fracture whose predictions do not agree with the experimental observations [Prabhakar et al. 1993], while Pei et al. reported a mechanistic model to predict MRR [Pei et al. 1995]. Then, Pei and Ferreira also reported the modeling of material removal in RUM by ductile mode [Pei and Ferreira 1998]. Zhang et al. introduced the effective number of diamond abrasives in RUM process into the MRR model based on brittle fracture [Zhang et al. 2000]. Ya et al. proposed that cavitation could be another material removal process in RUM [Ya et al. 2002].

2.5 REVIEW OF WHEEL WEAR MECHANISMS

A review of the literature shows that the wear of grinding wheels has been studied for workpiece materials such as ceramics (including alumina, silicon carbide, and silicon nitride), cermet, steel, and silicon with surface grinding, RUM, and wafer grinding [Kuriyagawa and Syoji 1990; Ilhan et al. 1992; Warkentin and Bauer 2003; Pecherer and Malkin 1984; Oliveira et al. 1999; Xie et al. 2003; Liao et al. 1997; Li et al. 1997; Hwang et al. 1999; Huang et al. 2003; Zeng et al. 2005; Tonshoff et al. 1997]. Table 2.2 summarizes the reported studies on wheel wear [Chu et al.].

Table 2.2 Summary of studies on wheel wear

Process	Workpiece material	Reference
Surface grinding	Cermet	[Kuriyagawa and Syoji 1990]
	Steel	[Ilhan et al 1992, Warkentin and Bauer 2003, Pecherer and Malkin 1984]
	Ceramics	[Oliveira et al 1999, Xie et al 2003, Liao et al 1997, Li et al 1997, Hwang et al 1997, Huang et al 2003]
Rotary ultrasonic machining	Silicon carbide	[Zeng et al 2005]
Wafer grinding	Silicon	[Shaw 1996]

Although a lot of research has been conducted on wheel wear mechanisms in grinding, there is no reported research on wheel wear mechanisms in RUM of titanium alloys. A brief review of wheel wear mechanisms in grinding will be conducive to the study on wheel wear mechanisms in RUM of titanium alloys.

Researchers have focused their attention mainly on the wheel wear mechanisms of individual abrasive particles (using single-grit wheels). An entire chapter is devoted to the wear mechanisms of individual abrasive particles in the book by Shaw [Shaw 1996]. There are four main types of wheel wear mechanisms [Shaw 1996; Malkin 1996; Jahanmir 1998; Malkin 1989; Cho et al. 1994] (Attritious wear, grain fracture, bond fractures, and grain pullout). Figure 2.3 shows the schematic illustration of these mechanisms. More discussion on each of the wear mechanisms is in chapter 6.

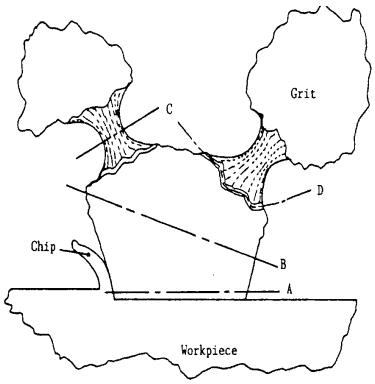

A- attritious wear, B- grain fracture, C- bond fracture, D- grain pullout

Figure 2.3 Illustration of wheel wear mechanisms [Sathyanarayanan 1985]

The overall wear and total weight loss of a grinding wheel is predominantly determined by grain fracture and bond fracture whereas attritious and grain pullout wear contribute only few percent [Yoshikawa and Sata 1963; Yoshikawa 1963; Yoshikawa 1963].

In the past, researchers have conducted more research on wear mechanisms of wheels comprising of alumina, silicon carbide and diamond wheels in grinding of metals and ceramic materials [Xie et al. 2003; Li et al. 1997; Tonshoff et al. 1997; Chu et al.; Shaw 1996; Malkin 1996]. Petrukha [1970] experimentally investigated the wheel wear in RUM by studying the effects of static load, ultrasonic vibration and amplitude, diamond concentration, diamond type, grit size, and bond strength on the specific wheel wear (as described by the following equation).

$$\text{Specific wheel wear} = \left[\frac{\text{Volume of material removed}}{\text{Volume of wheel wear}} \right]$$

But this hardly discloses any information on wheel wear mechanisms in RUM. Titanium alloys are gaining many applications in various industries such as aerospace [Boyer 1996; Peacock 1988], automotive [Anonymous 12 1989; Yamashita et al. 2002], chemical [Farthing 1979; Orr 1982], medical [Froes 2002; Abdullin et al. 1988] and sporting goods [Anonymous 13 2004; Yang and Liu 1999] due to their high strength to weight ratio at elevated temperatures, exceptional corrosion resistance, and superior fatigue strength. There is a crucial need for conducting a systematic study on wheel wear in rotary ultrasonic machining of titanium alloys. Such study may lead to findings practically useful to the wheel design and process control.

This investigation aims to understand the wheel wear mechanisms in RUM of a titanium alloy (Ti-6Al-4V). Results from this study can not only shed lights on the wheel wear mechanisms in RUM of titanium alloys, but also provide some practical guidance for the design and manufacture of RUM wheels.

2.6 SUMMARY

In this chapter, RUM process is reviewed historically. The literature review on studies of RUM process theoretically and experimentally shows many research papers about RUM on various hard-to-machine materials, but no study has ever been reported on RUM of titanium alloy, silicon carbide and dental ceramics. A question immediately raised is: is it possible to utilize RUM to machine titanium alloy, silicon carbide and dental ceramics. If it is possible, then what are the principles under the material removal process and what types of factors should be considered and studied further?

CHAPTER 3

ROTARY ULTRASONIC MACHINING OF TITANIUM ALLOY: A FEASIBILITY STUDY

This chapter presents the experimental results on feasibility study during rotary ultrasonic machining of a titanium alloy. The parameters studied are: tool wear, cutting force, material removal rate, and surface roughness.

3.1 SETUP AND CONDITIONS

Machining experiments were performed on a machine of Sonic Mill Series 10 (Sonic-Mill, Albuquerque, NM, USA). The experimental setup is schematically illustrated in Figure 3.1. It mainly consists of an ultrasonic spindle system, a data acquisition system, and a coolant system. The ultrasonic spindle system comprises of an ultrasonic spindle, a power supply, and a motor speed controller. The power supply converts 60 Hz electrical supply to high frequency (20 kHz) AC output. This is fed to the piezoelectric transducer located in the ultrasonic spindle. The ultrasonic transducer converts electrical input into mechanical vibrations. The motor attached atop the ultrasonic spindle supplies the rotational motion of the tool and different speeds can be obtained by adjusting the motor speed controller. The fixture to hold the specimens was mounted on a dynamometer that was attached to the machine table.

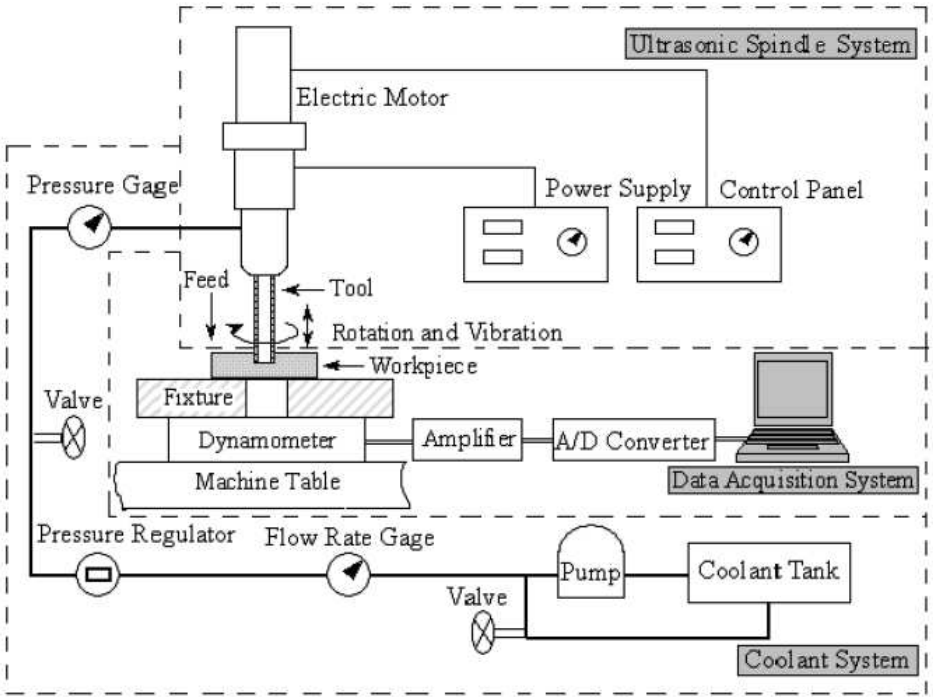

Figure 3.1 Experimental set-up

Table 3.1 Experimental conditions

Parameter	Unit	Value
Spindle speed	$rev \cdot s^{-1}$ (rpm)	67 (4000)
Feedrate	$mm \cdot s^{-1}$	0.06
Vibration power supply*	%	0 or 40
Vibration frequency	KHz	0 or 20

* Vibration power supply controls the amplitude of ultrasonic vibration

Table 3.1 shows the experimental conditions. Mobilemet® S122 water-soluble cutting oil (MSC Industrial Supply Co., Melville, NY, USA) was used as the coolant (diluted with water at 1 to 20 ratio). The workpiece material was titanium alloy (Ti-6Al-4V) provided

Table 3.2 Properties of titanium alloy (Ti-6Al-4V) [after Allen 1997].

Property	Unit	Value
Tensile strength	MPa	950
Thermal conductivity	$W \cdot m^{-1} \cdot K^{-1}$	21
Melting point	K	1941 ± 285
Density	$Kg \cdot m^{-3}$	4510
Coefficient of thermal expansion	K^{-1}	8.64×10^{-6}
Vickers hardness		300

by Boeing Company. The mechanical properties are shown in Table 3.2. The size of workpieces was 115×85×11.94 mm. Diamond core drills were provided by N.B.R. Diamond Tool Corp. (LaGrangeville, NY, USA). The outer and inner diameters of the core drills were 9.6 mm and 7.8 mm respectively. The mesh size of the diamond abrasives was 60/80.

Three different tools (two tools with slots and one tool without slots) were used. Figure 3.2 illustrates the cutting tool with slots.

The tools are designated as:

Tool #1 – The tool with slots (without ultrasonic vibration).

Tool #2 – The tool with slots (with ultrasonic vibration).

Tool #3 – The tool without slots (with ultrasonic vibration).

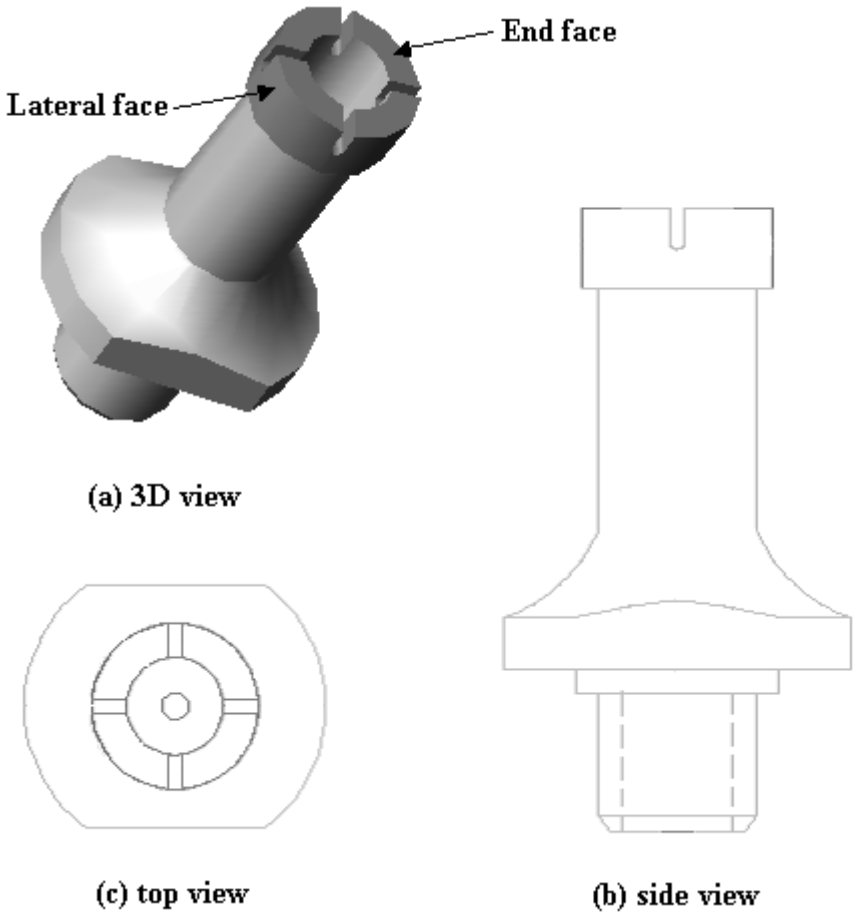

Figure 3.2 Illustration of the cutting tool with slots for rotary ultrasonic machining

3.2 MEASUREMENT PROCEDURES

During rotary ultrasonic machining, the cutting force along the feedrate direction was measured by a KISTLER 9257 dynamometer (Kistler Instrument Corp, Amherst, NY, USA). The dynamometer was mounted atop the machine table and beneath the workpiece, as shown in Figure 3.1. The electrical signals from the dynamometer were transformed into numerical signals by an A/D converter. Then the numerical signals to

measure the cutting force were displayed and saved on the computer with the help of LabVIEW™ (Version 5.1, National Instruments, Austin, TX, USA). The sampling frequency to obtain the cutting force signals was 100 Hz. The cutting force reported in this chapter is the maximum cutting force on the cutting force curve, as illustrated in Figure 3.3. The material removal rate (MRR) in the rotary ultrasonic machining was calculated using the following equation:

$$MRR = \frac{Volume of Material\ \mathrm{Re}moved}{Time}$$

$$MRR = \frac{\pi \cdot [(D_{out}/2)^2 - (D_{in}/2)^2] \cdot d}{T}$$

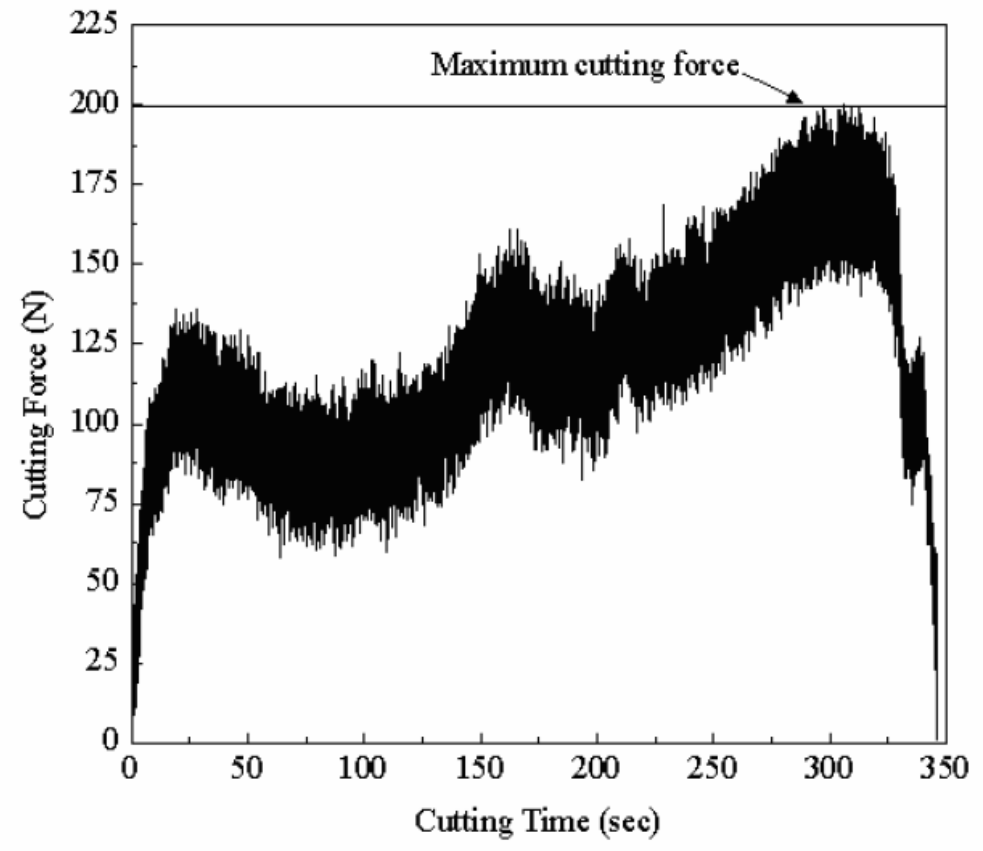

Figure 3.3 Measurement of maximum cutting force

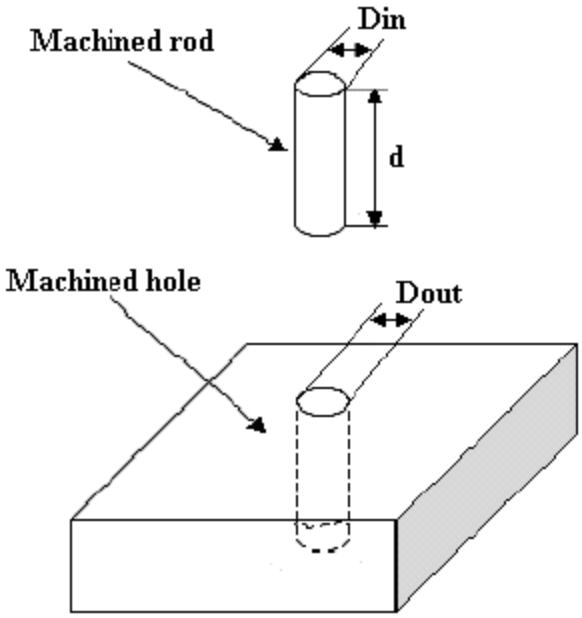

Figure 3.4 Illustration of the hole and rod machined by rotary ultrasonic machining

where, D_{out} is the diameter of machined hole, D_{in} the diameter of machined rod, d workpiece thickness, and T the time it takes to drill the hole. Figure 3.4 illustrates the machined hole and rod. After each drilling test, the cutting tool was removed from the machine for observation under a digital microscope (Olympus DVM-1, Olympus America Inc., New York, USA). The magnification of the digital microscope was from 50 to 200. The topography was observed on both the end face and lateral face of the tool (see Figure 3.5). In order to ensure that the same area of the tool surface was observed every time, a special fixture was designed for holding the tool. The position shown in Figure 3.5 was for observation of the tool lateral face.

A vernier caliper (Mitutoyo IP-65, Mitutoyo Corporation, Kanagawa, Japan) was used for measurements of the length of the core drill. The tool length was measured after each

test. The axial tool wear was determined by the difference between the two lengths measurements before and after each test. The surface roughness was measured on both the machined rod surface and the hole surface after each test with a surface profilometer (Mitutoyo Surftest-402, Mitutoyo Corporation, Kanagawa, Japan).

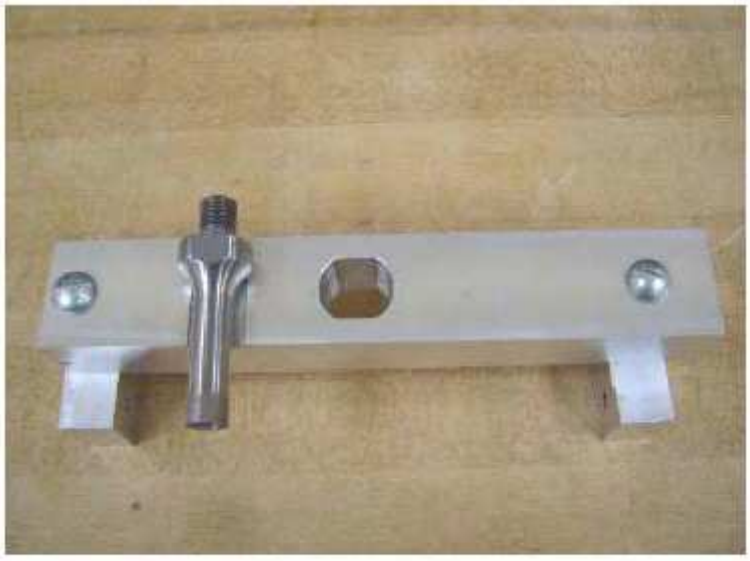

Figure 3.5 Position of tool holding for observation of tool lateral face

3.3 EXPERIMENTAL RESULTS

3.3.1 TOOL WEAR

The tool wear curves for the three tools are shown in Figure 3.6. For Tool #1 (with slots, without vibration), the tool wear rate was the highest. For Tool #2 (with slots, with vibration), the tool wear rate was lower than that for Tool #1. For Tool #3 (without slots, with vibration), the tool wear was the lowest. Sometimes, severe tool wear can be observed at the edge of the slots (Figure 3.7).

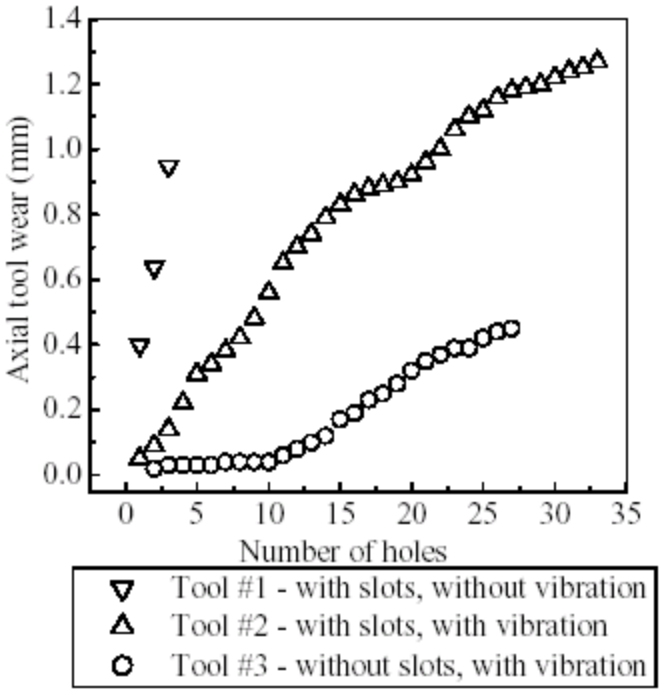

Figure 3.6 Tool wear vs. number of holes machined

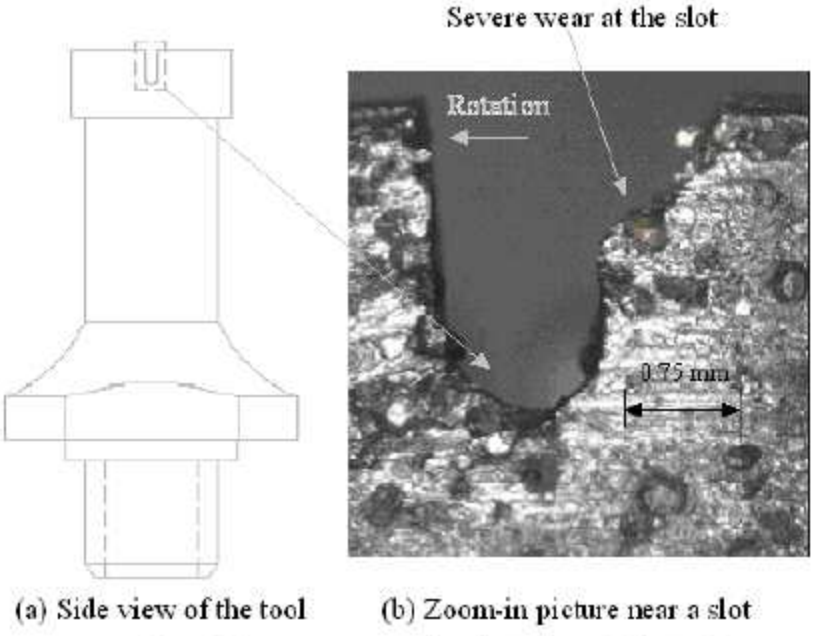

Figure 3.7 Severe wear at the slot edge of the tool

The above results about the effects of ultrasonic vibration on tool wear with the titanium alloy are consistent with those reported by Markov and Ustinov [1972] with workpiece material being quartz glass. They are also consistent with those reported by Egashira and Mizutani [2002] in a study on ultrasonic vibration assisted drilling of glass (Please note that ultrasonic vibration assisted drilling is different from rotary ultrasonic machining). They reported that the tool wear without vibration was approximately twice of that with vibration [Egashira and Mizutani 2002].

3.3.2 CUTTING FORCE

Cutting force data points are plotted in Figure 3.8 (a). The average value of cutting force data points for Tool #1, Tool #2, and Tool #3 are shown in Figure 3.8 (b). It can be seen that the cutting force was significantly reduced (about 20%) with rotary ultrasonic machining (Tool #1 and Tool #3) compared to diamond grinding. Presence of slots in the tool reduces the cutting forces by 7%. The above results about the effects of ultrasonic vibration on cutting forces are consistent with the observations by Li et al. [2005] when rotary ultrasonic machining of ceramic-matrix composites and alumina.

3.3.3 MRR

The results on material removal rate for the three tools are shown in Figure 3.9 (a). The average material removal rate values for Tool #1, Tool #2, and Tool #3 are shown in

Figure 3.9 (b). It can be observed that the material removal rates measured for the three tools do not vary significantly. The above results about the effects of ultrasonic vibration on material removal rate are consistent with the results reported by Li et al. [2005] when rotary ultrasonic machining of ceramic-matrix composites and alumina.

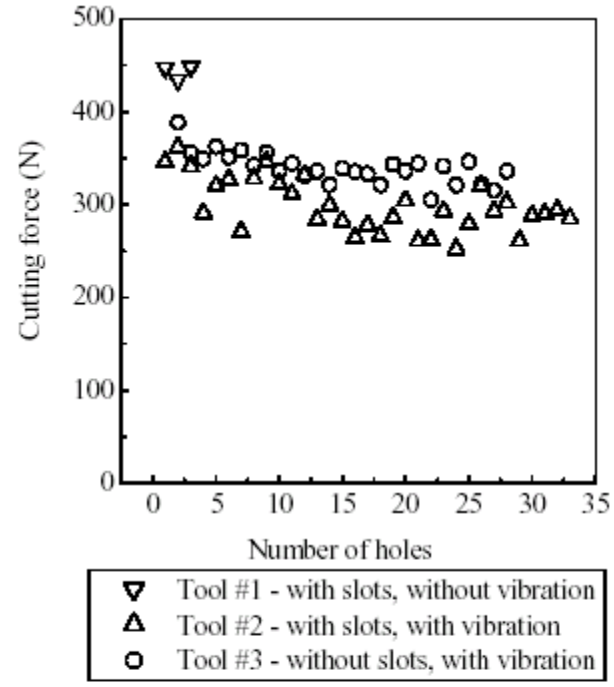

(a) Cutting force vs. number of holes

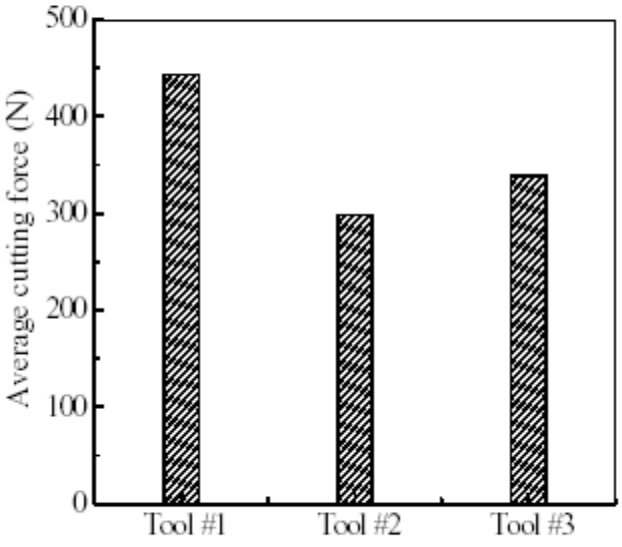

(b) Average cutting force for each tool

Figure 3.8 Effects on cutting force

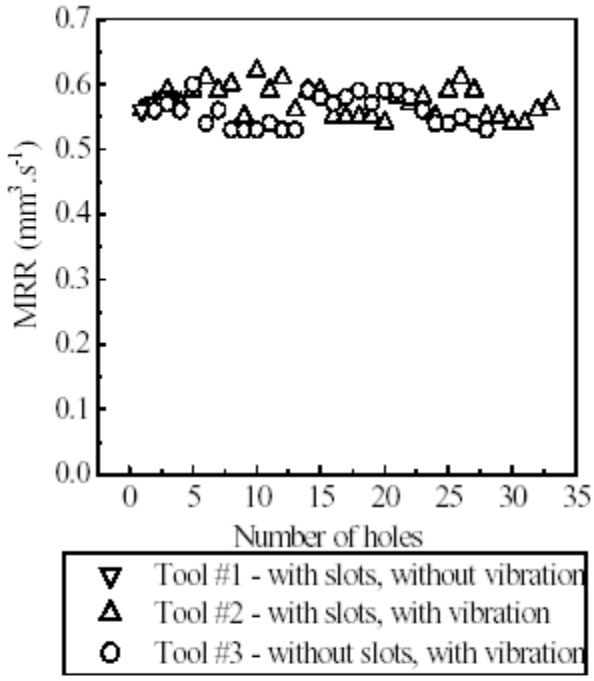

(a) MRR vs. number of holes

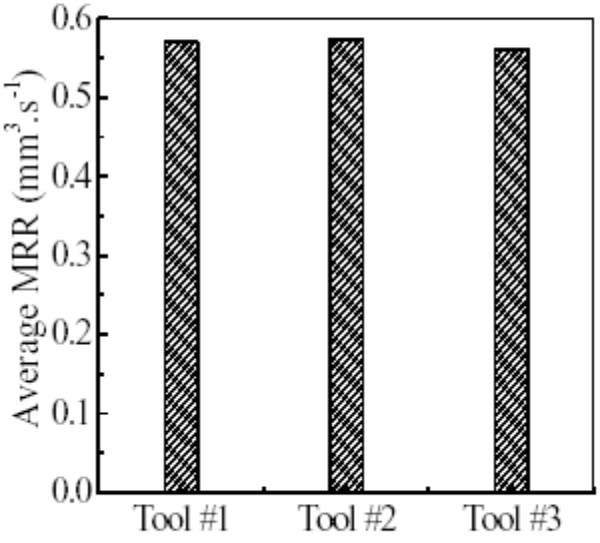

(b) Average MRR for each tool

Figure 3.9 Effects on material removal rate (MRR)

3.3.4 SURFACE ROUGHNESS

3.3.4.1 RFACE ROUGHNESS ON MACHINED HOLES

Surface roughness curves for machined holes are displayed in Figure 3.10 (a). The average surface roughness values for Tool #1, Tool #2, and Tool #3 are shown in Figure 3.10 (b). It can be seen that the average surface roughness with rotary ultrasonic machining is reduced by about 20% compared to diamond grinding. Furthermore, surface roughness when the tool has slots is lower than that when the tool has no slots.

3.3.4.2 RFACE ROUGHNESS ON MACHINED RODS

Surface roughness curves for machined rods are displayed in Figure 3.11 (a). The average surface roughness values for Tool #1, Tool #2, and Tool #3 are shown in Figure 3.11 (b). Similar to machined holes, the average surface roughness is lower when there is ultrasonic vibration. Note that the roughness value was reduced by 85% with ultrasonic vibration, a significant roughness improvement. Furthermore, surface roughness is improved by 43% when the tool has no slots. Markov and Ustinov [1972] studied the effects of ultrasonic vibration on surface roughness when machining of quartz glass. They found that the roughness could be either increased or decrease, depending on the vibration amplitude.

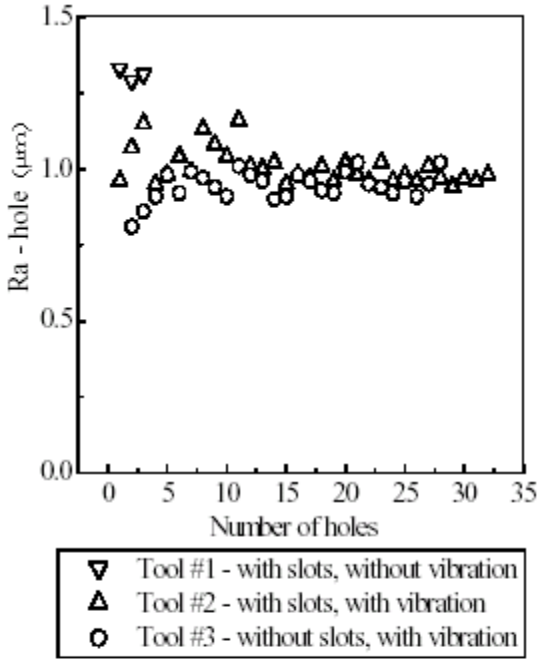

(a) Surface roughness vs. number of holes

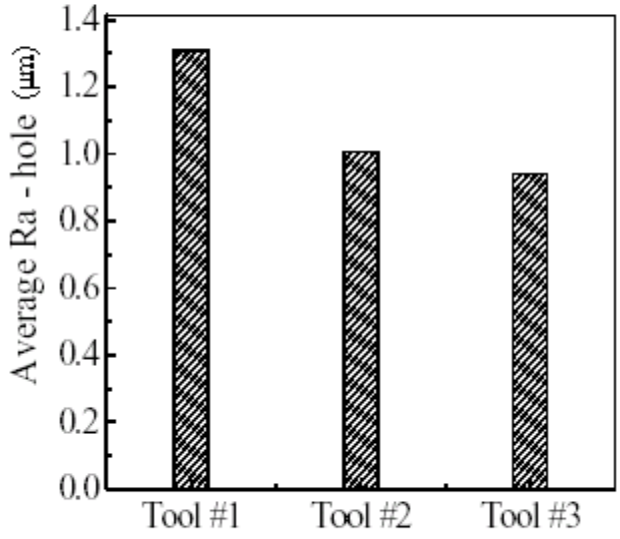

(b) Average surface roughness for each tool

Figure 3.10 Effects on surface roughness (machined holes)

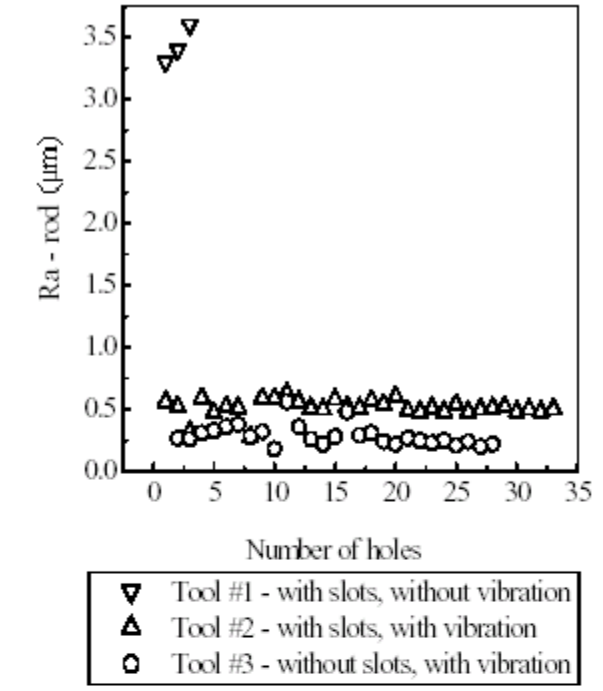

(a) Surface roughness vs. number of holes

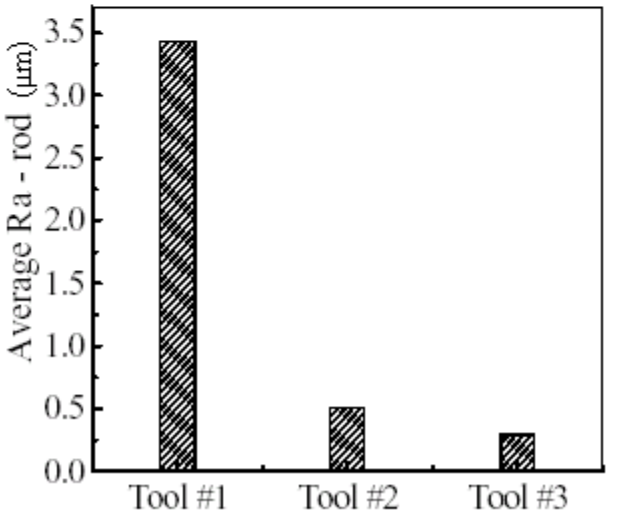

(b) Average surface roughness for each tool

Figure 3.11 Effects on surface roughness (machined rod)

3.4 SUMMARY

The experimental results presented here is the first attempt to drill titanium alloy with RUM. The tool wear, cutting forces, and surface roughness are compared with three different tools. The following conclusions can be drawn:

1. Compared with diamond drilling process, the tool wear rate with rotary ultrasonic machining is about 85 % lower.
2. The cutting force and surface roughness with rotary ultrasonic machining are lower than those with diamond grinding.
3. The tool with slots reduces cutting force but increases surface roughness and tool wear, compared with the tool without slots.

CHAPTER 4

ROTARY ULTRASONIC MACHINING OF TITANIUM ALLOY: EFECTS OF TOOL VARIABLES

This study reports the experimental results on the tool wear, cutting force, and surface roughness during rotary ultrasonic machining of a titanium alloy with four different tools.

4.1 EXPERIMENTAL CONDITIONS AND PROCEDURES

Workpiece material, machine, coolant and measurement equipment are the same as described in section 3.1. The experimental conditions are shown in Table 4.1. Four different tools were used. Table 4.2 shows their specifications. When 72 carats of diamond particles are added in 1 cubic inch of bond material then the diamond concentration is called as 100 concentration.

Table 4.1 Experimental conditions

Parameter	Unit	Value
Spindle speed	$rev \cdot s^{-1}$ (rpm)	67 (4000)
Feed rate	$mm \cdot s^{-1}$	0.06
Vibration power supply*	%	0, 40
Vibration frequency	KHz	0, 20

Table 4.2 Specifications of tool

Tool#	Grit size (mesh #)	Grain concentration	Bond type
1	60/80	100	B
2	60/80	100	C
3	60/80	80	B
4	80/100	100	B

4.2 EXPERIMENTAL RESULTS

The results of experiments are presented and discussed in this section. Experimental data has been processed using the software called MICROCAL ORIGIN (Version 6, Microcal Software, Inc., One Roundhouse Plaza, Northampton, MA, USA).

4.2.1 EFFECTS ON CUTTING FORCE

Figure 4.1 (a) shows the curves of cutting force vs. number of holes for the four tools. It can be clearly observed that tool #2 and tool #4 have the maximum and minimum cutting forces respectively. Furthermore, the cutting forces for all the four tools do not change much as the number of holes increases.

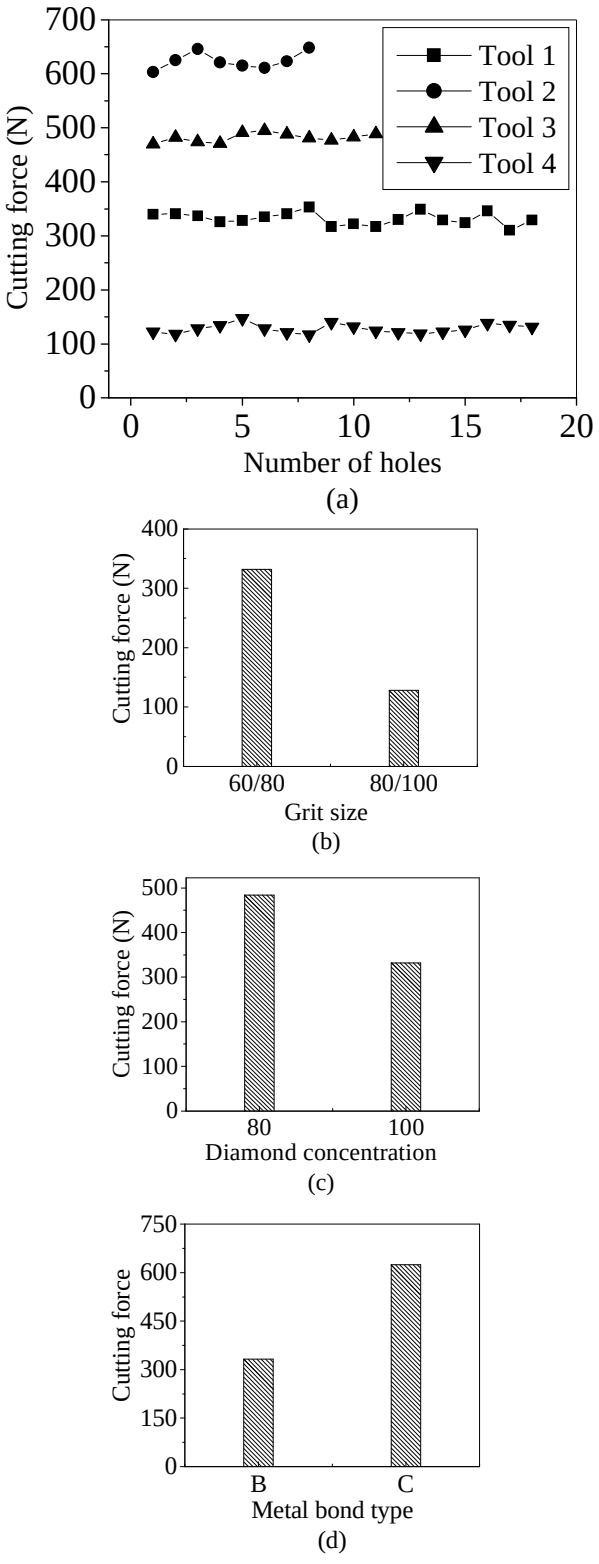

Figure 4.1 Effects on cutting force

4.2.1.1 GRIT SIZE

Figure 4.1 (b) shows the cutting force vs. grit size graph. It can be clearly observed that the cutting force is reduced by approximately half as the grit size changes from mesh #60/80 to 80/100. These results are similar to the results reported by Jiao et al. [2005] in rotary ultrasonic machining of alumina.

4.2.1.2 DIAMOND CONCENTRATION

Figure 4.1 (c) shows the effect of diamond concentration on cutting force. It can be seen that the cutting force is reduced significantly as the diamond concentration increases from 80 to 100.

4.2.1.3 METAL BOND TYPE

Figure 4.1 (d) shows the relation between cutting force and metal bond type. It can be observed that the cutting force is lower for bond type B as compared to bond type C.

4.2.2 EFFECTS ON SURFACE ROUGHNESS OF MACHINED HOLE

Figure 4.2 (a) shows the experimental data of surface roughness of hole vs. number of holes for the four tools. It can be clearly observed that tool #1 and tool #4 produce the maximum and minimum surface roughness values of hole respectively. Large variation is

observed while machining first few holes with tool #1. The surface roughness of hole for the other three tools remains relatively constant.

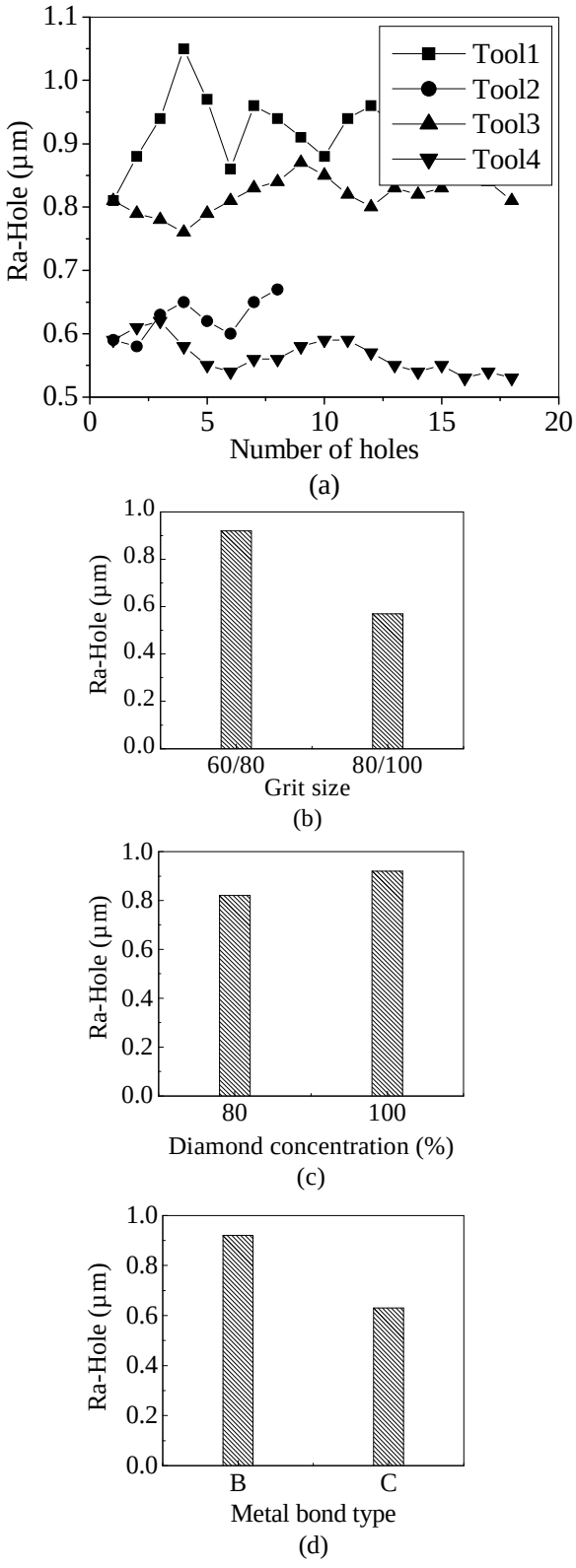

Figure 4.2 Effects on surface roughness of hole

4.2.2.1 GRIT SIZE

Figure 4.2 (b) shows the effect of grit size on surface roughness of hole. It can be clearly observed that the surface roughness of hole is reduced significantly as the grit size changes from mesh #60/80 to 80/100. These results are consistent with the results stated by Li et al. [2004] and Pei et al. [1995] for rotary ultrasonic machining of ceramics. They reported that the surface roughness increases till an optimum value and then decreases as the grit size increases.

4.2.2.2 DIAMOND CONCENTRATION

Figure 4.2 (c) shows the graph of surface roughness of hole vs. diamond concentration. As the diamond concentration increases from 80 to 100, the surface roughness of the hole increases. It is interesting to observe that these results are different from those reported by Li et al. [2004] and Pei et al. [1995] for rotary ultrasonic machining of ceramics. They reported that the surface roughness decreases with increasing diamond concentration.

4.2.2.3 METAL BOND TYPE

Figure 4.2 (d) shows the effect of bond type on surface roughness of hole. It can be observed that surface roughness is higher for bond type B as compared to bond type C.

4.2.3 EFFECTS ON SURFACE ROUGHNESS OF MACHINED ROD

Figure 4.3 (a) shows the curves of surface roughness of rod vs. number of holes curves for the four tools. It can be observed that tool #2 and tool #4 produce the maximum and minimum surface roughness values of rod respectively. Surface roughness of rod remains more or less constant for all the four tools as the number of holes increases.

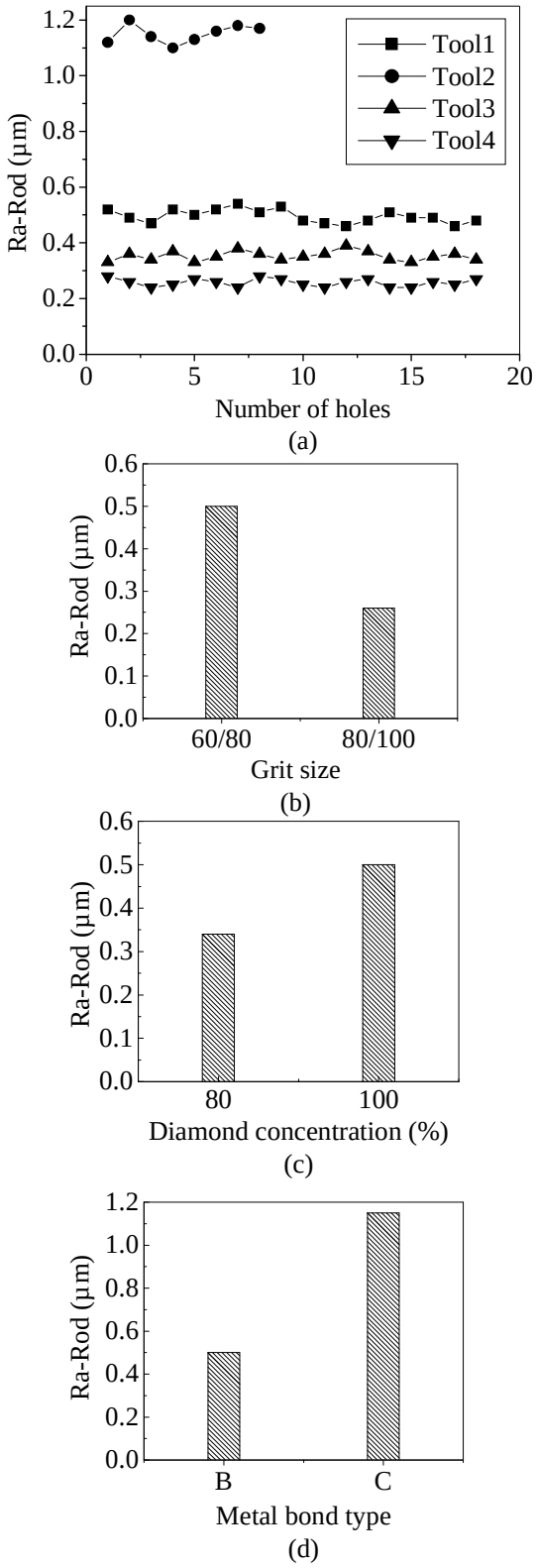

Figure 4.3 Effects on surface roughness of rod

4.2.3.1 GRIT SIZE

Figure 4.3 (b) shows the effect of grit size on surface roughness of rod. The surface roughness reduces significantly when the grit size changes from 60/80 to 80/100. This finding is similar to the results stated by Li et al. [2004] and Pei et al. [1995] for rotary ultrasonic machining of ceramics.

4.2.3.2 DIAMOND CONCENTRATION

Figure 4.3 (c) shows the graph of surface roughness of rod vs. diamond concentration. Surface roughness of rod increases significantly as the diamond concentration increases from 80 to 100. This result is different from those stated by Li et al. [2004] and Pei et al. [1995] for rotary ultrasonic machining of ceramics.

4.2.3.3 METAL BOND TYPE

Figure 4.3 (d) shows the graph of surface roughness of rod vs. types of metal bond. It can be observed that the surface roughness is lower for metal bond type B as compared to metal bond type C.

4.2.4 EFFECTS ON TOOL WEAR

Figure 4.4 (a) shows the curves of cumulative tool wear vs. number of holes for the four tools. It can be observed that tool #2 and tool #3 have the maximum and minimum axial tool wear respectively.

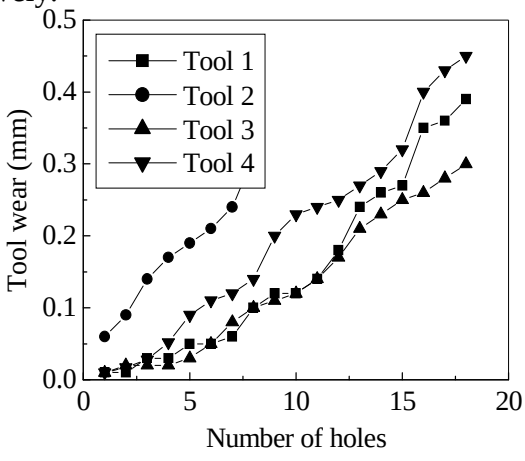

(a)

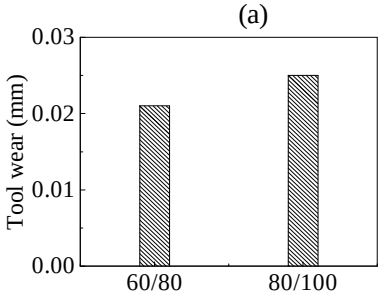

(b)

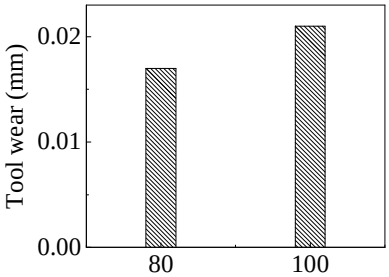

(c)

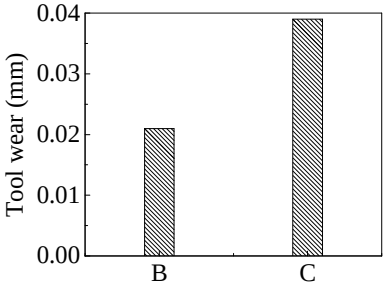

(d)

Figure 4.4 Effects on tool wear

4.2.4.1 GRIT SIZE

Figure 4.4 (b) shows the effect of grit size on tool wear. The tool wear increases slightly as the grit size changes from mesh # 60/80 to 80/100. This result is similar to the results reported by Li et al. [2004], Pei et al [1995], Ferreira and Pei [1999], and Zeng et al. [2004] for rotary ultrasonic machining of ceramics.

4.2.4.2 DIAMOND CONCENTRATION

Figure 4.4 (c) shows the graph of tool wear vs. diamond concentration. The axial tool wear increases slightly as the diamond concentration increases from 80 to 100. This result is similar to the results reported by Li et al. [2004], Pei et al. [1995], Ferreira and Pei [1999], and Zeng et al. [2004] for rotary ultrasonic machining of ceramics.

4.2.4.3 METAL BOND TYPE

Figure 4.4 (d) shows the graph of tool wear vs. types of metal bond. It is observed that the tool wear is lower for metal bond type B as compared to metal bond type C. Note that the effects of bond type on tool wear and on surface roughness are similar.

4.3 SUMMARY

Rotary ultrasonic machining (RUM) of titanium alloy with four different tools has been studied. The effects of different tool variables (grit size, metal bond type, and diamond concentration) on output variables (tool wear, cutting force, surface roughness) has been investigated. The following conclusions can be drawn from the study:

1. The tool with grit size of mesh #60/80 gives higher cutting force and surface roughness but lower tool wear compared to the tool with grit size of mesh #80/100.
2. The tool with lower diamond concentration (80) gives lower surface roughness and tool wear but higher cutting force compared to the tool with higher diamond concentration (100).
3. The tool with bond type B gives lower cutting force, surface roughness for rod, and tool wear but higher surface roughness for hole compared to the tool with bond type C.

CHAPTER 5

ROTARY ULTRASONIC MACHINING OF TITANIUM ALLOY: EFFECTS OF MACHINING VARIABLES

5.1 EXPERIMENTAL CONDITIONS AND PROCEDURES

Table 5.1 shows the experimental conditions. Other conditions including workpiece material, machine, coolant and measurement equipment are the same as described in section 3.1.

Table 5.1 Experimental conditions

Order of tests			Spindle speed ($rev \cdot s^{-1}$)	Feedrate ($mm \cdot s^{-1}$)	Ultrasonic vibration power (%)
Tool 1	Tool 2	Tool 3			
1	1	1	66.7	0.06	40
2	2	2	33.4	0.06	40
3	3	9	100	0.06	40
4	4	10	50	0.06	40
5	5	11	66.7	0.06	40
6	6	12	66.7	0.25	40
7	7	3	66.7	0.14	40
8		4	66.7	0.19	40
9		5	66.7	0.06	60
10		6	66.7	0.06	40
11		7	66.7	0.06	30
12		8	66.7	0.06	50

The outer and inner diameters of the core drills were 9.6 mm and 7.8 mm respectively. The mesh size of the diamond abrasives was 80/100. Three sets of experiments were conducted with three identical tools. Four different levels of the three machining variables (spindle speed, feedrate, and ultrasonic power) were studied, one variable was varied at a time while keeping the other two variables constant to study the effects on the output.

5.2 EXPERIMENTAL RESULTS

In this section, the results of the experiments are presented. The cutting force, MRR, and surface roughness results are shown in Table 5.2, Table 5.3, and Table 5.4 respectively.

Table 5.2 Results on cutting force (N)

Spindle speed ($rev \cdot s^{-1}$)	Feedrate ($mm \cdot s^{-1}$)	Ultrasonic vibration power (%)	Tool 1	Tool 2	Tool 3
66.7	0.06	40	118	111	123
33.4	0.06	40	547	534	565
100	0.06	40	98	102	97
50	0.06	40	298	264	244
66.7	0.06	40	118	119	134
66.7	0.25	40	680	750	695
66.7	0.14	40	390	385	402
66.7	0.19	40	448		468
66.7	0.06	60	145		138
66.7	0.06	40	118		106
66.7	0.06	30	161		172
66.7	0.06	50	109		101

Table 5.2 Results on MRR ($mm^3 \cdot s^{-1}$)

Spindle speed ($rev \cdot s^{-1}$)	Feedrate ($mm \cdot s^{-1}$)	Ultrasonic vibration power (%)	Tool 1	Tool 2	Tool 3
66.7	0.06	40	0.56	0.418	0.47
33.4	0.06	40	0.582	0.447	0.481
100	0.06	40	0.539	0.441	0.464
50	0.06	40	0.539	0.43	0.487
66.7	0.06	40	0.56	0.49	0.56
66.7	0.25	40	1.68	2.01	1.81
66.7	0.14	40	1.27	1.3	1.28
66.7	0.19	40	1.4		1.5
66.7	0.06	60	0.565		0.474
66.7	0.06	40	0.56		0.452
66.7	0.06	30	0.591		0.448
66.7	0.06	50	0.567		0.452

Table 5.3 Results on surface roughness (μm)

Spindle speed ($rev \cdot s^{-1}$)	Feedrate ($mm \cdot s^{-1}$)	Ultrasonic vibration power (%)	Tool 1		Tool 2		Tool 3	
			hole	rod	hole	rod	hole	rod
66.7	0.06	40	0.69	0.48	0.76	0.5	0.75	0.52
33.4	0.06	40	2.01	1.75	1.98	1.8	1.93	1.69
100	0.06	40	0.63	0.3	0.65	0.31	0.58	0.33
50	0.06	40	1.29	0.93	1.35	0.88	1.31	0.94
66.7	0.06	40	0.69	0.48	0.79	0.48	0.81	0.54
66.7	0.25	40	4.64	3.51	4.23	3.8	4.19	3.89
66.7	0.14	40	1.27	0.7	1.19	0.63	1.22	0.69
66.7	0.19	40	2.91	2.32			2.79	2.2
66.7	0.06	60	0.63	0.28			0.58	0.22
66.7	0.06	40	0.69	0.48			1.01	0.5
66.7	0.06	30	1.66	1.44			1.47	1.89
66.7	0.06	50	0.66	0.31			0.57	0.35

5.2.1 EFFECTS ON CUTTING FORCE

5.2.1.1 SPINDLE SPEED

The maximum cutting force vs. spindle speed curve is shown in Figure 5.1. The cutting force decreases significantly as the spindle speed increases.

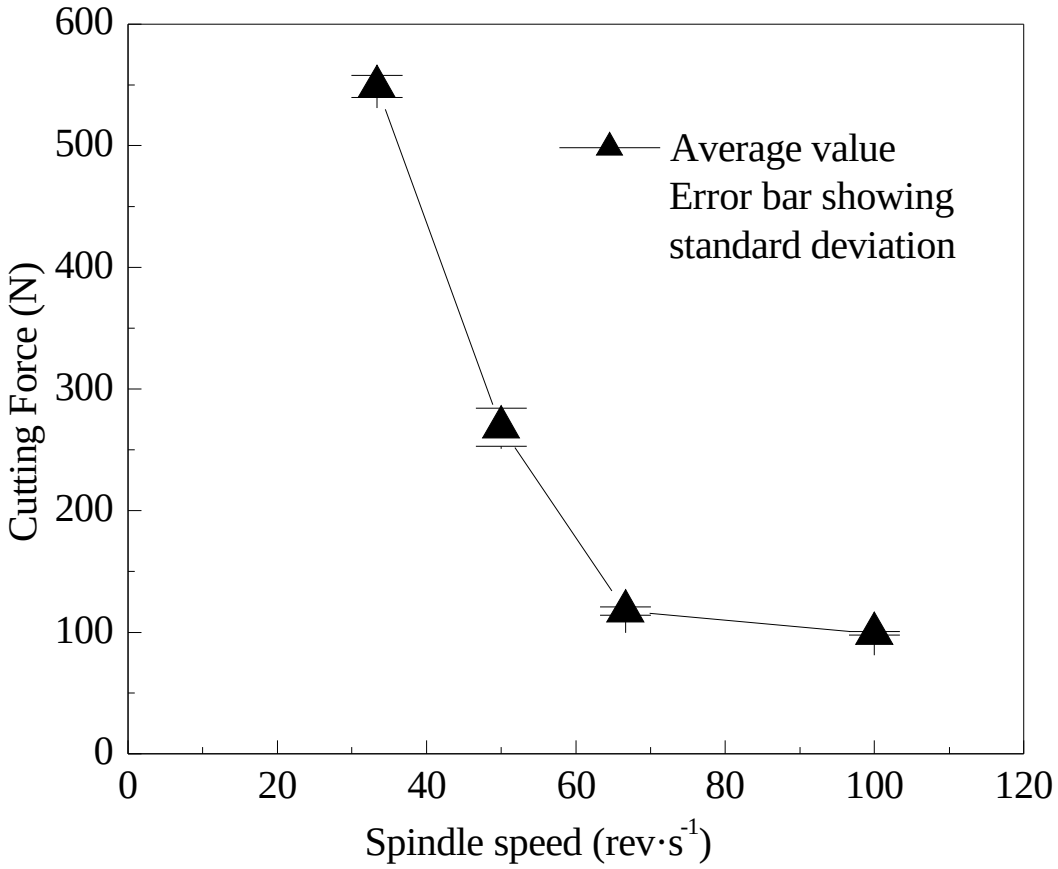

Figure 5.1 Effects of spindle speed on cutting force

These results are consistent with those reported by Jiao et al. [2005] for rotary ultrasonic machining of alumina. However, it is interesting to notice that these results are different from those reported by Li et al. [2005]. They reported that the spindle speed did not have

significant effects on cutting force for rotary ultrasonic machining of ceramic matrix composite materials. Therefore, it can be said that the effects of spindle speed on cutting force vary for different workpiece materials.

It is also observed that the rate of decrease in the cutting force decreases when the spindle speed increases. In summary, the spindle speed has significant effects on cutting force; the lower the spindle speed, the higher the cutting force.

5.2.1.2 FEEDRATE

The feedrate has significant effects on cutting force, as shown in Figure 5.2. The cutting force increases significantly as the feedrate increases, which are consistent with the observation by Jiao et al. [2005] and Li et al. [2005] for rotary ultrasonic machining of alumina and ceramic matrix composite material respectively.

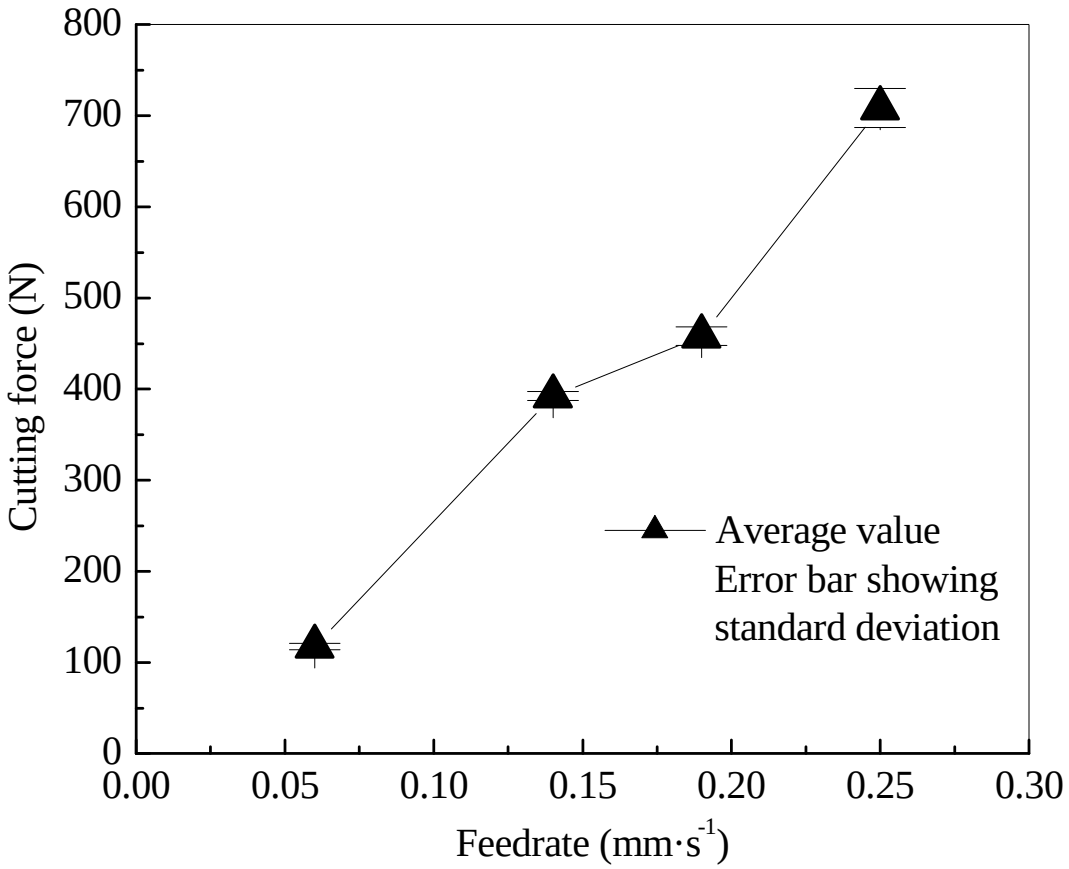

Figure 5.2 Effects of feedrate on cutting force

5.2.1.3 ULTRASONIC VIBRATION POWER

The ultrasonic power has significant effect on cutting force, as shown in Figure 5.3. Cutting force decreases initially as ultrasonic power level increases and then increases at higher power level. This observation is different from that previously reported by Jiao et al. [2005] and Li et al. [2005]. Jiao et al. found no significant effects of ultrasonic power on cutting force when rotary ultrasonic machining of alumina. Li et al. reported that cutting force increases as the ultrasonic power increases for rotary ultrasonic machining

of ceramic matrix composites. Please note that both Jiao et al. and Li et al. used much smaller range of ultrasonic power in their experiments.

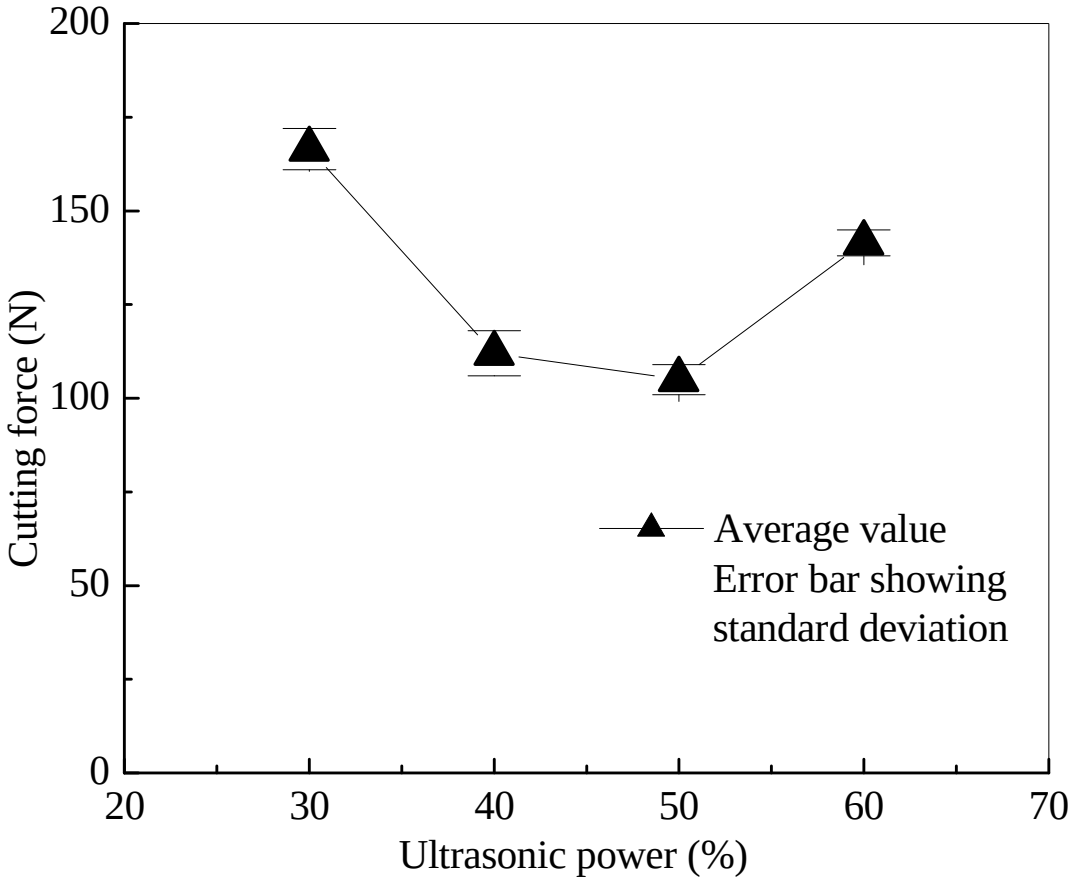

Figure 5.3 Effects of ultrasonic power on cutting force

5.2.2 EFFECTS ON MATERIAL REMOVAL RATE

5.2.2.1 SPINDLE SPEED

The effects of spindle speed on MRR are shown in Figure5.4. It can be seen that the spindle speed has no obvious effects on MRR. This is consistent with the results reported by Jiao et al. [2005] for rotary ultrasonic machining of alumina. However, it is interesting

to notice that this observation is different from those previously reported by Li et al. [2005]. They found that MRR increases as the spindle speed increases for rotary ultrasonic machining of ceramic matrix composite materials.

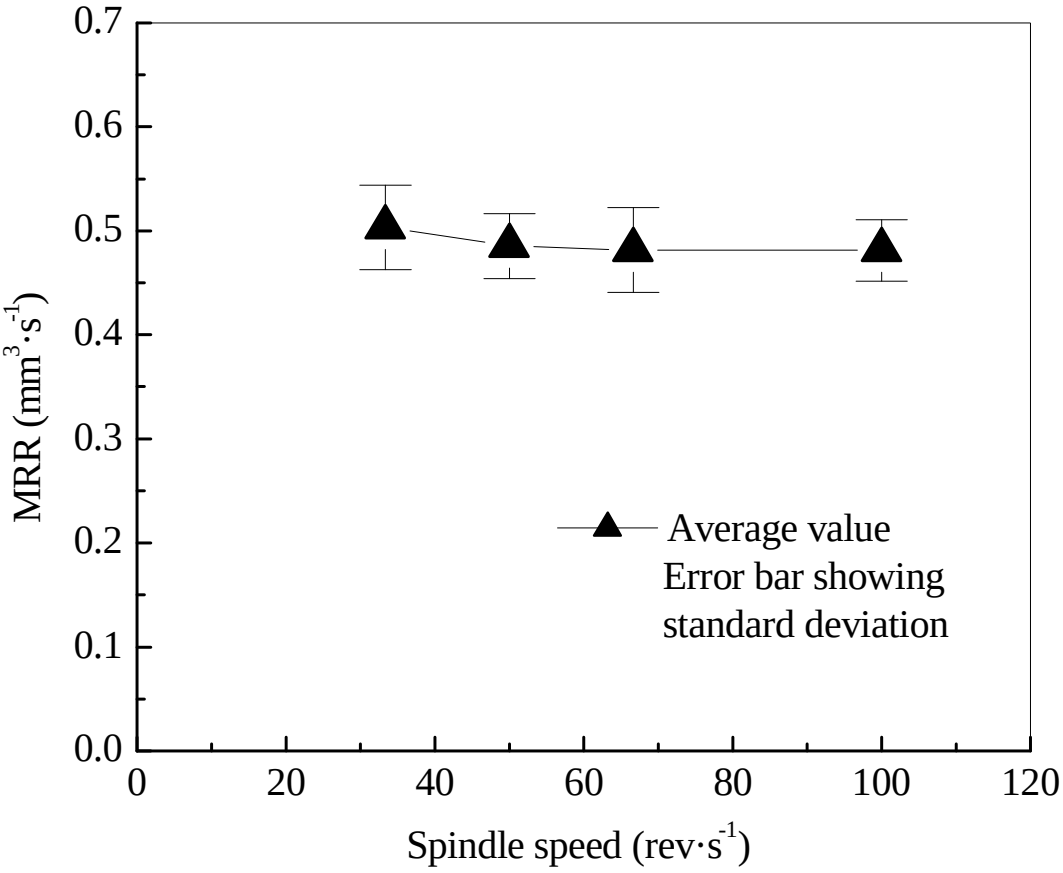

Figure 5.4 Effects of spindle speed on MRR

5.2.2.2 FEEDRATE

As shown in Figure 5.5, when the feedrate increases, MRR increases. This is because as the feedrate increases, the tool travels faster in downward direction causing increase in material removal rate. Jiao et al. [2005] and Li et al. [2005] reported a similar relationship

between MRR and feedrate for rotary ultrasonic machining of alumina and ceramic matrix composite material respectively. Thus, even for different material properties, MRR always increases with feedrate.

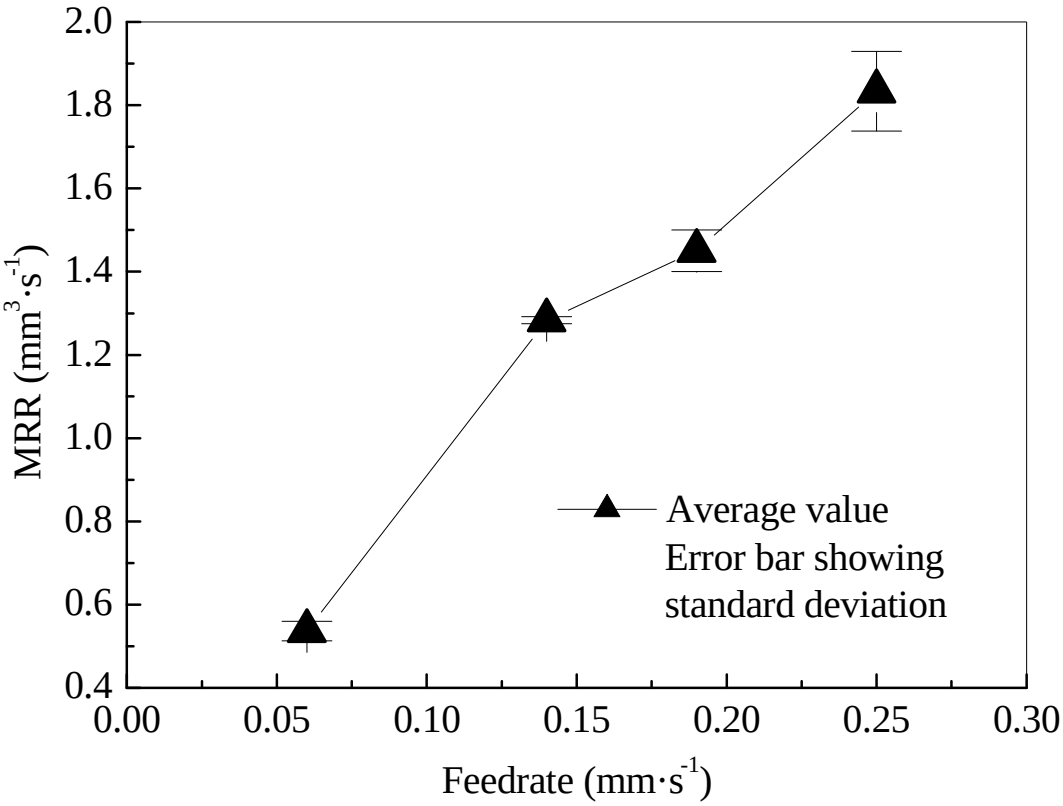

Figure 5.5 Effects of feedrate on MRR

5.2.2.3 ULTRASONIC VIBRATION POWER

The ultrasonic power has no significant effects on MRR, as shown in Figure 5.6. The MRR observed at various levels of ultrasonic power is almost constant. This is consistent with the results reported by Jiao et al. [2005]. However, it is interesting to notice that this observation is different from those previously reported by Li et al. [2005]. They reported

that MRR increases as the ultrasonic power increases for rotary ultrasonic machining of ceramic matrix composites.

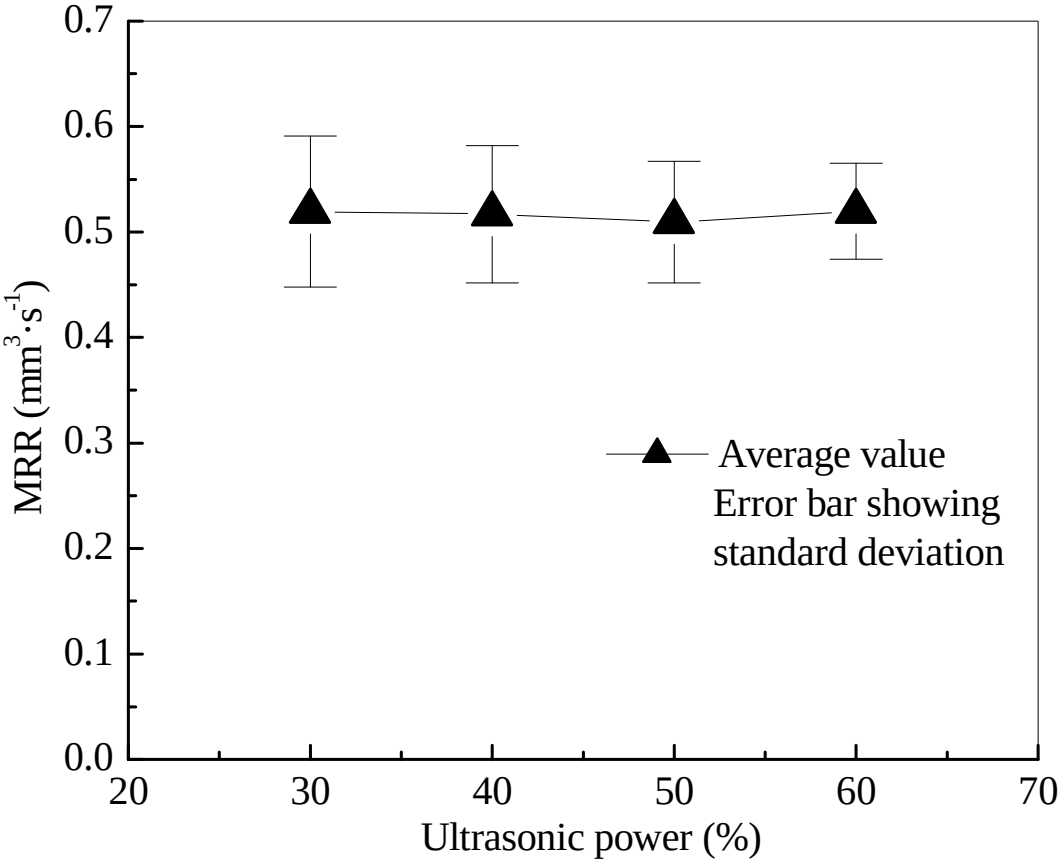

Figure 5.6 Effects of ultrasonic power on MRR

5.2.3 EFFECTS ON SURFACE ROUGHNESS

5.2.3.1 SPINDLE SPEED

The surface roughness curve for the machined hole is depicted in Figure 5.7. The surface roughness becomes significantly lower as the spindle speed increases. This observation is

consistent with those reported by Jiao et al. [2005] for rotary ultrasonic machining of alumina. It is also observed that the rate of decrease of surface roughness decreases with the increase in spindle speed. It can be concluded that spindle speed has significant effects on surface roughness on the machined hole.

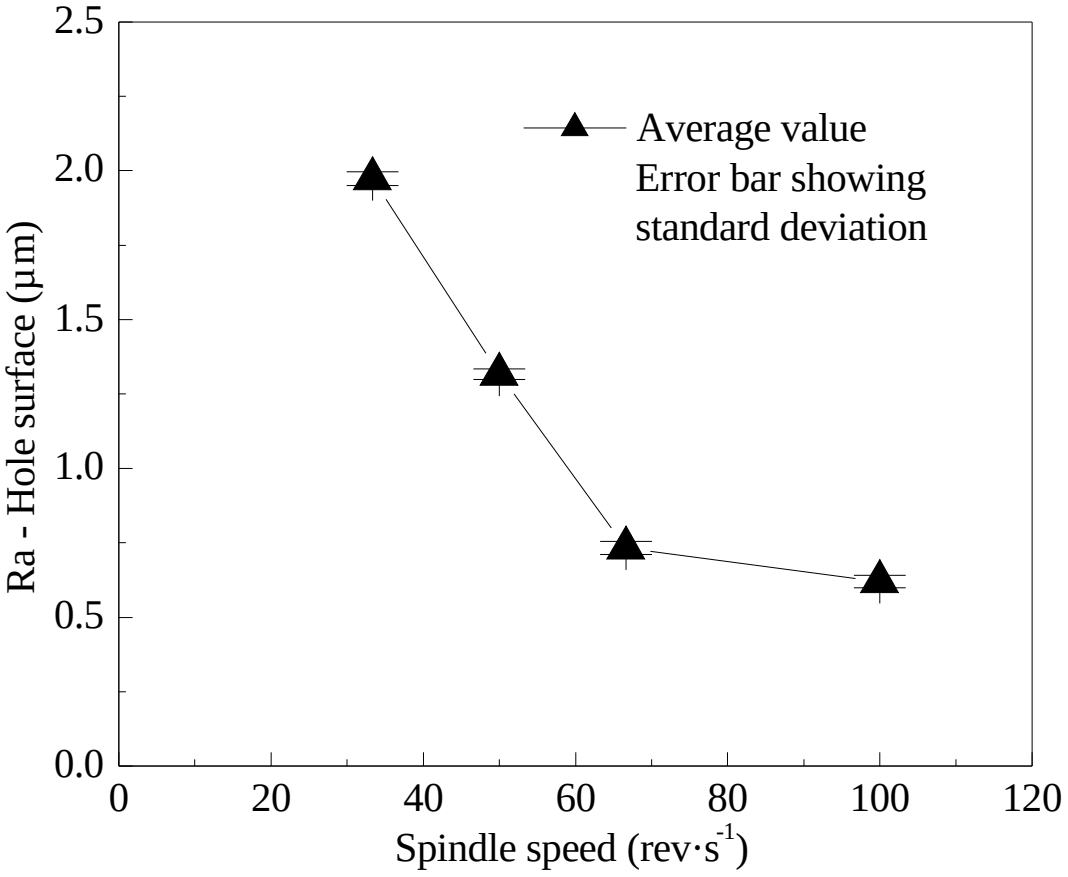

Figure 5.7 Effects of spindle speed on surface roughness measured on machined hole

5.2.3.1.1 ON SURFACE ROUGHNESS MEASURED ON MACHINED HOLE

The surface roughness curve for machined rod is depicted in Figure 5.8. The surface roughness becomes significantly lower as the spindle speed increases. This observation is consistent with those reported by Jiao et al. [2005] for rotary ultrasonic machining of

alumina. It is also observed that the rate of decrease of surface roughness decreases with the increase in spindle speed. Compared with the machined hole, the surface roughness observed on the rod is lower. It is concluded that spindle speed has significant effects on surface roughness on the machined rod.

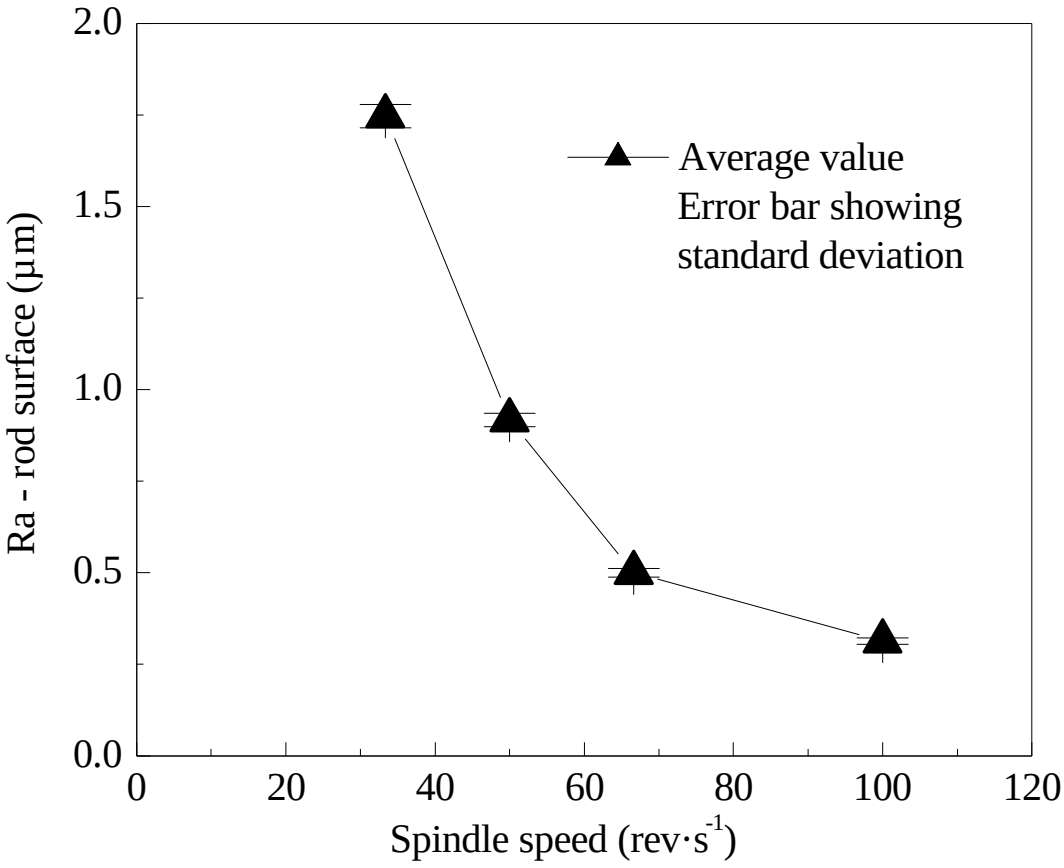

Figure 5.8 Effects of spindle speed on surface roughness measured on machined rod

5.2.3.2 FEEDRATE

The effects of feedrate on the machined hole surface roughness are depicted in Figure 5.9. The surface roughness measured on the hole increases significantly as the feedrate

increases. This is consistent with the results from the study of Jiao et al. [2005] for rotary ultrasonic machining of alumina.

The effects of feedrate on surface roughness on the machined rod are depicted in Figure 5.10. At lower feedrates, there is no significant increase in surface roughness as feedrate increases. However, at higher feedrates, the surface roughness increases significantly with feedrate. Comparison of surface roughness values shows that roughness values for the machined rod are lower than those for the machined hole.

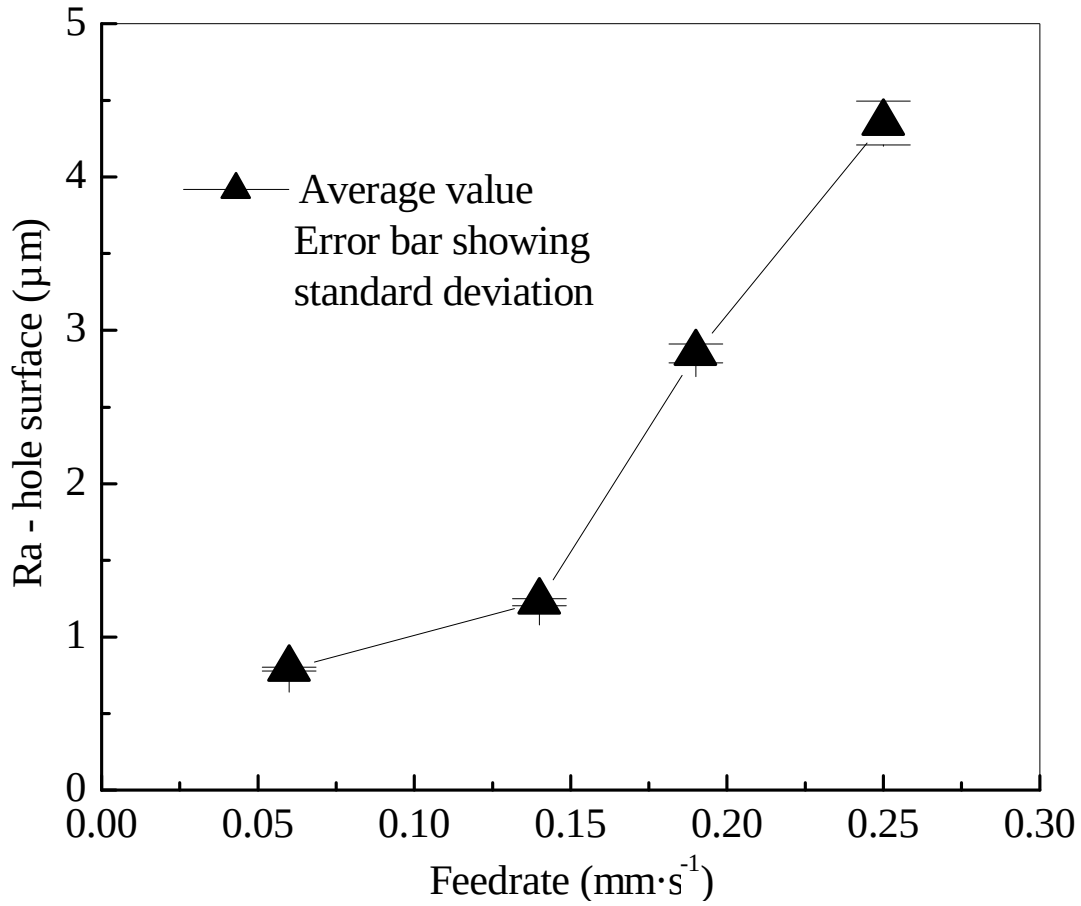

Figure 5.9 Effects of feedrate on surface roughness measured on machined hole

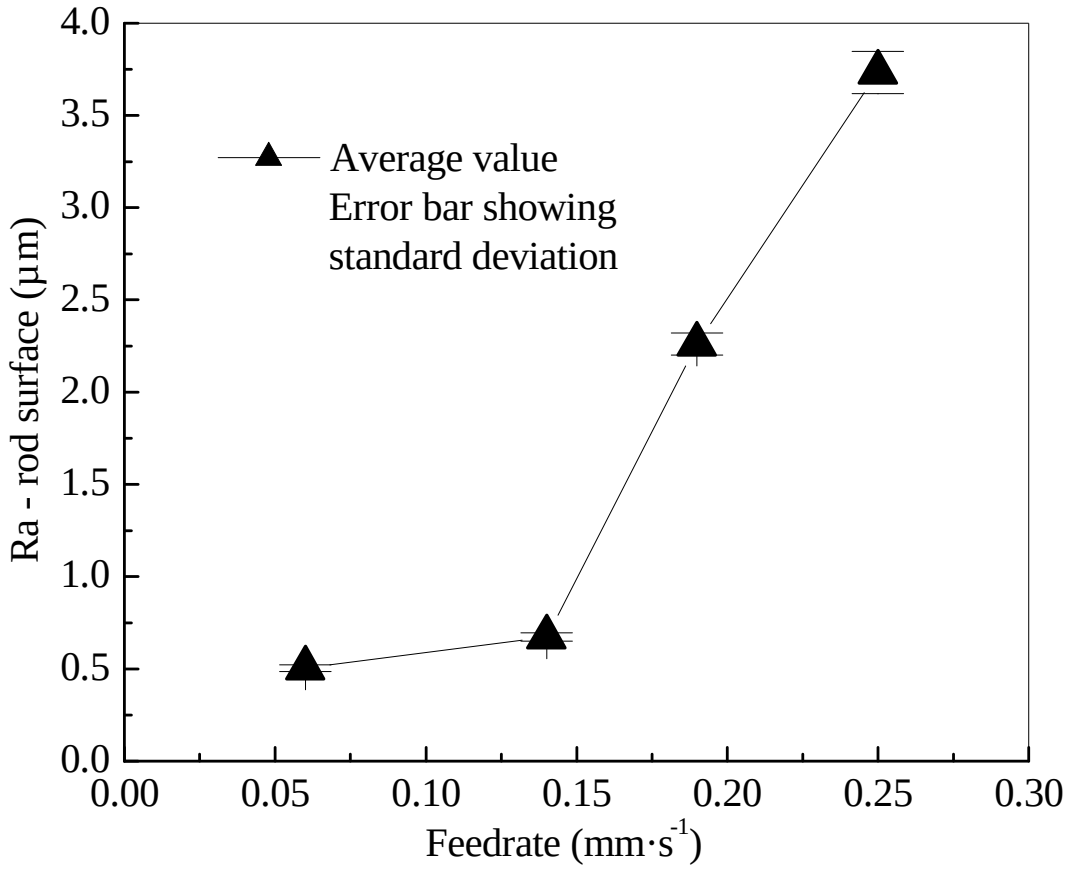

Figure 5.10 Effects of feedrate on surface roughness measured on machined rod

5.2.3.3 ULTRASONIC VIBRATION POWER

The effects of ultrasonic power on surface roughness measured on the machined hole are depicted in Figure 5.11. The surface roughness measured on the machined hole decreases significantly as the ultrasonic power increases. These results are consistent with those reported by Jiao et al. [2005] and Li et al. [2005] for rotary ultrasonic machining of alumina and technical glasses respectively.

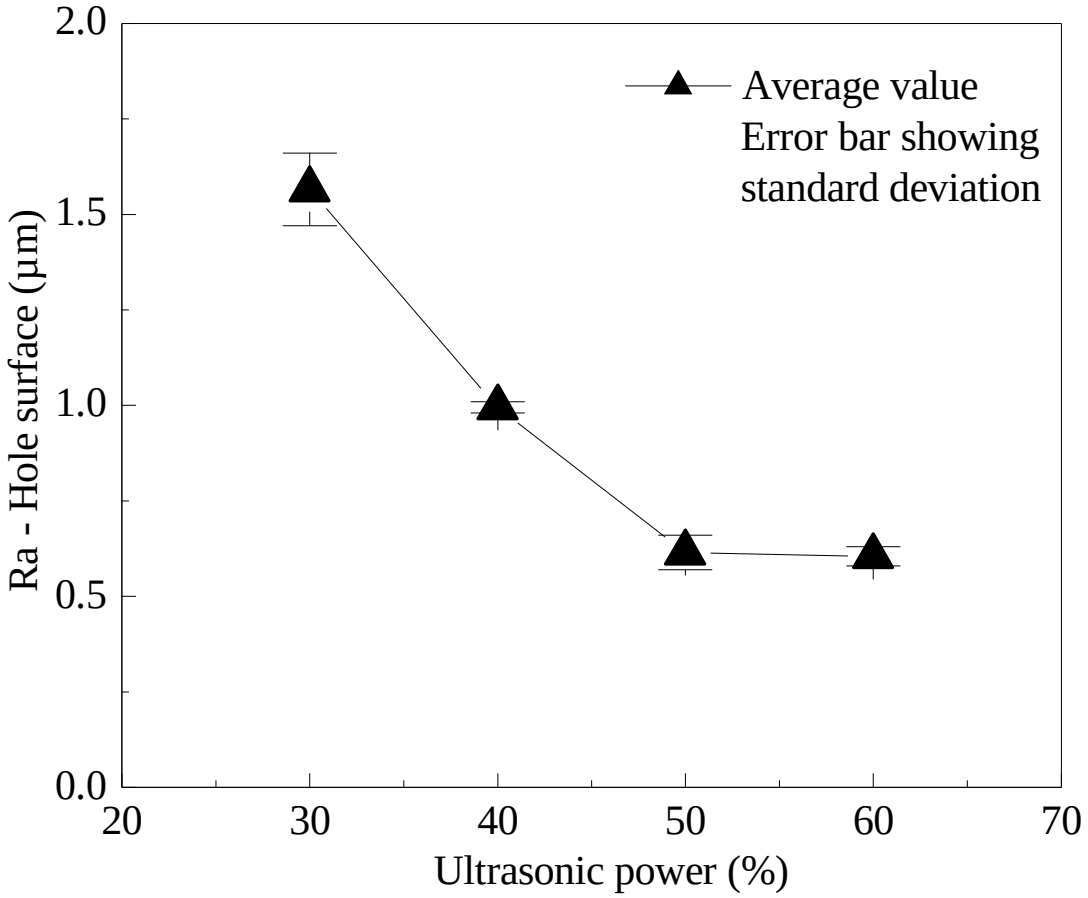

Figure 5.11 Effects of ultrasonic power on surface roughness measured on machined hole

5.2.3.4 ON SURFACE ROUGHNESS MEASURED ON MACHINED ROD

The effects of ultrasonic power on measured surface roughness measured on the machined rod are depicted in Figure 5.12. It is observed that as the ultrasonic power increases, the surface roughness measured on the rod surface decreases significantly.

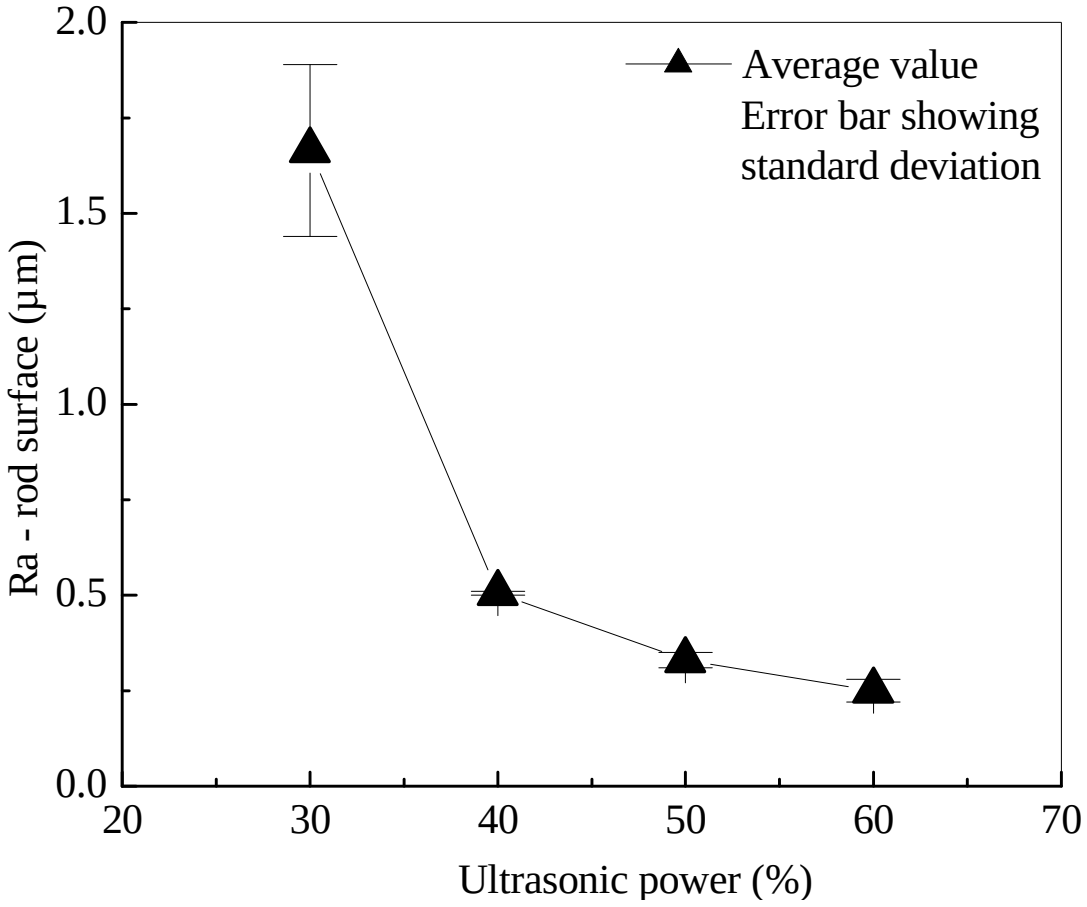

Figure 5.12 Effects of ultrasonic power on surface roughness measured on machined rod

5.3 SUMMARY

In this chapter, the effects of three machining variables (spindle speed, feedrate, and ultrasonic power) on three output variables (cutting force, MRR, and surface roughness) while rotary ultrasonic machining of a titanium alloy are studied. The following conclusions can be drawn from the study:

1) The spindle speed has significant effects on cutting force and surface roughness, but its effects on material removal rate are not significant. Cutting force and surface roughness decrease as the spindle speed increases.
2) The feedrate has significant effects on cutting force, material removal rate, and surface roughness. Cutting force, material removal rate, and surface roughness increase significantly as the feedrate increases.
3) The ultrasonic power has significant effects on cutting force and surface roughness, but its effects on material removal rate are not significant. Cutting force decreases initially and then increases as the ultrasonic power increases. Surface roughness decreases as the ultrasonic power increases.

CHAPTER 6

ROTARY ULTRASONIC MACHINING OF TITANIUM ALLOY: WHEEL WEAR MECHANISMS

6.1 EXPERIMENTAL CONDITIONS AND PROCEDURES

Table 6.1 shows the experimental conditions. Other conditions including workpiece material, machine, coolant and measurement equipment are the same as described in section 3.1. Seven different wheels were used and their specifications are shown in Table 6.2.

Table 6.1 Experimental conditions

Parameter	Unit	Value
Spindle speed	$rev \cdot s^{-1}$ (rpm)	67 (4000)
Feedrate	$mm \cdot s^{-1}$	0.06
Vibration power supply*	%	0 or 40
Vibration frequency	KHz	0 or 20

* Vibration power supply controls the amplitude of ultrasonic vibration.

Table 6.2 Specifications of the tools and testing conditions

Wheel	Slots	Grit size	Grain concentration	Bond type	Ultrasonic vibration
1	Yes	60/80	100	B	No
2	Yes	60/80	100	B	Yes
3	No	60/80	100	B	Yes
4	No	60/80	100	C	Yes
5	No	60/80	80	C	Yes
6	No	60/80	80	B	Yes
7	No	80/100	100	B	Yes

6.2 MEASUREMENT PROCEDURES

After each drilling test, the grinding wheel was removed from the machine for observation under a digital microscope (Olympus DVM-1, Olympus America Inc., New York, USA). The magnification of the digital microscope was from 50 to 200. The topography was observed on the end face of the wheel. In order to ensure that the same area of the wheel surface was observed every time, a special fixture was designed for holding the wheel.

6.3 WEAR MECHANISMS

6.3.1 ATTRITIOUS WEAR

Attritious wear [Malkin 1989] is referred to a type of wear where sharp edges of an abrasive grain become dull due to attrition by workpiece material, developing flat areas. The sharp edges of diamond grains are converted into dull or flat areas. Attritious wear increases the area of wear flats and determines the magnitude of the grinding force and quality of the ground surface. Attritious wear has been observed by Shi et al. [Shi and Malkin 2003] in grinding of hardened bearing steel with electroplated CBN wheels. Sathyanarayanan et al. [Satyanarayanan and Pandit 1985] conducted a study on attritious wear rates in grinding of steel.

Larger flat areas on diamond abrasives due to attritious wear were observed for every RUM tool tested. Figure 6.1 shows two examples of the attritious wear mechanism (marked in the circle). A certain amount of material is removed from the diamond grain making the top surface to be flat after a few drilling tests.

Wheel# 4

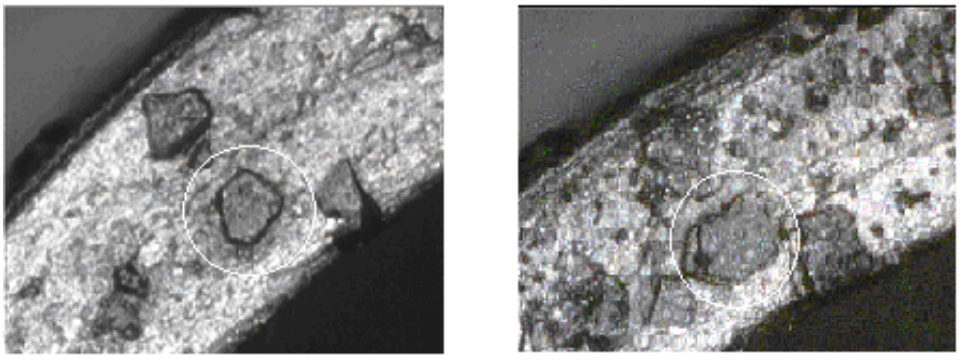

(a) Initial condition (b) After 5 drilling tests

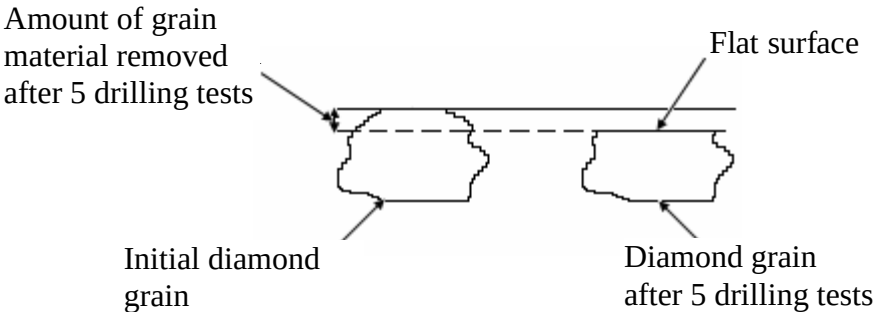

Wheel# 6

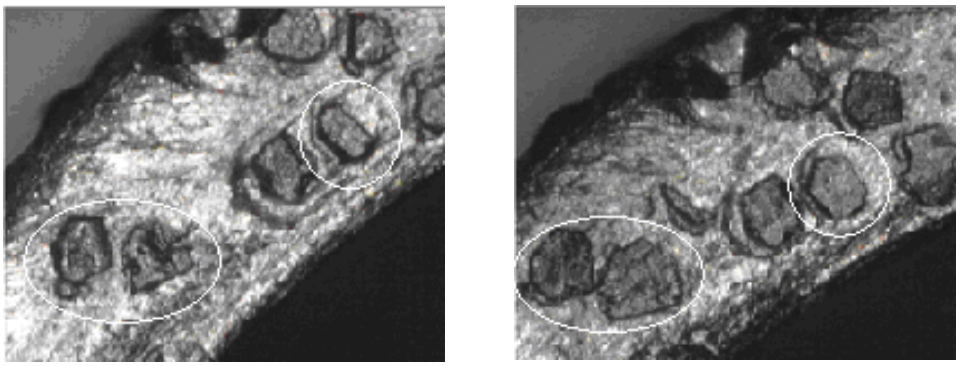

(a) Initial condition (b) After 4 drilling tests

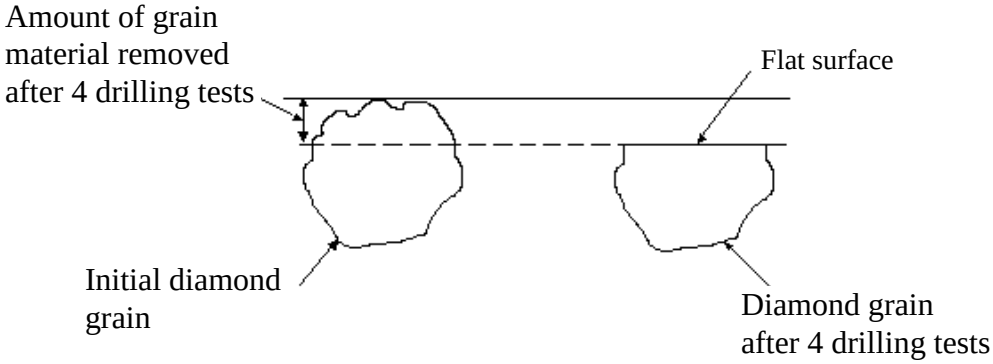

Figure 6.1 Attritious wear

6.3.2 GRAIN PULLOUT

Grain pullout has been observed by Cho et al. [Cho et al 1994] for grinding of Si3N4, ZrO2, SiC and Al_2O_3 with resin-bonded diamond wheels. Xie et al. [2003] observed this type of wear (grain pullout) during grinding of three tailored α-sialon microstructures. In the experiments of RUM of titanium alloy, many diamond grains on the wheels were dislodged prematurely, before completing their effective working lives. Figure 6.2 shows two examples of the grain pullout type wear mechanism. In these figures, it can be clearly observed that the diamond grain that is present in Figure 6.2 (a) (marked by circles) is seen to be dislodged in Figure 6.2 (b). A certain amount of metal bond material was removed leading to the grain to be completely pulled leaving a cavity in the metal bond after the next drilling test.

Wheel# 3

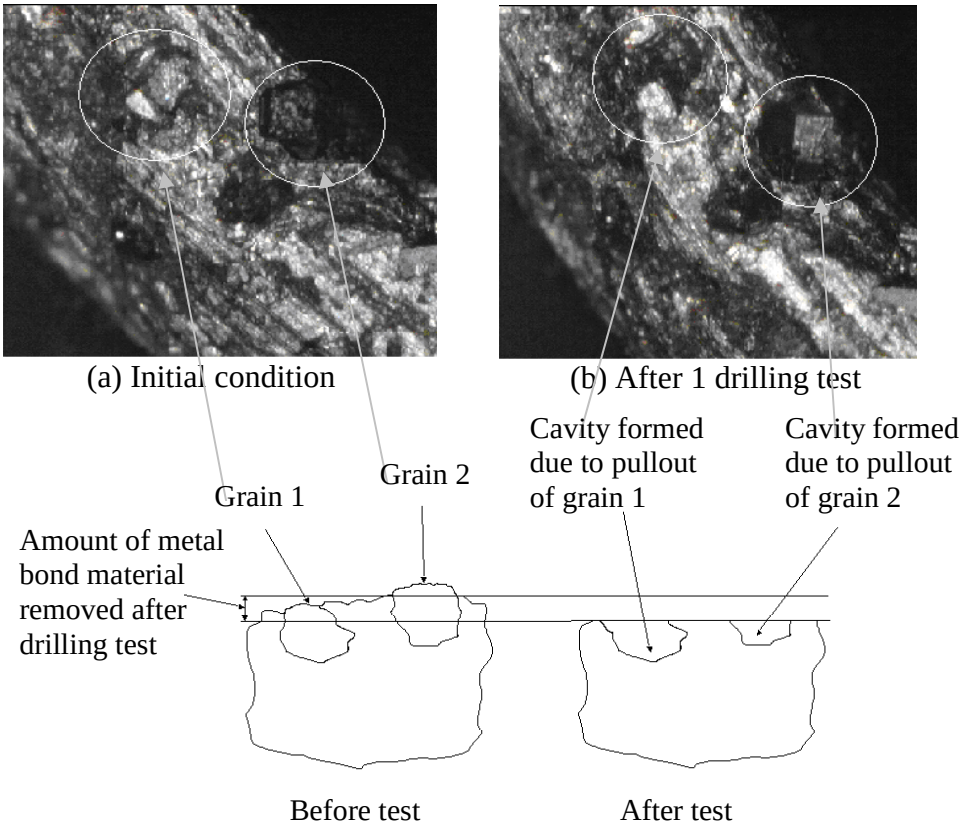

Wheel# 5

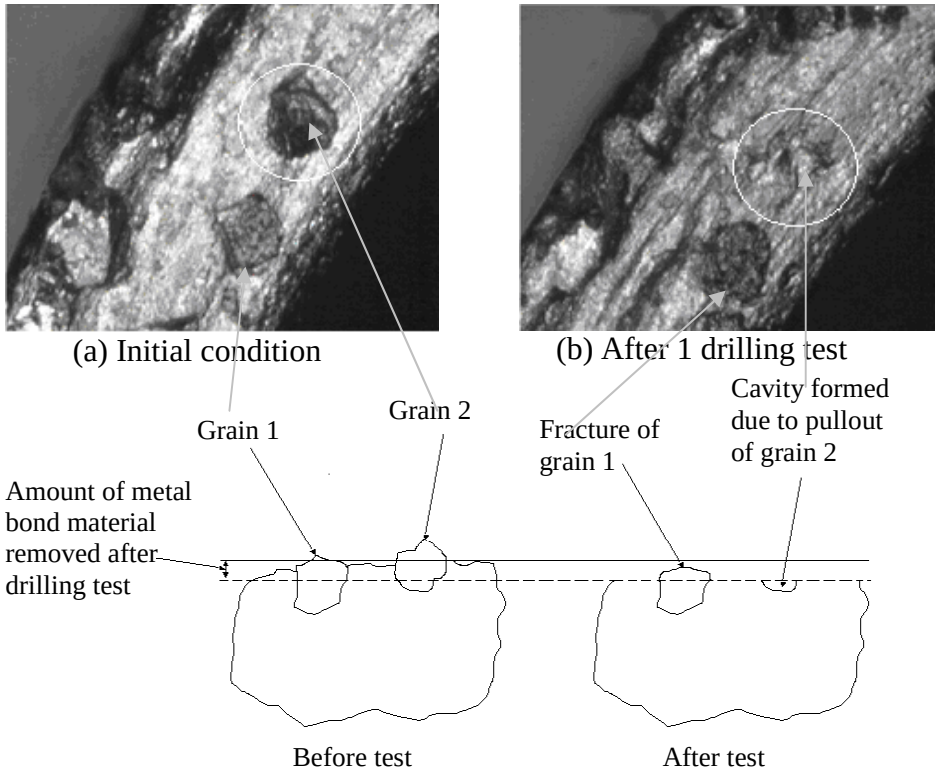

Figure 6.2 Diamond grain pullout

6.3.3 GRAIN FRACTURE

For grain fracture, the abrasive fragment is removed by fracture within the grain and the fractured area exposes new cutting edges [Malkin 1989]. Hagiwara et al. [1994] evaluated the grain fracture characteristics of diamond grains in stone grinding process. Shih and Akemon [2001].

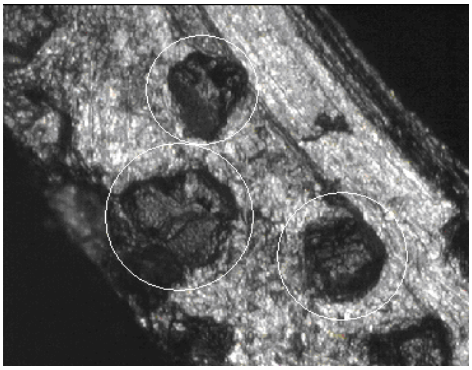

Wheel# 3

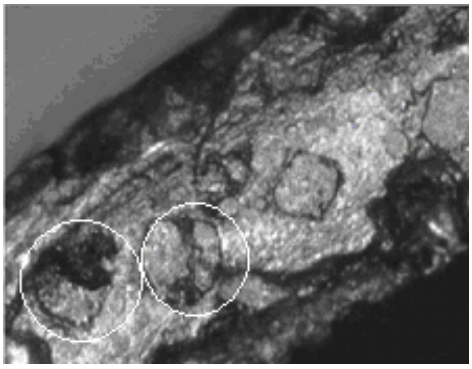

Wheel# 5

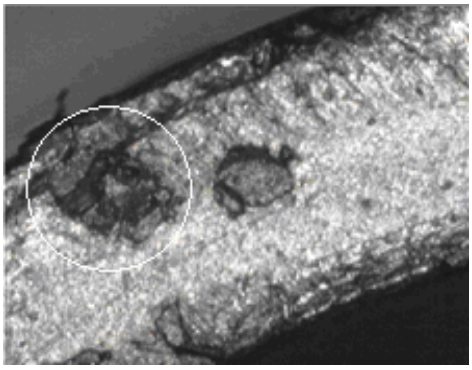

Wheel# 6

Figure 6.3 Diamond grain fracture

reported brittle fracture of diamond abrasives when vitreous-bond diamond wheels were trued using blade diamond tools.

Figure 6.3 shows the grain fracture type wear mechanism (marked by circles) on seven different wheels used in the investigation. It can be seen that the grains were cracked or their top surfaces were fractured abruptly. Abrupt grain surfaces and depressions on the grain surface are visible.

6.3.4 BOND FRACTURE

In this type of wear, the bond material is eroded [Malkin 1989]. The bond strength is reduced and diamond grain dislodgement is promoted due to bond fracture. Bond fracture is responsible for the self-sharpening of grinding wheels and loss of form and size of the grinding wheels. Shih and Akemon [2001] have reported fracture of vitreous-bond in diamond wheels when the wheels were trued by blade diamond tools.

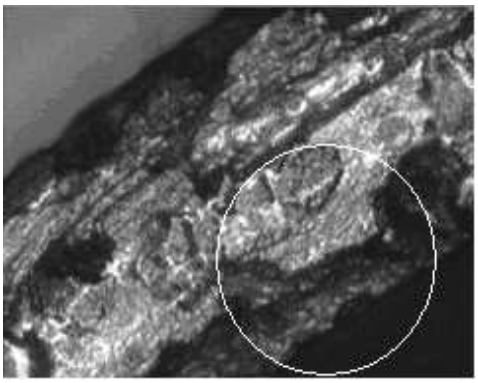

Wheel# 2

Wheel# 5

Figure 6.4 Metal bond fracture

Figure 6.4 shows two examples of the bond fracture type of wear mechanism (marked by circles). It can be observed that the majority of the bond fracture occurred along the edges of the wheel rather than towards the center.

6.3.5 CATASTROPHIC FRACTURE

Figure 6.5 shows some pictures of cracking of metal bond and diamond grains (marked by circles). They are also classified as catastrophic failure because they occur at macroscopic scale; the tool fails (or breaks) after occurrence of these types of failures. Figure 6.5 shows cracking of the metal bond. These cracks grew with the number of

drilled holes and eventually caused sudden failure (breakage) of the wheel. Cracking of metal bond is

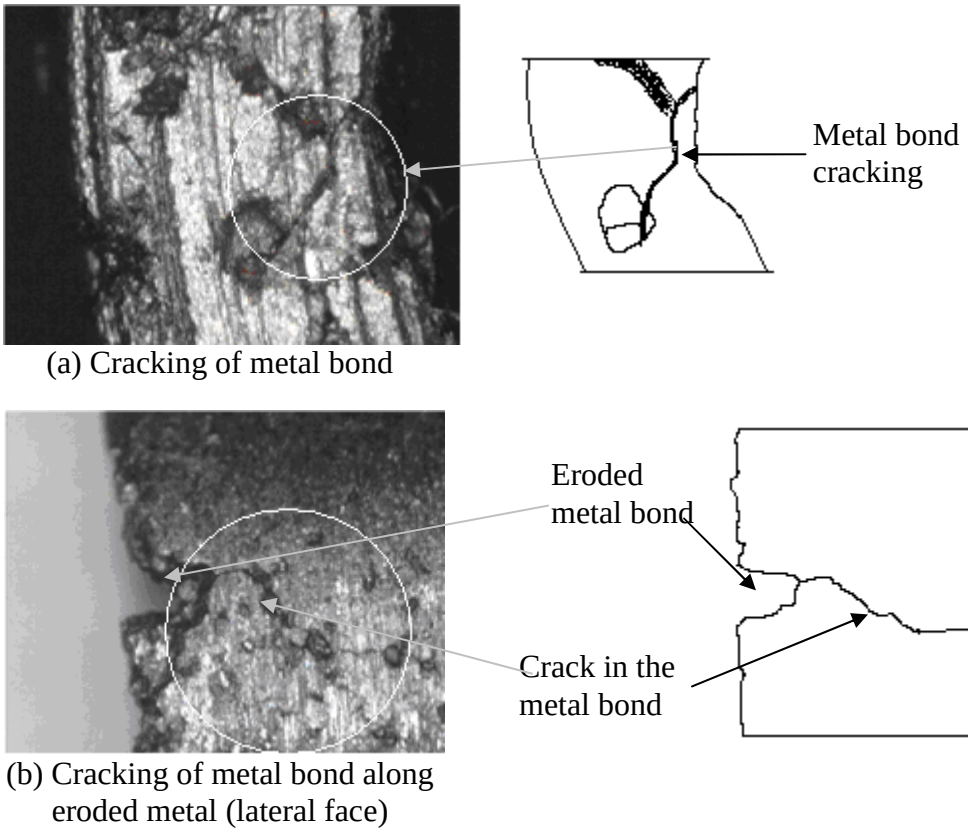

(a) Cracking of metal bond

(b) Cracking of metal bond along eroded metal (lateral face)

Figure 6.5 Cracking of metal bond

more undesirable than cracking of diamond grain because it has more significant effects on wheel life. The crack shown in Figure 6.5 (b) is for wheel # 5 after drilling 7 holes. This crack grew rapidly and the wheel failed while drilling the 8th hole. The catastrophic type of wear mechanism occurred only once during the whole set of experiments.

6.4 SUMMARY

Wheel wear mechanisms in RUM of titanium alloy (Ti-6Al-4V) have been studied by observing the topography of the end faces of metal-bond diamond wheels under a digital microscope. The following conclusions can be drawn:

1. Attritious wear, grain pullout, grain fracture, bond fracture, cracking of metal were observed in RUM of titanium alloy.

2. In RUM of titanium alloy, more severe bond fracture and grain pullout were observed on the edges of the wheel end face than at the center.

CHAPTER 7

ROTARY ULTRASONIC MACHINING OF SILICON CARBIDE

Literature review shows that no study on rotary ultrasonic machining of silicon carbide has been reported. This chapter presents an experimental study on designed experiments of RUM of SiC. A two-level four-factor experimental design has been employed to study the effects of spindle speed, ultrasonic power, feedrate and grit size on the cutting force, chipping size and surface roughness. Other conditions including machine, coolant and measurement equipment are the same as described in section 3.1.

7.1 EXPERIMENTAL CONDITIONS AND PROCEDURES

7.1.1 SETUP AND CONDITIONS

Table 7.1. Properties of silicon carbide (SiC)

Property	Unit	Value
Tensile strength	MPa	3440
Thermal conductivity	$W \cdot m^{-1} \cdot K^{-1}$	120
Melting point	K	56
Density	$Kg \cdot m^{-3}$	3100
Coefficient of thermal expansion	$in \cdot in^{-1} F^{-1}$	2.2×10^{-6}
Vickers hardness		2150

The workpiece material was silicon carbide (SiC) provided by Saint-Gobain Ceramics (Niagara Falls, N.Y). The size of workpiece was 120 mm × 50 mm × 6 mm. Table 7.1 shows the properties of silicon carbide.

7.1.2 DESIGN OF EXPERIMENTS

A 2^4 (two-level four-factor) full factorial design was employed. There were 16 unique experimental conditions. Based on preliminary experiments and due to the limitations of the experimental set-up, the following four process variables were studied:

- Spindle speed: rotational speed of the core drill.
- Ultrasonic power: percentage of power from ultrasonic power supply, which controls the ultrasonic vibration amplitude.
- Feedrate: feedrate of the core drill.
- Grit size: abrasive particle size of the core drill.

Table 7.2 shows the low and high levels of the process variables. Test matrix is shown in Table 7.3. The high and low levels of the process variables were determined according to the preliminary experiments. Furthermore, considering the variations associated with ceramic machining experiments, two tests were conducted for each of the 16 unique experiment conditions, bringing the total number of tests to 32. The output variables studied include cutting force, surface roughness, and chipping size.

Table 7.2 Low and high levels of process variables

Process Variable	Unit	Low level (−)	High level (+)
Spindle speed	$rev \cdot s^{-1}$	33.3	66.6
Feedrate	$mm \cdot s^{-1}$	0.008	0.015
Ultrasonic power*	%	25	50
Grit size	mesh	60/80	80/100

* To control ultrasonic vibration amplitude.

Table 7.3 Test matrix

Test #	Test order		Spindle speed	Vibration power	Feedrate	Grit size
	Test 1	Test 2				
1	1	14	-	-	-	-
2	10	8	+	-	-	-
3	4	3	-	+	-	-
4	5	16	+	+	-	-
5	3	10	-	-	+	-
6	7	2	+	-	+	-
7	2	9	-	+	+	-
8	16	15	+	+	+	-
9	6	1	-	-	-	+
10	12	11	+	-	-	+
11	11	5	-	+	-	+
12	13	12	+	+	-	+
13	9	4	-	-	+	+
14	8	7	+	-	+	+
15	15	6	-	+	+	+
16	14	13	+	+	+	+

A digital video microscope of Olympus DVM-1 (Olympus America Inc., Melville, NY, US) was utilized to inspect the chippings at the exit side of the machined hole. The hole quality is quantified by the size of the edge chipping formed on the machined rod as illustrated in Figure 7.1. The chipping size was measured with a vernier caliper (Mitutoyo IP-65, Mitutoyo Corporation, Kanagawa, Japan).

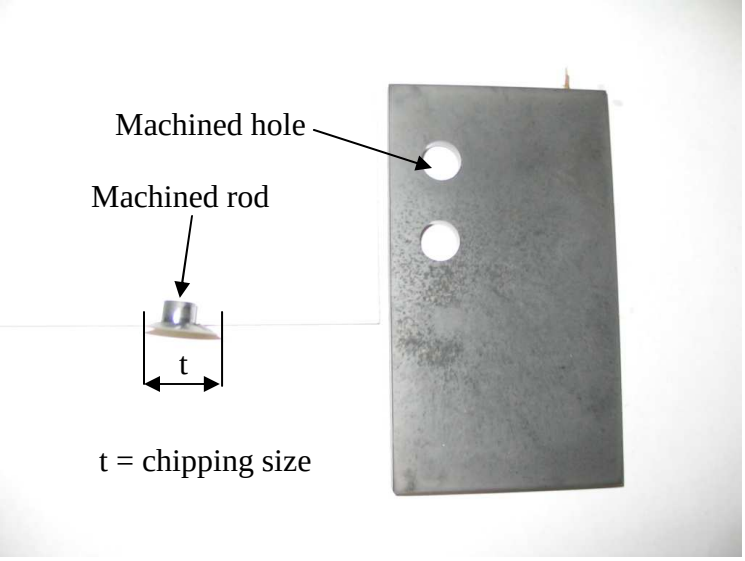

Figure 7.1 Illustration of chipping size

7.2 EXPERIMENTAL RESULTS

Table 7.4 displays the experimental data. The software called MINITAB Statistical Software (Version 13.31, Minitab Inc., State College, PA, USA) was used to process the data and to obtain the main effects, two-factor interaction and three-factor interaction effects. Geometric representations of these effects are presented in Figs. 7.2-7.7. Analysis of variance (ANOVA) has been conducted to determine the significance of each effect. However, ANOVA tables are omitted in this chapter.

Table 7.4 Experimental results

Test #	Cutting force (N)		Chipping size (mm)		Surface roughness Ra (μm)	
	Test 1	Test 2	Test 1	Test 2	Test 1	Test 2
1	1400	1350	14	16	0.38	0.40
2	1010	980	10	11	0.32	0.35
3	1230	1205	16	18	0.33	0.37
4	990	950	13	12	0.27	0.29
5	1930	1965	17	16	0.49	0.51
6	1420	1450	15	17	0.41	0.43
7	2120	2145	20	22	0.41	0.42
8	1650	1710	19	20	0.36	0.38
9	1290	1230	13	13	0.29	0.29
10	970	950	9	10	0.24	0.27
11	1090	1060	14	13	0.25	0.27
12	850	900	12	14	0.23	0.23
13	1810	1770	15	16	0.38	0.40
14	1340	1390	14	14	0.36	0.37
15	2080	2180	17	16	0.34	0.37
16	1340	1310	15	16	0.30	0.33

7.2.1 MAIN EFFECTS

7.2.1.1 ON CUTTING FORCE

The main effects of the four process variables (spindle speed, feedrate, vibration power, and grit size) on cutting force are shown in Figure 7.2. The effect of feedrate is the most significant (with P-value = 0.031). The secondly significant effect is spindle speed (P-value = 0.045). It can be seen that, as spindle speed decreases and feedrate increases, cutting force will increase. These trends are consistent with those observed by Jiao et al. [2005] for RUM of alumina and by Li et al. [2005] for RUM of ceramic matrix composites.

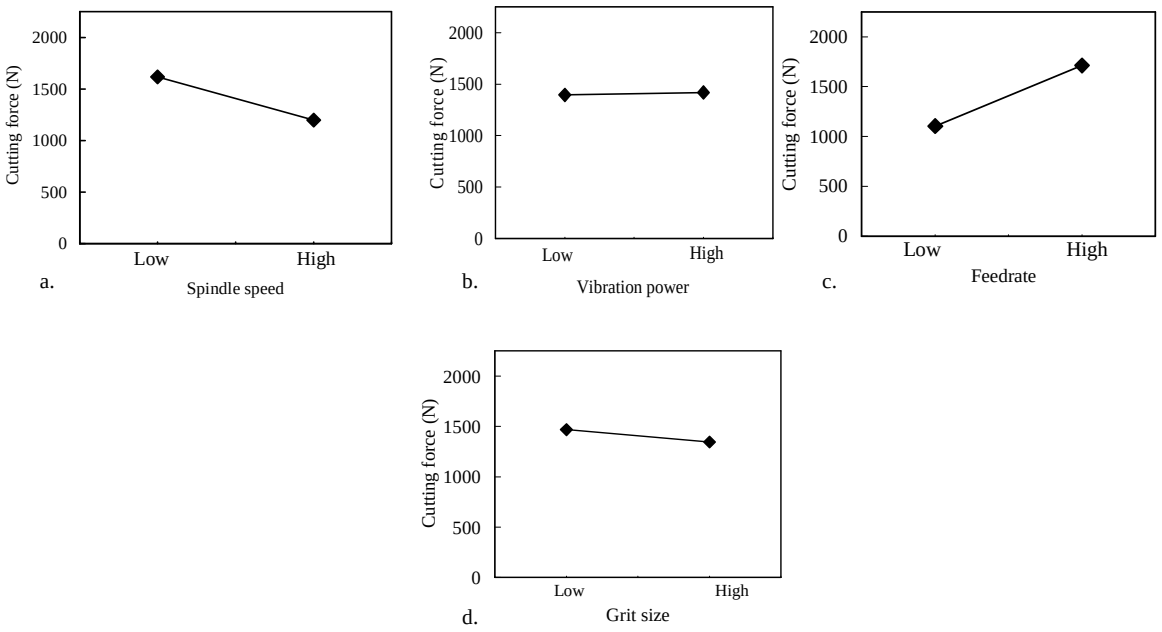

Figure 7.2 Main effects on cutting force

7.2.1.2 ON SURFACE ROUGHNESS

The main effects of the four process variables (spindle speed, feedrate, vibration power and grit size) on surface roughness are shown in Figure 7.3. The effect of feedrate is the most significant (with P-value = 0.069). The secondly significant effect is grit size (P-value = 0.087) followed by spindle speed (P-value = 0.132), and vibration power (P-value = 0.132). As it can be seen, surface roughness (Ra) decreases as spindle speed, vibration power and grit size increases, and as feedrate decreases. These trends are consistent with those reported by Jiao et al. [2005] for RUM of alumina.

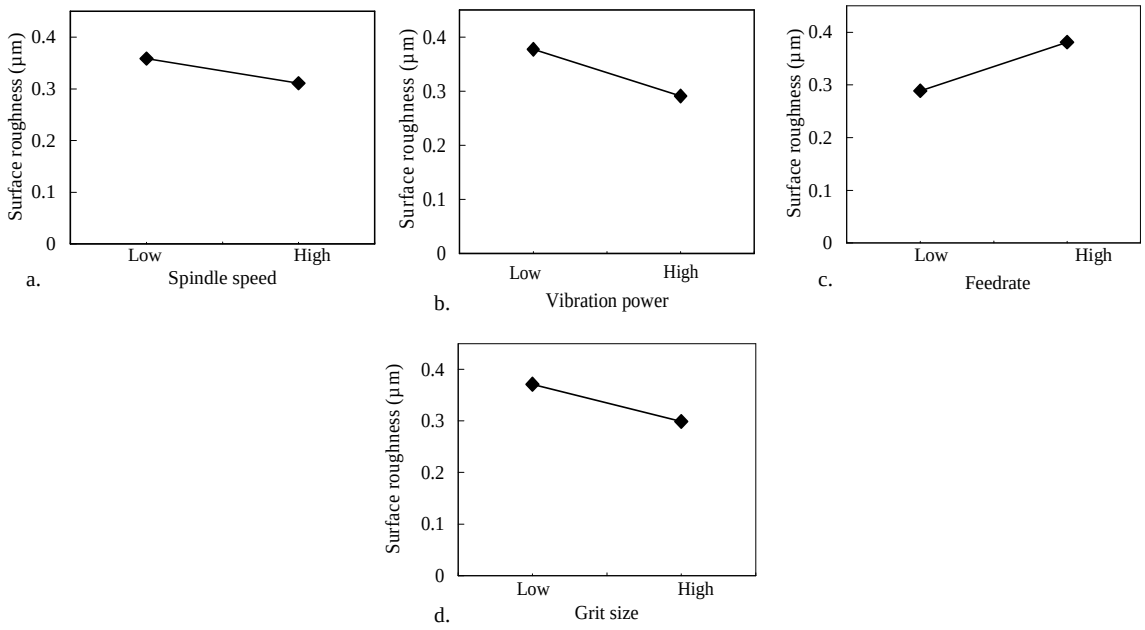

Figure 7.3 Main effects on surface roughness

7.2.1.3 ON CHIPPING SIZE

The main effects of the four process variables (spindle speed, feedrate, vibration power and grit size) on chipping size are shown in Figure 7.4. The effect of feedrate is the most significant (with P-value = 0.061). The secondly significant effects are spindle speed and vibration power (both have P-value = 0.1). As it can be seen, as spindle speed and grit size increase, or feedrate decreases, chipping size decreases. These trends are consistent with those reported by Jiao et al. [2005] for RUM of alumina and by Li et al. [2005] for RUM of ceramic matrix composite.

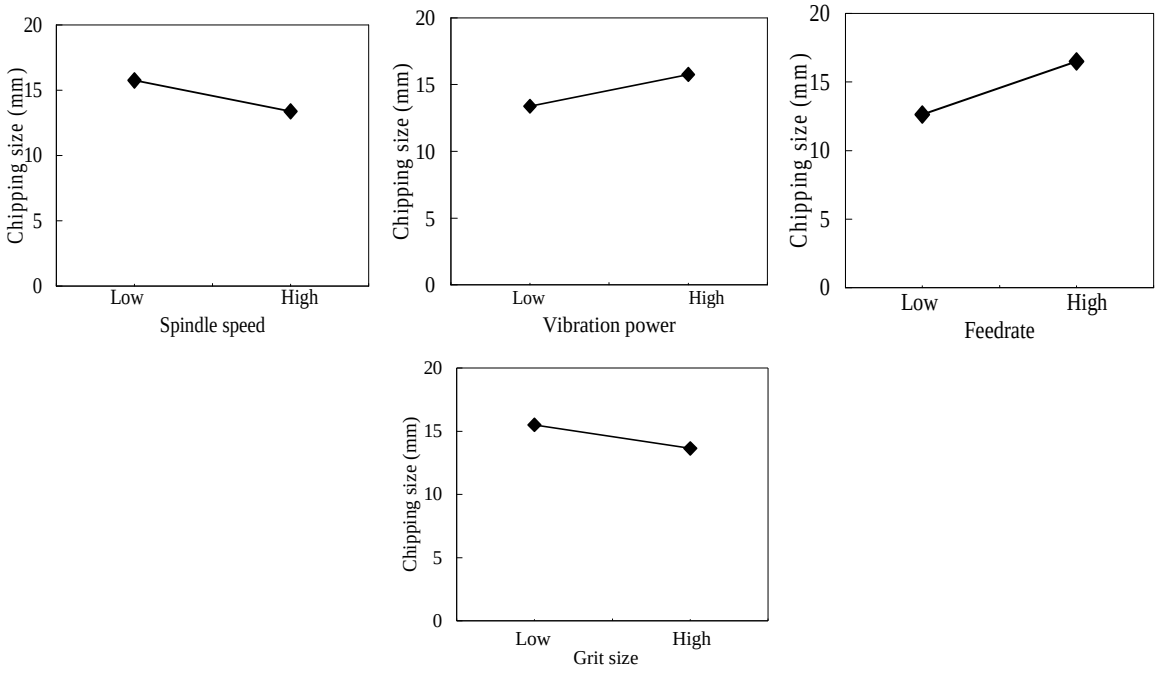

Figure 7.4 Main effects on chipping size

7.2.2 TWO FACTOR INTERACTIONS

7.2.2.1 ON CUTTING FORCE

For the four-factor two-level factorial design, 6 two-factor interactions can be obtained. The results are shown in Figure 7.5. The interactions between spindle speed and feedrate (P-value = 0.15) as shown in Figure 7.5 (b), between vibration power and feedrate (P-value = 0.126) as shown in Figure 7.5 (d), between vibration power and grit size (P-value = 0.151) as shown in Figure 7.5 (e), are significant on cutting force at a significance level of $\alpha = 0.2$.

As shown in Figure 53(b), at the high level of feedrate, the change of spindle speed causes a larger change in cutting force than at the low level of feedrate. As shown in Figure 53(d), at

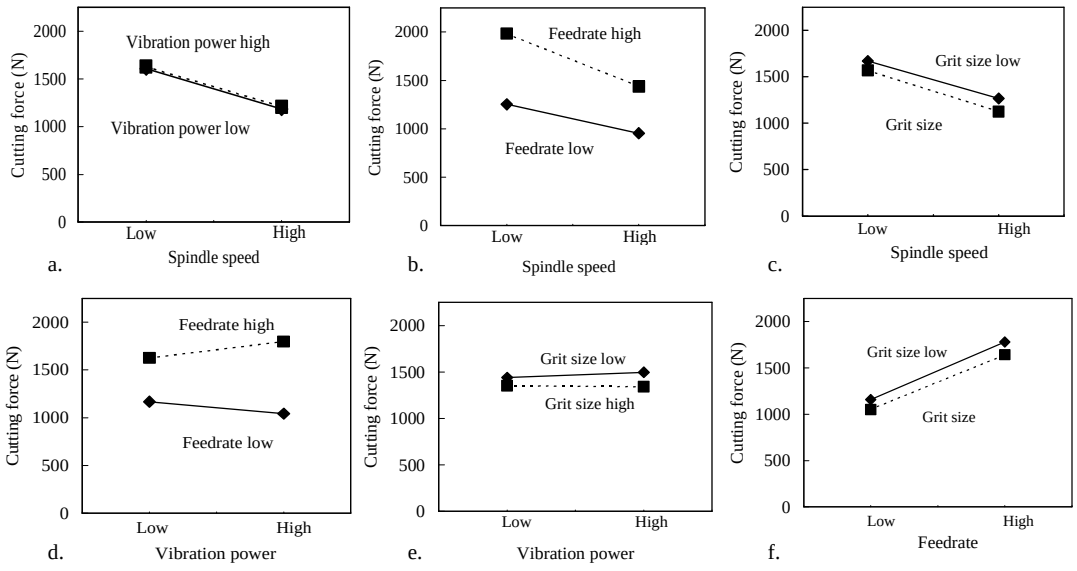

Figure 7.5 Two-factor interactions on cutting force

the high level of feedrate, the cutting force increases with the change of vibration power from low level to high level, whereas, at the low level of feedrate, the cutting force decreases with the change of vibration power from low level to high level. As shown in Figure 7.5 (e), at low level of grit size, the cutting force increases with change of vibration power from low level to high level, whereas, at high level of grit size, the cutting force remains about the same with change of vibration power from low level to high level.

7.2.2.2 ON SURFACE ROUGHNESS

The 6 two-factor interaction effects on surface roughness are shown in Figure 7.6. The interaction effect between spindle speed and grit size (P-value = 0.174) as shown in Figure 7.6 (c) is significant at a significance level of $\alpha = 0.2$. It can be seen that at the low level of grit size, the change of spindle speed causes a larger change in surface roughness than at the high level of grit size.

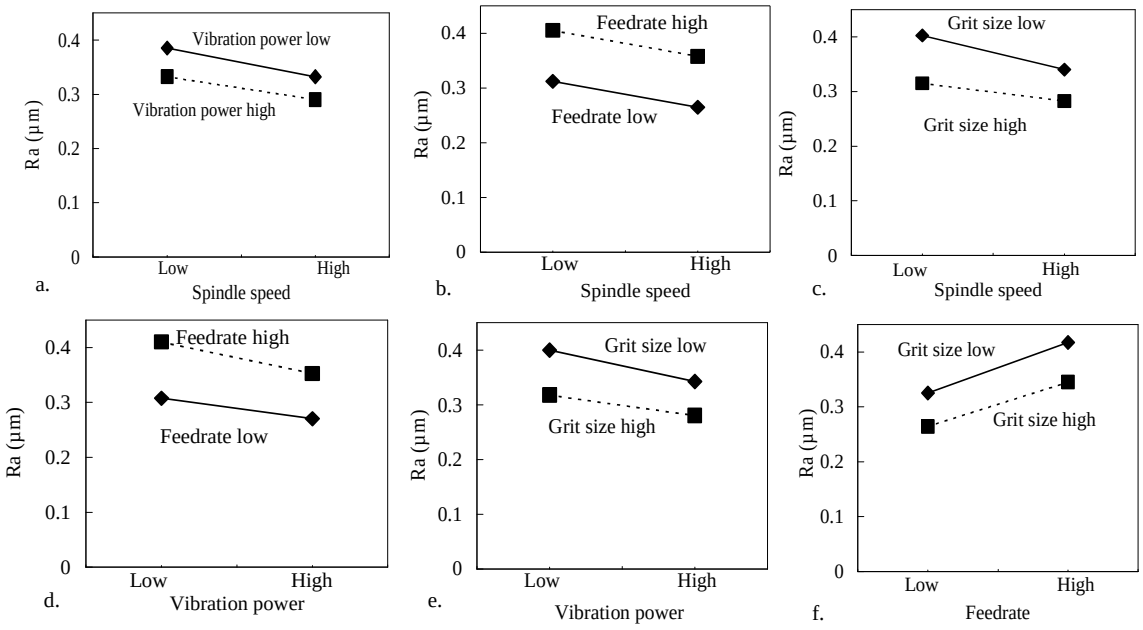

Figure 7.6 Two factor interactions on surface roughness

7.2.2.3 ON CHIPPING SIZE

The 6 two-factor interaction effects on chipping size are shown in Figure 7.7. The interaction effect between spindle speed and vibration power (P-value = 0.2) as shown in Figure 7.7 (a) is significant at a significance level of $\alpha = 0.2$.

It can be seen that at the high level of vibration power, the change of spindle speed causes a smaller change in chipping size than at the low level of vibration power.

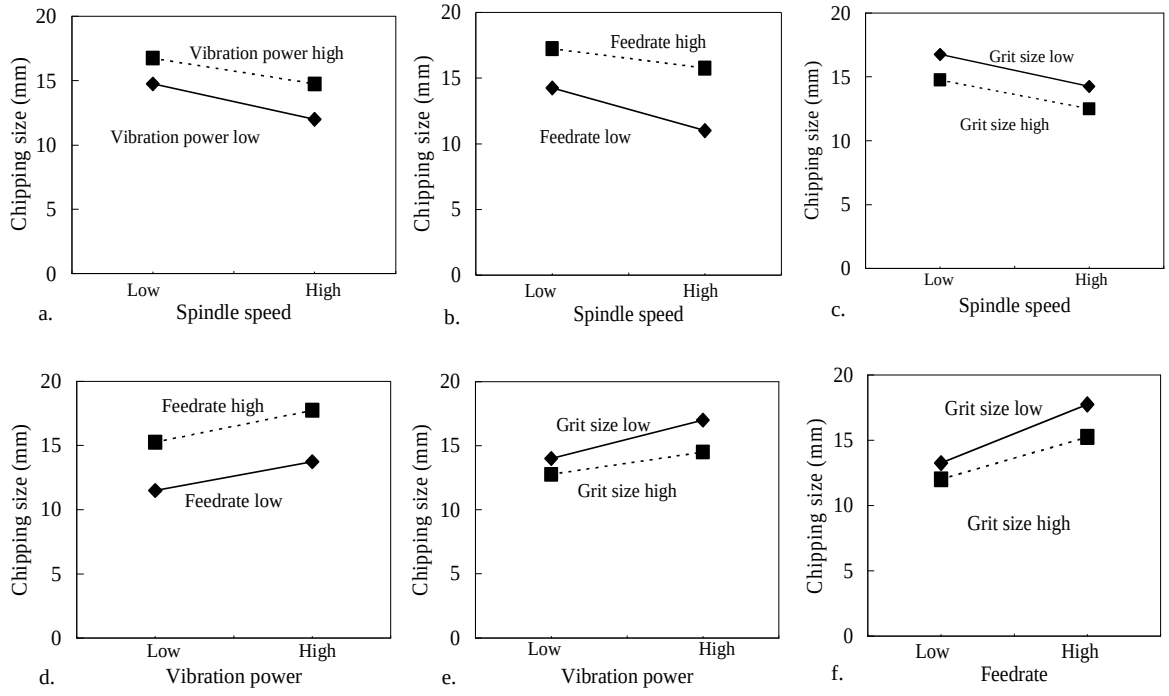

Figure 7.7 Two-factor interactions on chipping size

7.2.3 THREE FACTOR INTERACTIONS

At the significance level of $\alpha = 0.3$, none of the three-factor interactions is significant. Therefore, their geometric representations and discussion are omitted in the chapter.

7.3 SUMMARY

A four-factor two-level factorial design is used to study the relationships between the outputs (cutting force, surface roughness, and chipping size) and the four process variables (spindle speed, feedrate, vibration power, and grit size). The following conclusions are drawn from this study:

1) The main effects of spindle speed and feedrate have significant effects ($\alpha = 0.05$) on the cutting force. As spindle speed decreases and feedrate increases, cutting force increases.
2) Spindle speed, vibration power, feedrate, and grit size have significant effects on surface roughness. Surface roughness decreases as spindle speed, vibration power and grit size increases, and as feedrate decreases.
3) Spindle speed, feedrate, and vibration power have significant effects on chipping size. As spindle speed and grit size increase, or feedrate and vibration power decrease, chipping size decreases.
4) Some of the two-factor interactions are also significant.

CHAPTER 8

ROTARY ULTRASONIC MACHINING OF DENTAL CERAMICS

This chapter presents an experimental study on designed experiments of RUM of dental ceramics. Literature review shows that no study on rotary ultrasonic machining of dental ceramics has been reported. The effects of spindle speed, feedrate and ultrasonic vibration power on cutting force, surface roughness and chipping size have been reported.

8.1 EXPERIMENTAL CONDITIONS

Macor panels (Corning Incorporated, Macor products Group, Corning NY, USA) (55 mm × 55 mm × 4.5 mm) were used in this study. The composition of the material is shown in Table 8.1. The mechanical properties of macor are listed in Table 8.2. Other conditions including machine, coolant and measurement equipment are the same as described in section 3.1.

Table 8.1 Composition of macor [after Noort, 2004]

Compound	Approximate weight %
SiO_2	46
MgO	17
Al_2O_3	16
K_2O	10
B_2O_3	7
F	4

Table 8.2 Mechanical properties of macor [after Noort, 2004]

Property	Value
Density	2.52 g/cm^3
Young's Modulus (at 25° C)	66.9 GPa
Poisson's Ratio	0.29
Shear Modulus (at 25° C)	25.5 GPa
Rockwell Hardness	48
Modulus of Rupture (at 25° C)	94 MPa
Compressive Strength	345 MPa
Fracture Toughness	1.53 MPa m$^{0.5}$

The process parameters that were investigated were spindle speed (rotational speed of the diamond core drill), feedrate (linear velocity of the drill in the direction normal to the workpiece surface), and ultrasonic vibration power (percentage of electrical power, which controls the amplitude of ultrasonic vibration). Four different levels of these process parameters were studied. One parameter was varied at a time keeping the other two parameters constant. The order of the RUM tests was randomized. The values of the parameters for the feasibility experiments are presented in Table 8.3.

Table 8.3 Experimental conditions

Test #	Spindle speed ($rev \cdot s^{-1}$)	Feedrate ($mm \cdot s^{-1}$)	Ultrasonic power (%)
1	2000	0.0635	40
2	3000	0.0635	40
3	4000	0.0635	40
4	5000	0.0635	40
5	4000	0.0635	40
6	4000	0.138	40
7	4000	0.1957	40
8	4000	0.2475	40
9	4000	0.0635	20
10	4000	0.0635	30
11	4000	0.0635	40
12	4000	0.0635	50

8.2 EXPERIMENTAL RESULTS

8.2.1 EFFECTS ON CUTTING FORCE

8.2.1.1 SPINDLE SPEED

Figure 8.2 shows the cutting force curve as spindle speed increases. It is observed that the cutting force decreases with the increase in spindle speed. This finding is consistent with that by Jiao et al. [2005] for alumina and that by Churi et al. [2006] for silicon carbide. However, Li et al. [2005] reported that the cutting force increased with the increase of spindle speed when RUM of ceramic matrix composite (CMC).

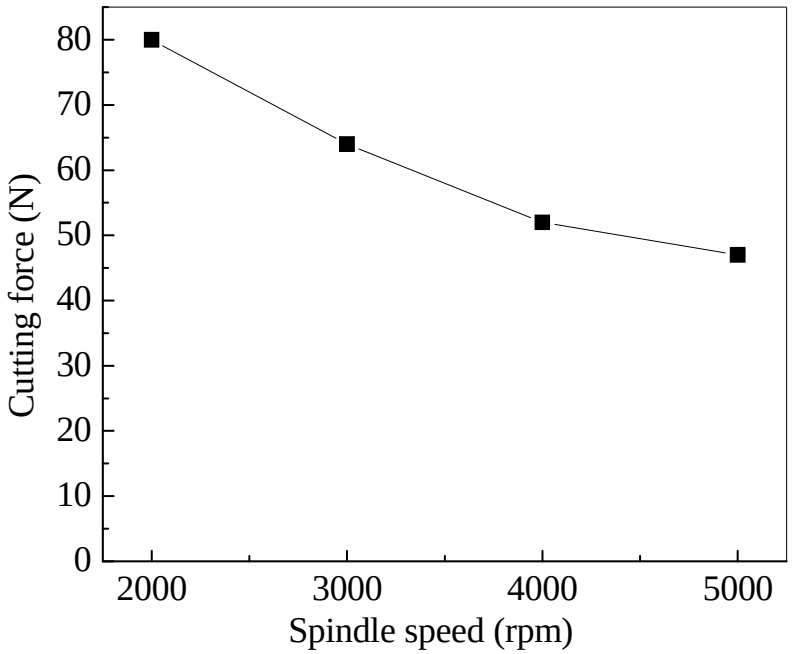

Figure 8.2 Cutting force vs. spindle speed

8.2.1.2 FEEDRATE

Figure 8.3 shows the cutting force curve as feedrate increases. It can be seen that the cutting force increases with the increase in feedrate. This result is consistent with those reported by Jiao et al. [2005] for alumina, by Churi et al. [2006] for silicon carbide, and by Li et al. [2005] for CMC.

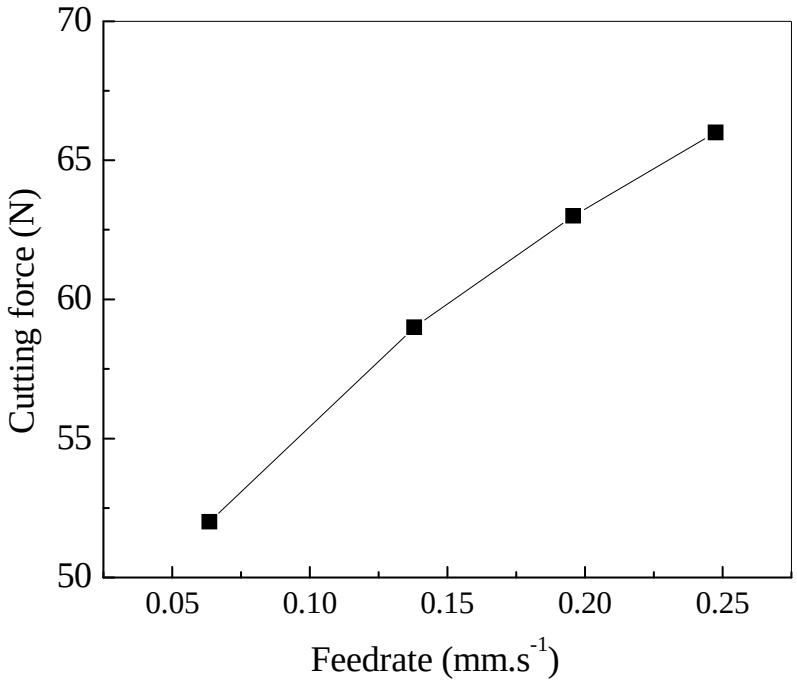

Figure 8.3 Cutting force vs. feedrate

8.2.1.3 ULTRASONIC VIBRATION POWER

Figure 8.4 shows the cutting force curve as ultrasonic vibration power increases. It is observed that the cutting force reduces when the ultrasonic vibration power increases from 20 % to 30 %, then remains almost stable when the ultrasonic power changes from 30 % to 40 %, and then starts increasing with the increase in ultrasonic vibration power. This result is different from those reported by others on RUM of different materials. As ultrasonic vibration power increased, the cutting force decreased for alumina [2005], increased for CMC [2005], and did not vary much for silicon carbide [2006].

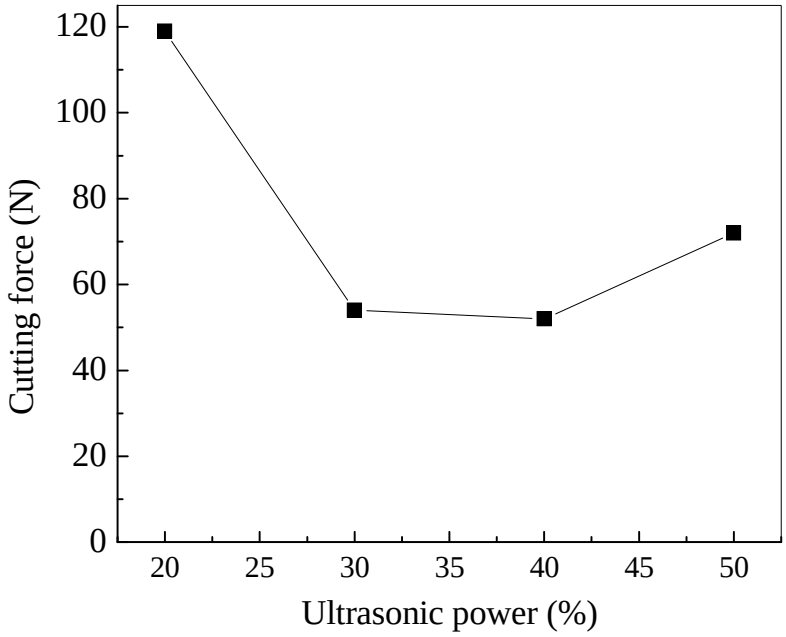

Figure 8.4 Cutting force vs. ultrasonic power

8.2.2 EFFECTS ON SURFACE ROUGHNESS

8.2.2.1 SPINDLE SPEED

Figure 8.5 shows the surface roughness curve as spindle speed increases. It can be observed that the surface roughness decreases when the spindle speed increases from 2000 rpm to 3000 rpm, then it increases with the increase in spindle speed from 3000 rpm to 5000 rpm. These findings are different from those reported by Jiao et al. [2005] for alumina and Churi et al. [2006] for silicon carbide. Both Jiao et al. [2005] and Churi et al. [2006] reported that the surface roughness decreased with the increase in spindle speed.

8.2.2.2 FEEDRATE

Figure 8.6 shows the surface roughness curve as feedrate increases. It can be seen that the surface roughness increases as the feedrate increases from 0.06 to 0.14 $mm \cdot s^{-1}$, then decreases as feedrate increases from 0.06 to 0.25 $mm \cdot s^{-1}$. These findings are different from those reported by Jiao et al. [2005] for alumina and Churi et al. [2006] for silicon carbide. They stated that the surface roughness increased with the increase in feedrate.

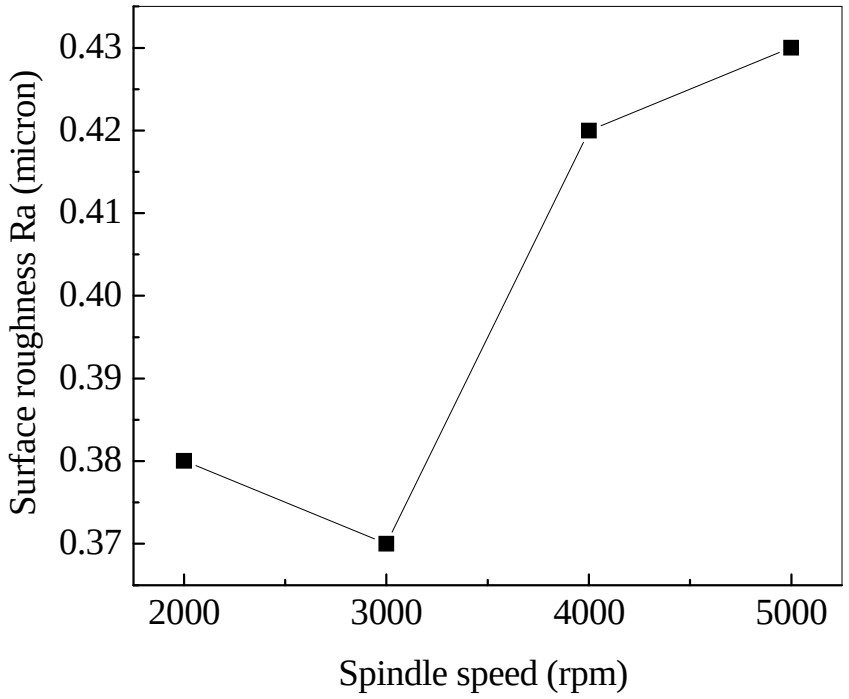

Figure 8.5 Surface roughness vs. spindle speed

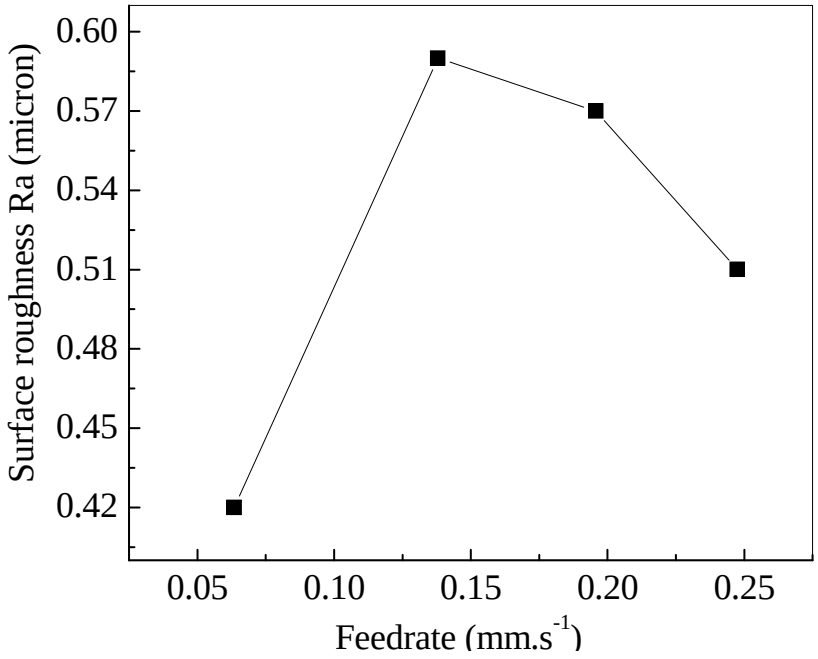

Figure 8.6 Surface roughness vs. feedrate

8.2.2.3 ULTRASONIC VIBRATION POWER

Figure 8.7 shows the surface roughness curve as ultrasonic vibration power increases. It is observed that the surface roughness increases rapidly when ultrasonic vibration power increases from 20% to 40%, and then decreases. This implies that there exists an ultrasonic vibration power level at which the surface roughness is minimum. These findings are different from those reported by Jiao et al. [2005] for alumina and Churi et al. [2006] for silicon carbide. They stated that the surface roughness decreased with the increase in ultrasonic vibration power.

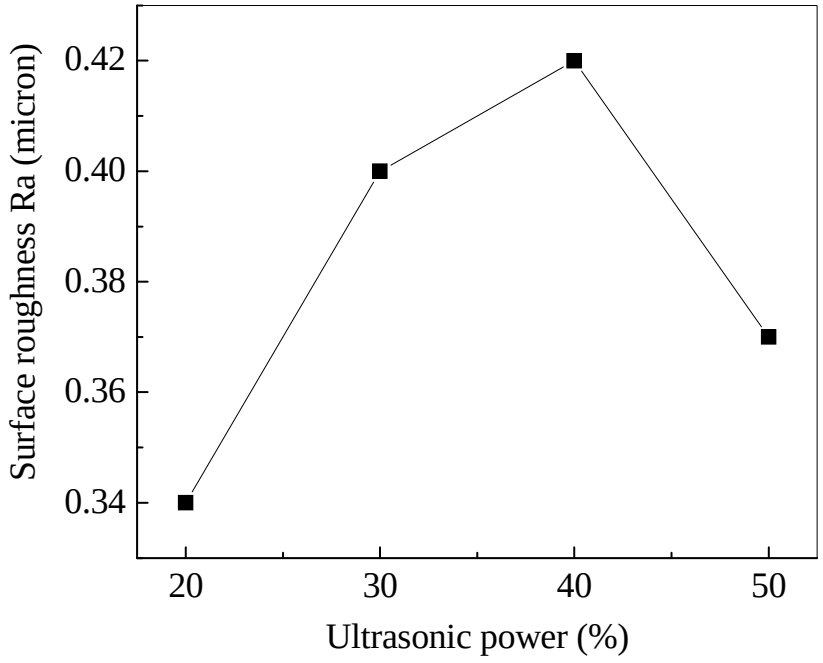

Figure 8.7 Surface roughness vs. ultrasonic power

8.2.3 EFFECTS ON CHIPPING SIZE

8.2.3.1 SPINDLE SPEED

Figure 8.8 shows the chipping size curve as spindle speed increases. It can be observed that the chip size decreases rapidly initially when the spindle speed increases from 2000 rpm to 4000 rpm, then decreases at a lower rate till the spindle speed reaches 5000 rpm. These results are consistent with those reported by Churi et al. [2006] for silicon carbide. But Li et al. [2005] reported that, for CMC, the chipping size increased with the increase in spindle speed.

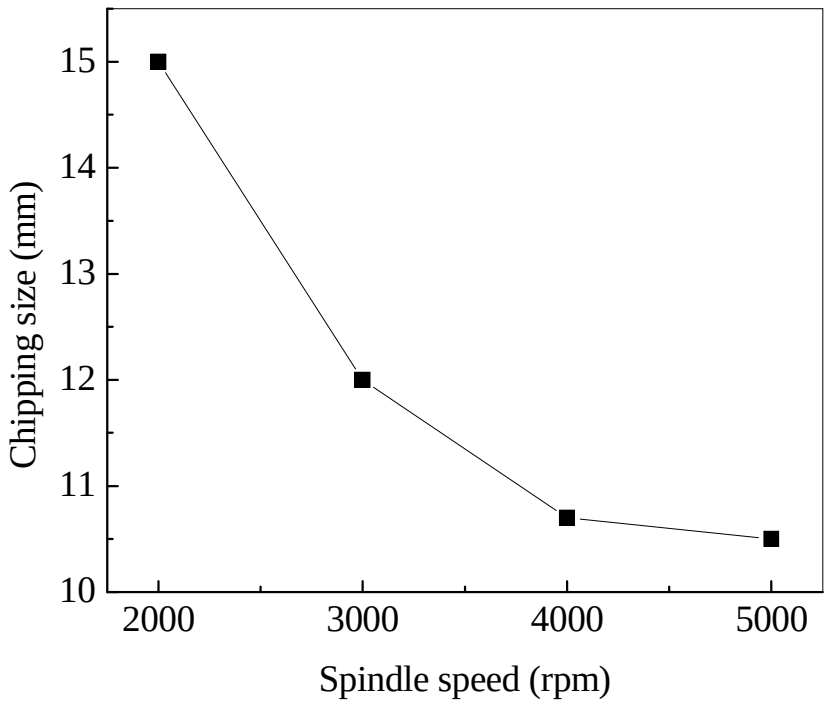

Figure 8.8 Chipping size vs. spindle speed

8.2.3.2 FEEDRATE

Figure 8.9 shows the relation between chipping size and feedrate. It can be observed that the chipping size increases with the increase in feedrate. These results are consistent with those reported by Churi et al. [2006] for silicon carbide. But Li et al. [2005] reported that, for CMC, the chipping size decreased with increase in feedrate.

8.2.3.3 ULTRASONIC VIBRATION POWER

Figure 8.10 shows the change of chipping size with ultrasonic vibration power. It can be observed that the chipping size increases slowly when the ultrasonic power increases from 20% to 40%, and then increases rapidly when the ultrasonic power increases from 40% to 50%. These results are consistent with those reported by Churi et al. [2006] for silicon carbide. But Li et al. [2005] reported that, for CMC, the chipping size decreased with the increase in ultrasonic vibration power.

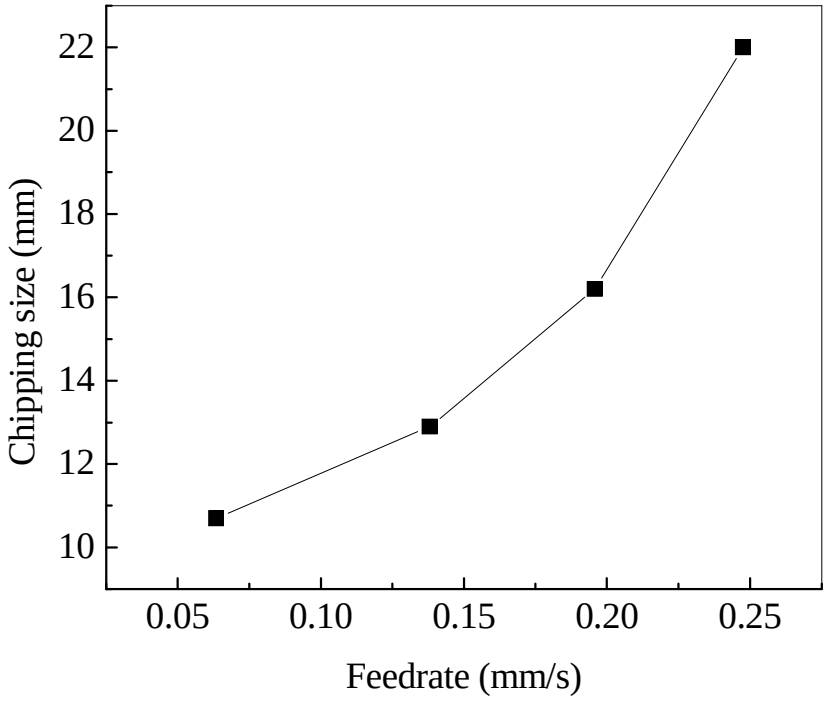

Figure 8.9 Chipping size vs. feedrate

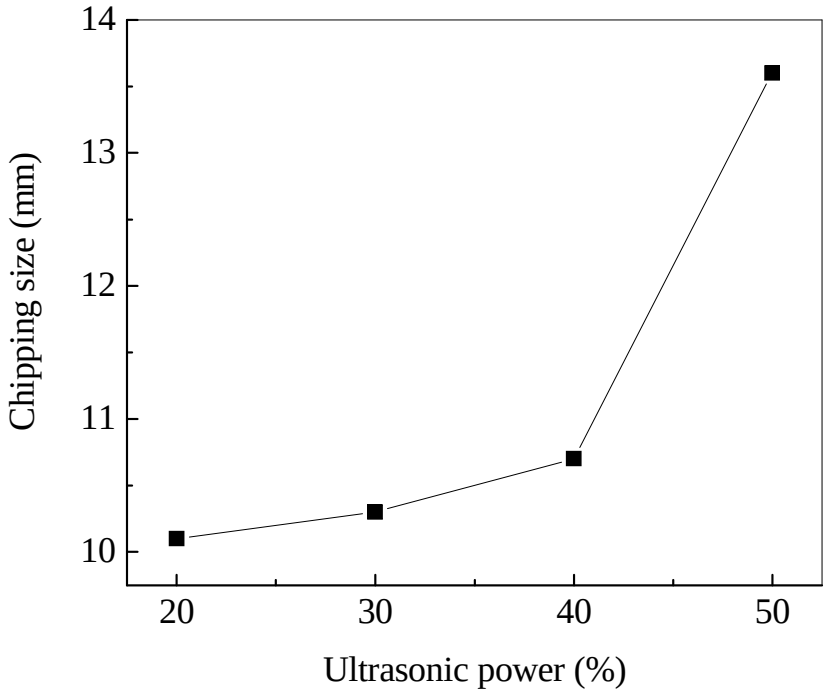

Figure 8.10 Chipping size vs. ultrasonic power

8.3 SUMMARY

This chapter reports a study on the effects of three process parameters (spindle speed, feedrate, and ultrasonic power) on three output variables (cutting force, surface roughness, and chipping size) while rotary ultrasonic machining of a dental ceramic material (macor). The following conclusions can be drawn from the study:

1) As spindle speed increases, cutting force and chipping size decrease while surface roughness decreases initially and then increases.
2) As feedrate increases, cutting force and chipping size increase while surface roughness increases initially and then decreases.
3) As ultrasonic vibration power increases, cutting force decreases initially and then increases; surface roughness increases initially and then decreases, while the chipping size increases.

CHAPTER 9 PREDICTIVE FORCE MODEL IN ROTARY ULTRASONIC MACHINING OF TITANIUM

9.1 ASSUMPTIONS

Rotary ultrasonic machining is considered as a hybrid process that combines the material removal mechanisms of diamond grinding and ultrasonic machining. Therefore, there are two principle approaches for development of a model to predict cutting force. In the first approach the process is considered as ultrasonic machining and the effect of diamond grinding is superimposed as a rotational effect of the tool. In the second approach, the effects of these processes are reversed. The first approach is used in this study.

The list of assumptions and terminology used are stated below:

1. Workpiece material = rigid plastic
2. Diamond abrasive = rigid sphere
3. Diamond abrasive size = same for all
4. Working particle height = all particles are at same height
5. All abrasive particles take part in cutting during each ultrasonic cycle
6. Volume of material removed by one abrasive particle = interaction volume of abrasive particle swept volume
7. Material removal rate for a tool is constant
8. Tool thickness remains constant for all the tools. Tool thickness = 1.8 mm

TERMINOLOGY

D_o = Outer diameter of the tool (mm)

D_i = Inner diameter of the tool (mm)

h = Workpiece thickness (mm)

S = Spindle speed (rpm)

f = Ultrasonic vibration frequency (Hz)

A = Ultrasonic vibration amplitude (mm)

d = Diameter of diamond particle (mm)

r = Radius of diamond particle (mm)

L = Distance moved by diamond particle during penetration in workpiece (mm)

δ = Depth of maximum penetration (mm)

T = Time of machining (sec)

n = Number of diamond particles taking part in machining

MRR = Material removal rate (mm^3/sec)

F = Maximum contact force between tool and workpiece (N)

σ_y = Compressive strength of workpiece

B = Projected area (mm^2)

9.2 INDENTION DEPTH OF A DIAMOND GRIT INTO THE WORKPIECE

$$L = \left[\frac{\pi D_o S}{60 f}\right] \times \left\{\frac{\pi}{2} - \arcsin\left(1 - \frac{\delta}{A}\right)\right\} \quad \text{----------Equation (1)}$$

Detailed derivation of the equation can be found in (Pei et al. 1995). L and δ are the two unknowns in Equation (1).

The material removal rate can be given by:

MRR = volume of material removed per unit time

$$MRR = \frac{\pi\left[D_o{}^2 - D_i{}^2\right] \times h}{4T}$$ ----------Equation (2)

Material removal rate is also given by Pei et al. (1995) as -

$$MRR = nf\pi\left[1 + \frac{L}{d}\right] \times \left[\frac{d}{2} - \frac{\delta}{3}\right] \times \delta^2$$ ----------Equation (3)

L and δ is the unknowns in Equation (3).

The value of δ can be derived by solving Equations (1), (2) and (3).

9.3 ESTIMATION OF CUTTING FORCE

When A diamond particle acts against workpiece surface, an indentation is formed. Diamond abrasive is rigid sphere and titanium workpiece is rigid plastic. Therefore, the following equation can be derived:

$$\frac{F}{n} = \sigma_y B$$ ----------Equation (4)

Where B = projected area of the contact between the diamond particle and workpiece.

B can be further simplified as:

$$B = \pi \times r_B{}^2$$ ----------Equation (5)

And by Hypotenuse theorem,

$$r^2 = (r-\delta)^2 + {r_B}^2$$

$$r^2 = r^2 - 2r\delta + \delta^2 + {r_B}^2$$

$${r_B}^2 = \delta(2r-\delta)$$----------Equation (6)

Substituting Equation (6) into Equation (5)

$$B = \pi\delta(2r-\delta)$$ ----------Equation (7)

Substituting Equation (5) in Equation (4)

$$\frac{F}{n} = \sigma_y[\pi\delta(2r-\delta)]$$

$$F = n\sigma_y[\pi\delta(2r-\delta)]$$ ----------Equation (8)

9.4 THE INFLUENCE OF DIFFERENT PARAMETERS ON CUTTING FORCE

In the previous sections, we have developed a simplified analytical model for cutting force in rotary ultrasonic machining for titanium material. In this section, we will use this model to study how individual machining parameters influence the cutting force and compare the trends predicted by the model with those observed by experimental results. It must be noted here that only trends can be compared because our model is based on some assumptions; and the predicted values from the model and the experimental results may not exactly match. The model is applied to predict the relations between the cutting force and the different parameters for rotary ultrasonic machining of titanium alloy.

9.4.1 GRIT DIAMETER

The predicted relation between cutting force at 5 different levels of grit diameter are plotted against tool diameter, number of grains, spindle speed, machining time and amplitude (Fig. 9.1 to 9.5). The experimental results presented in Chapter 4 also show that cutting force increased with increase in grit diameter. This may be because as the diameter of the grain increases, the projected area of contact also increases. The cutting force is directly proportional to the projected area of contact. Figure 9.6 shows the variation of different important components of Equation 1 (the cutting force equation) with variation in grit diameter. Specifically, the depth of indentation (δ), the distance moved by an indenter when in contact with the workpiece (L), material removal rate (MRR) and cutting force (F) are shown in this figure. Two important effects are visible. First, the depth of indentation and length of contact decrease at a decreasing rate with increase in grit diameter. Second, the cutting force increases with a decrease in depth of indentation and length of contact.

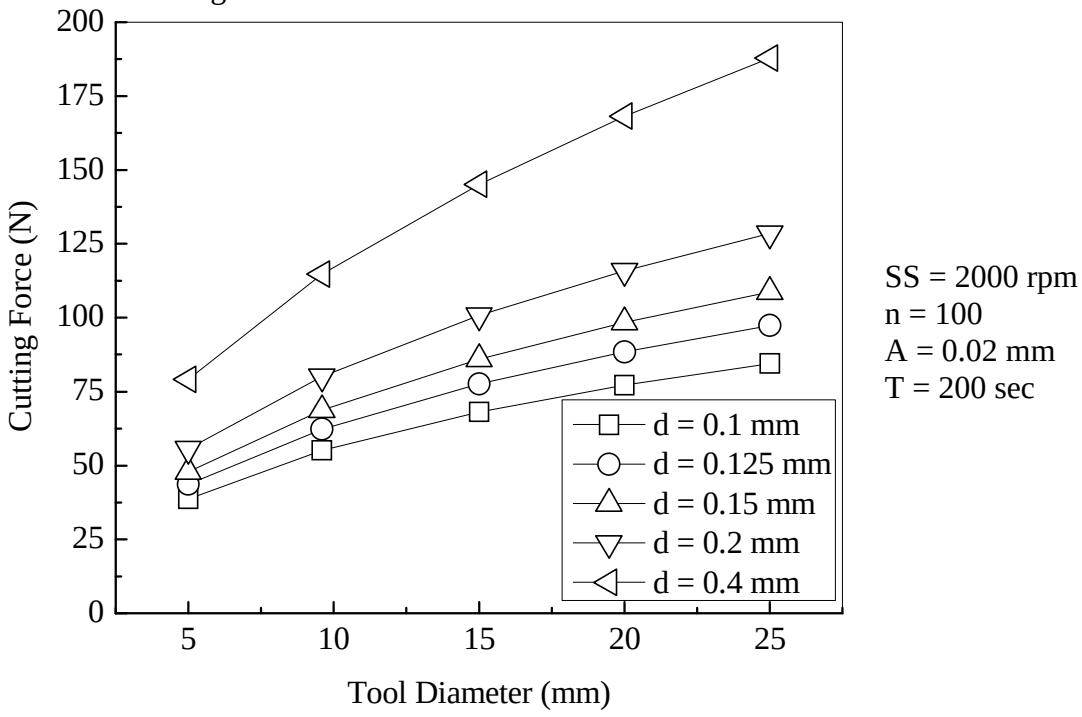

Figure 9.1 Relation between tool diameter and cutting force at 5 different levels of grit diameter

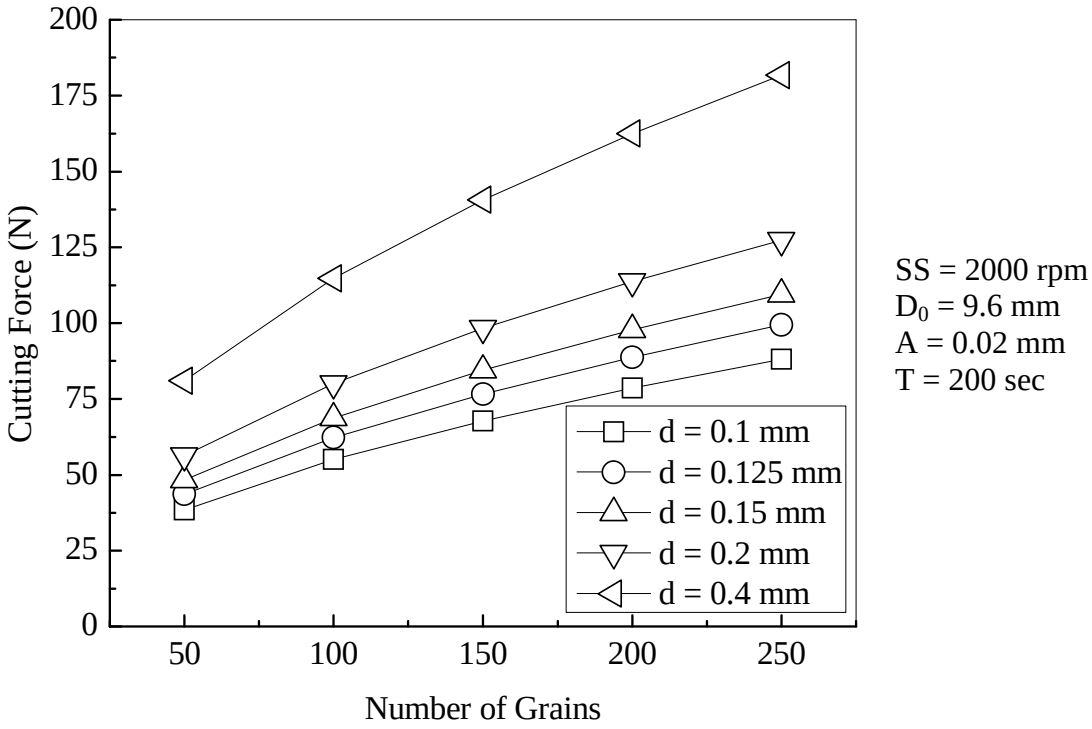

Figure 9.2 Relation between number of grains and cutting force at 5 different levels of grit diameter

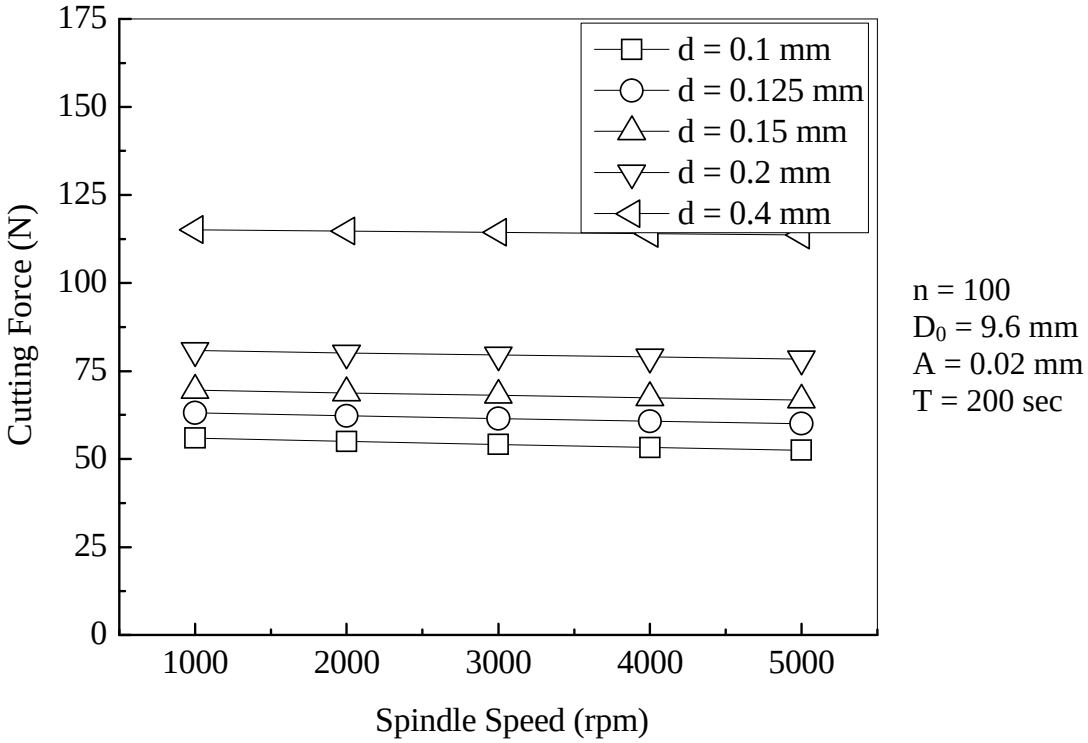

Figure 9.3 Relation between spindle speed and cutting force at 5 different levels of grit diameter

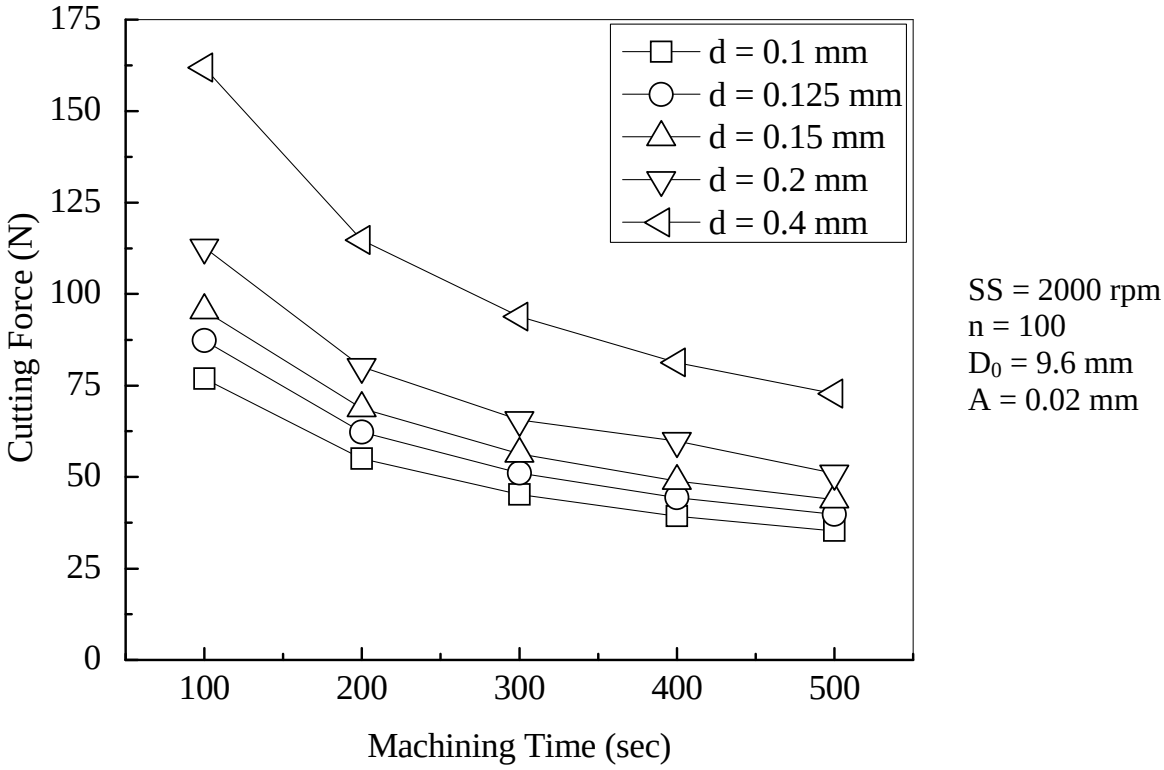

Figure 9.4 Relation between machining time and cutting force at 5 different levels of grit diameter

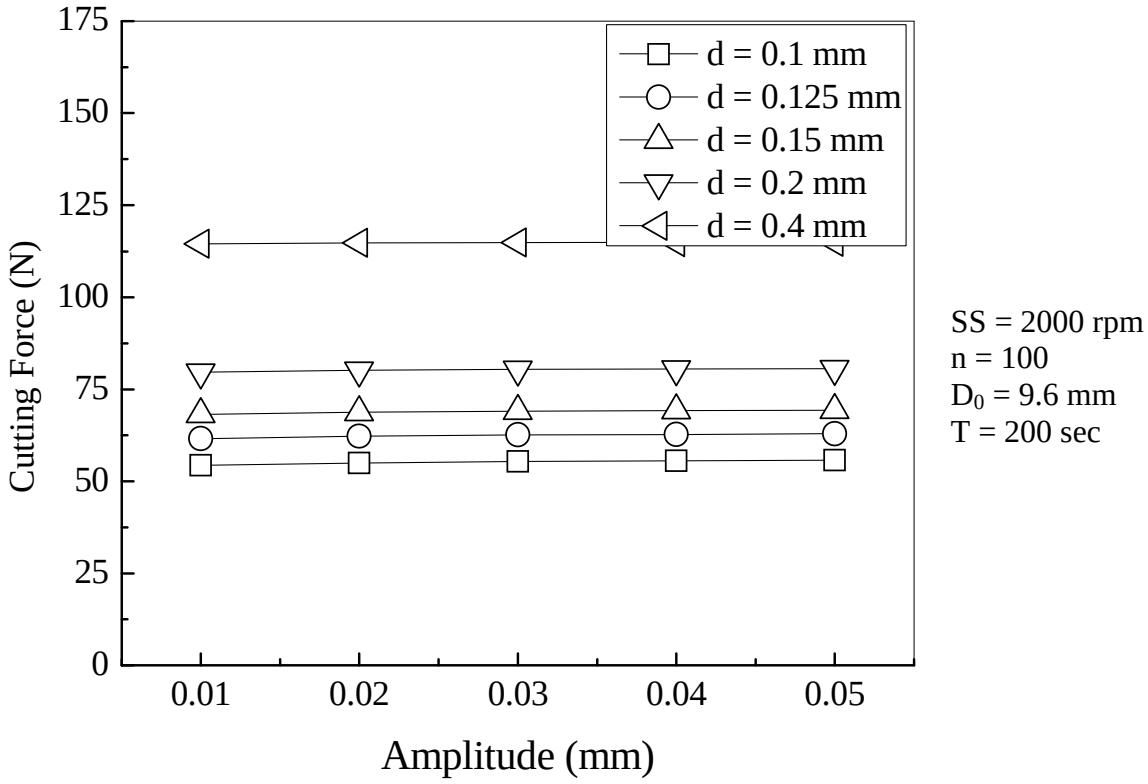

Figure 9.5 Relation between amplitude and cutting force at 5 different levels of grit diameter

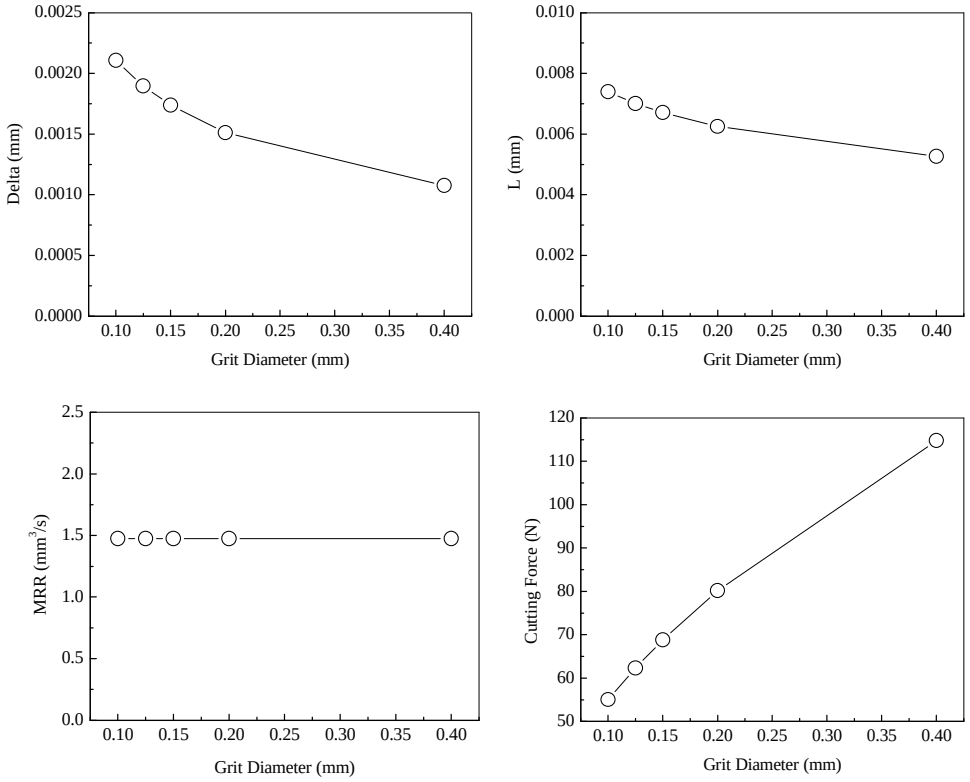

SS = 2000 rpm
n = 100
D_0 = 9.6 mm
A = 0.02 mm
T = 200 sec

Figure 9.6 Influence of grit diameter

9.4.2 A

The predicted relation between cutting force at 5 different levels of amplitude are plotted against grit diameter, tool diameter, number of grains, spindle speed and machining time (Fig. 9.7 to 9.11). It is observed that the cutting force steadily increases with increase in grit diameter, tool diameter and number of grains. Whereas, it decreases at a very low rate with increase in spindle speed and it has a tendency to decrease at a higher rate with increase in machining time. The experimental results presented in Chapter 5 shows a different trend. They reported that the cutting force decreases initially, then remains constant for a certain level of amplitude and then increase beyond certain limit. The variation in trends between our model and the reported results may be due to the difference in basic assumptions. Also the results presented in Chapter 5were for specific

sets of conditions. The results may be different for different conditions. Figure 9.12 shows the variation of different important components of Equation 1 (the cutting force equation) with variation in amplitude. Two important effects are visible. First, the depth of indentation increases at a decreasing rate with amplitude. Second, the length of contact decreases with amplitude. This clearly states that the depth of indentation and length of contact are related inversely. This inverse effect causes the cutting force to remain fairly constant.

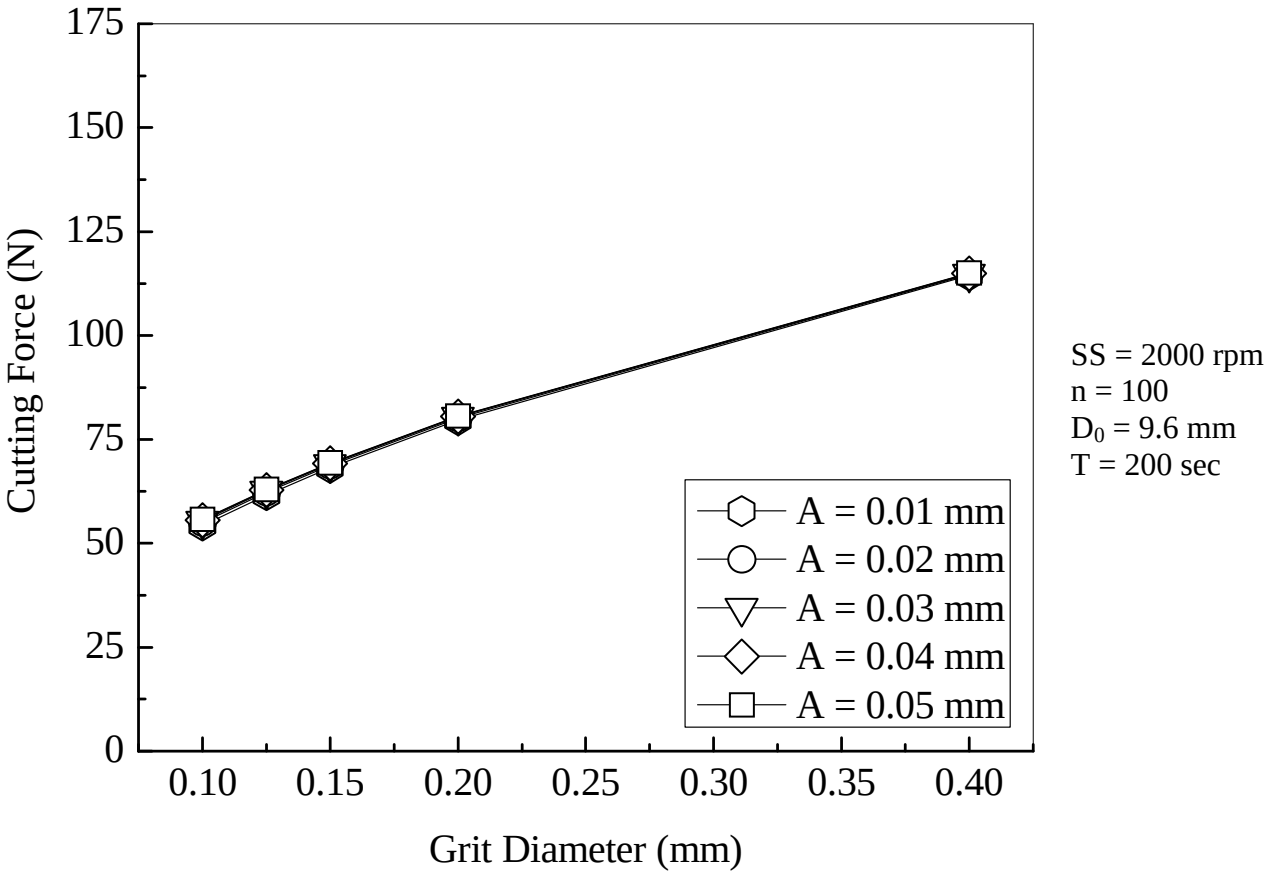

Figure 9.7 Relation between grit diameter and cutting force at 5 different levels of amplitude

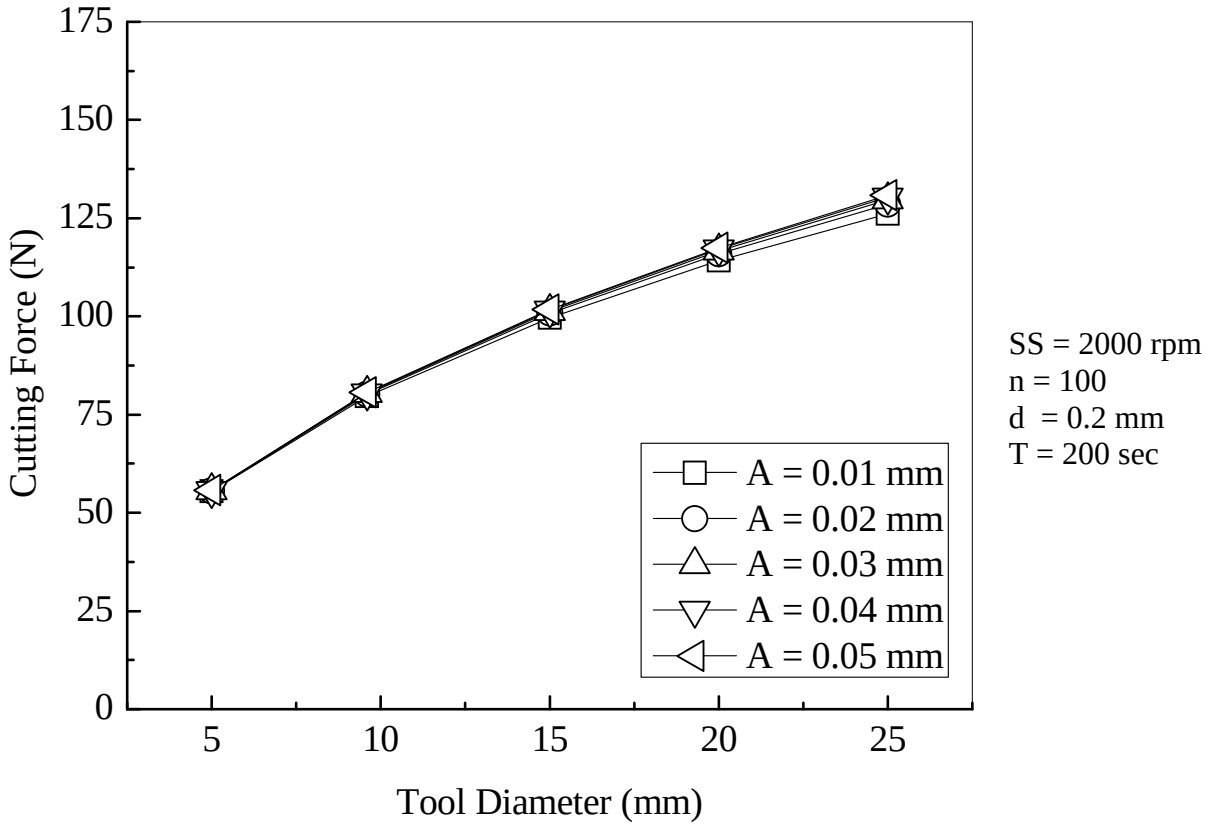

Figure 9.8 Relation between tool diameter and cutting force at 5 different levels of amplitude

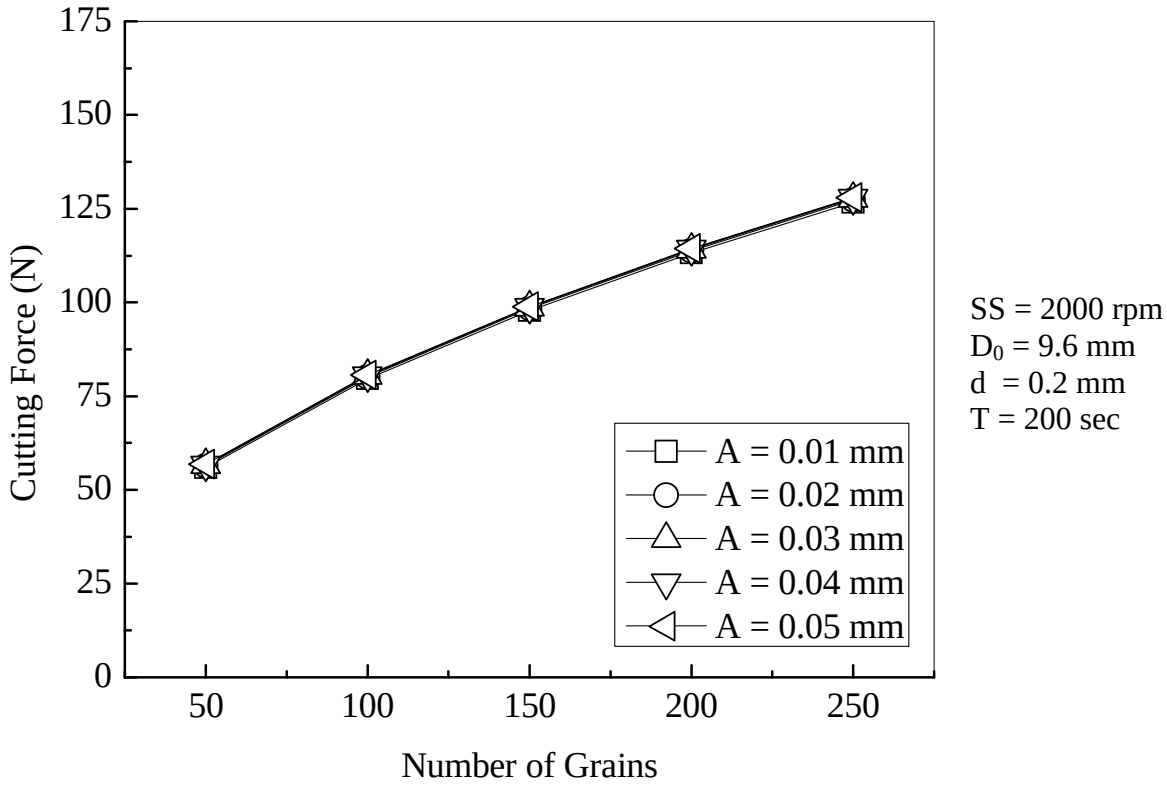

Figure 9.9 Relation between number of grains and cutting force at 5 different levels of amplitude

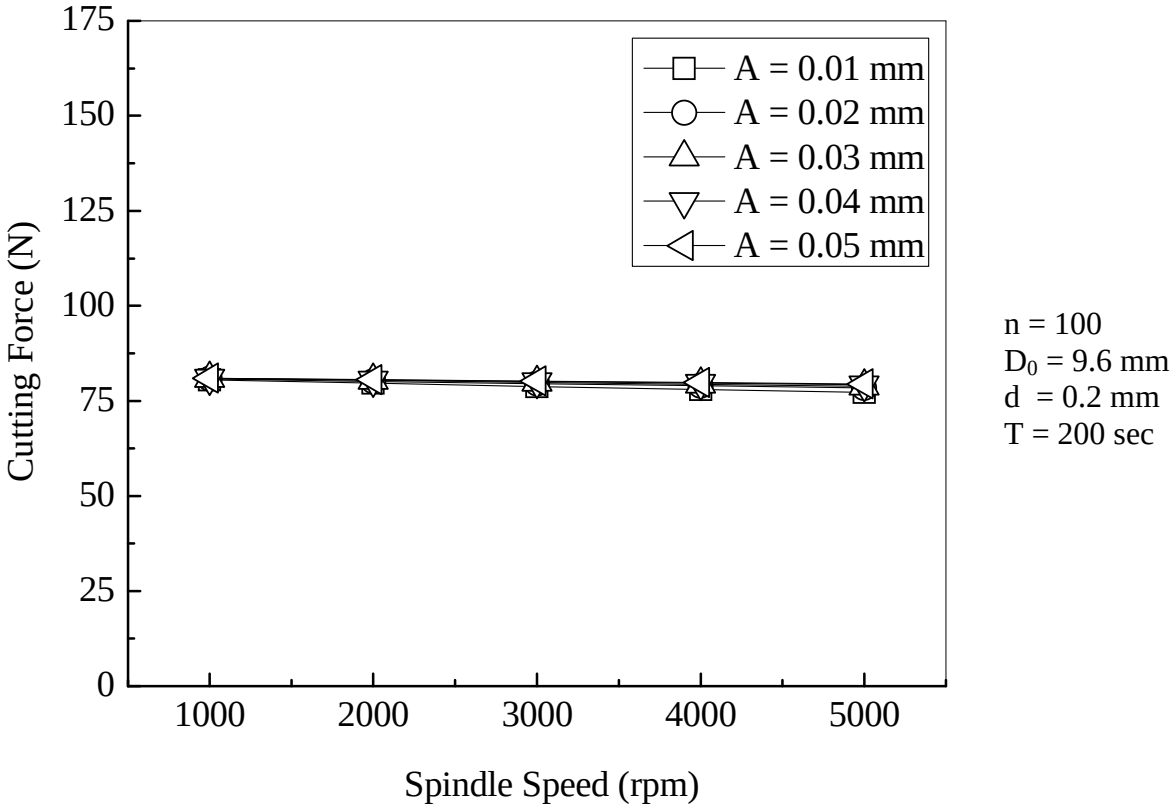

Figure 9.10 Relation between spindle speed and cutting force at 5 different levels of amplitude

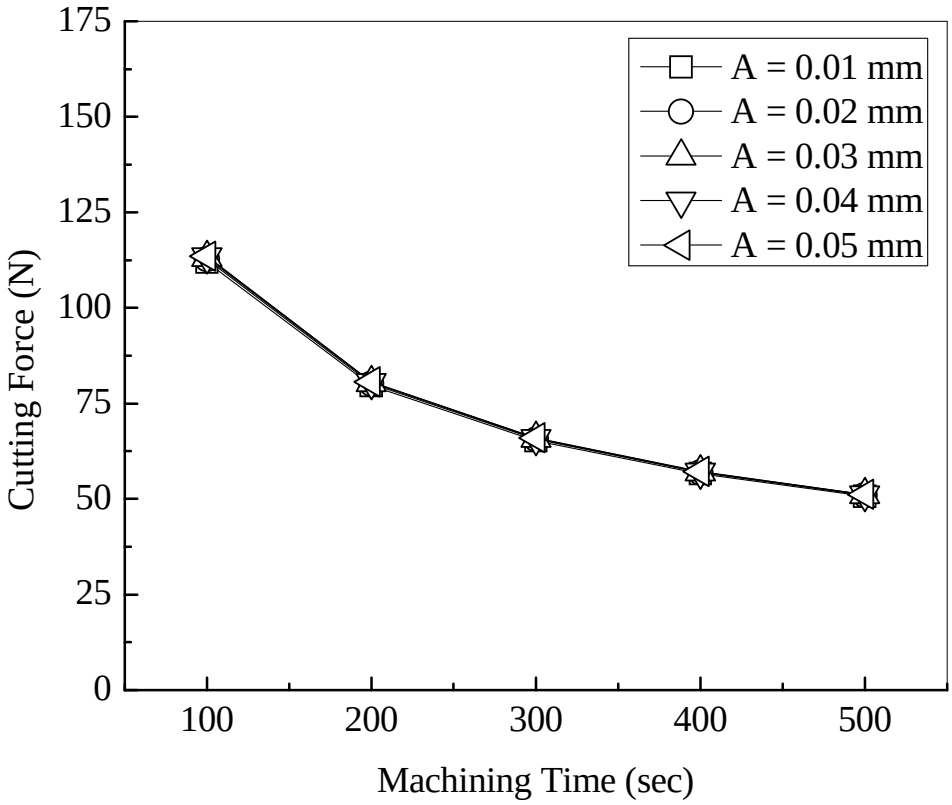

Figure 9.11 Relation between machining time and cutting force at 5 different levels of amplitude

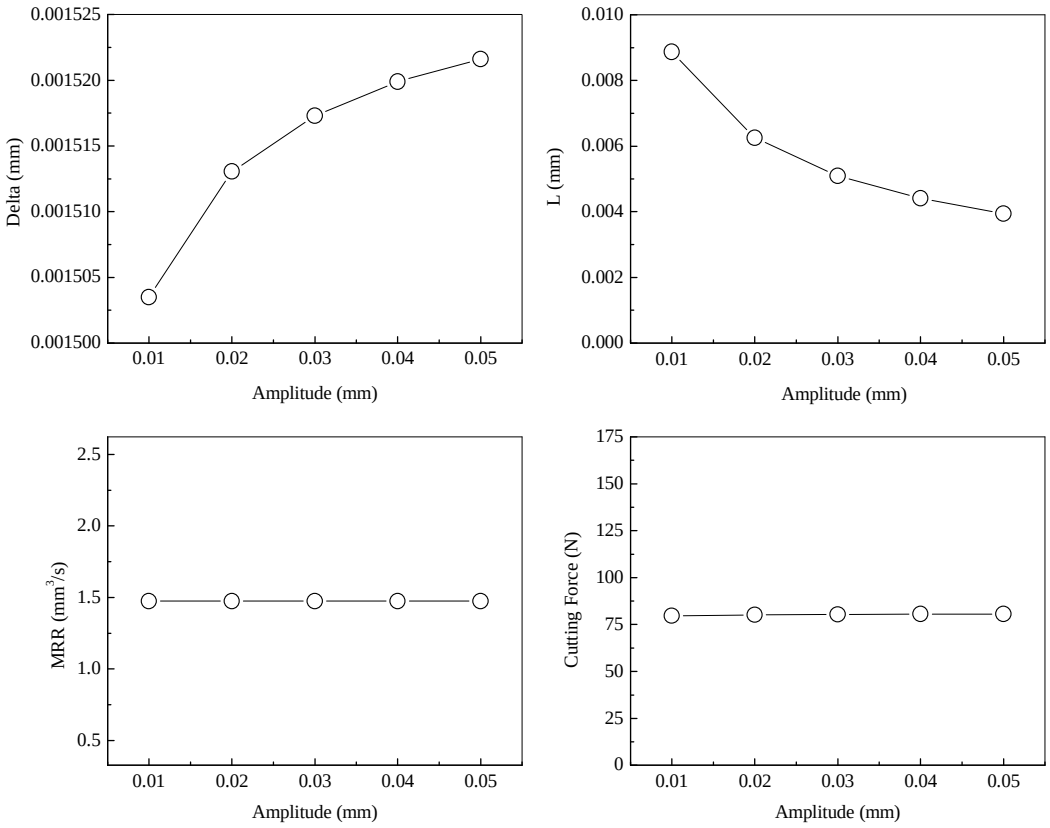

SS = 2000 rpm
n = 100
D_0 = 9.6 mm
d = 0.2 mm
T = 200 sec

Figure 9.12 Influence of amplitude

9.4.3 TOOL DIAMETER

The predicted relation between cutting force at 5 different levels of tool diameter are plotted against grit diameter, number of grains, spindle speed, machining time and amplitude (Fig. 9.13 to 9.17). It is observed that the cutting force steadily increases with increase in grit diameter and number of grains. It decreases at a very low rate with increase in spindle speed and it has a tendency to decrease at a higher rate with increase in machining time; and it fairly remains constant with increasing amplitude. Figure 9.18 shows the variation of different important components of Equation 1 (the cutting force equation) with variation in tool diameter. The only visible effect is that the depth of indentation, length of contact and material removal rate increase with increase in tool diameter. And this causes the cutting force to increase.

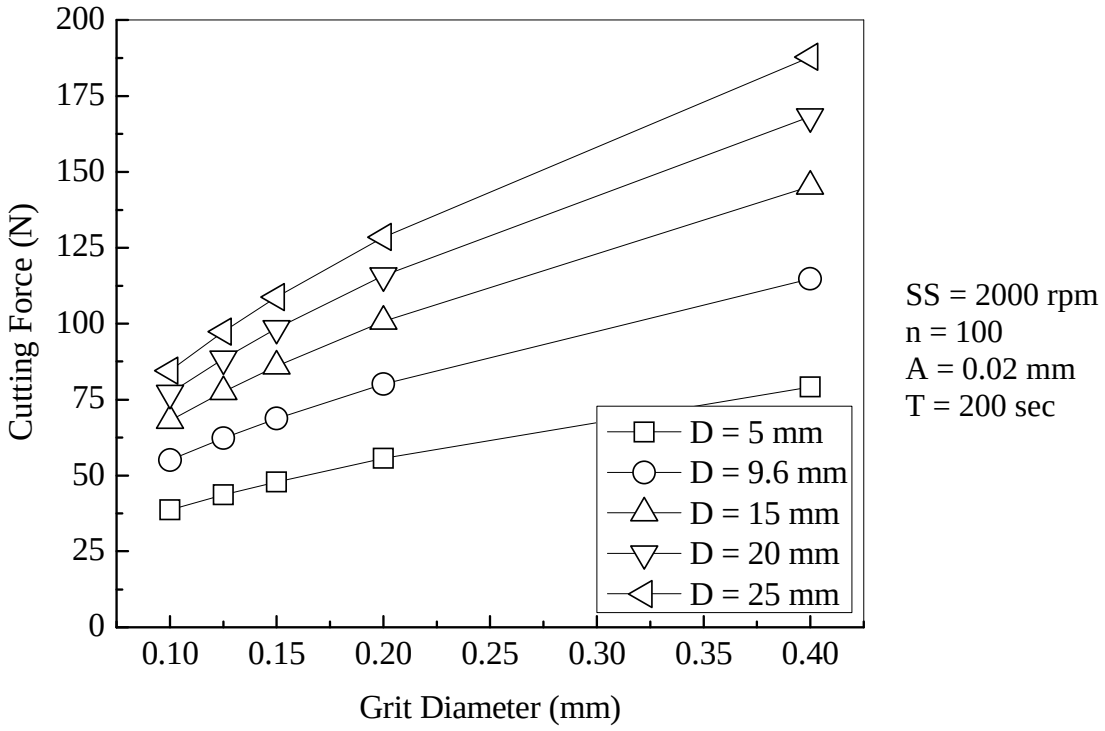

Figure 9.13 Relation between grit diameter and cutting force at 5 different levels of tool diameter

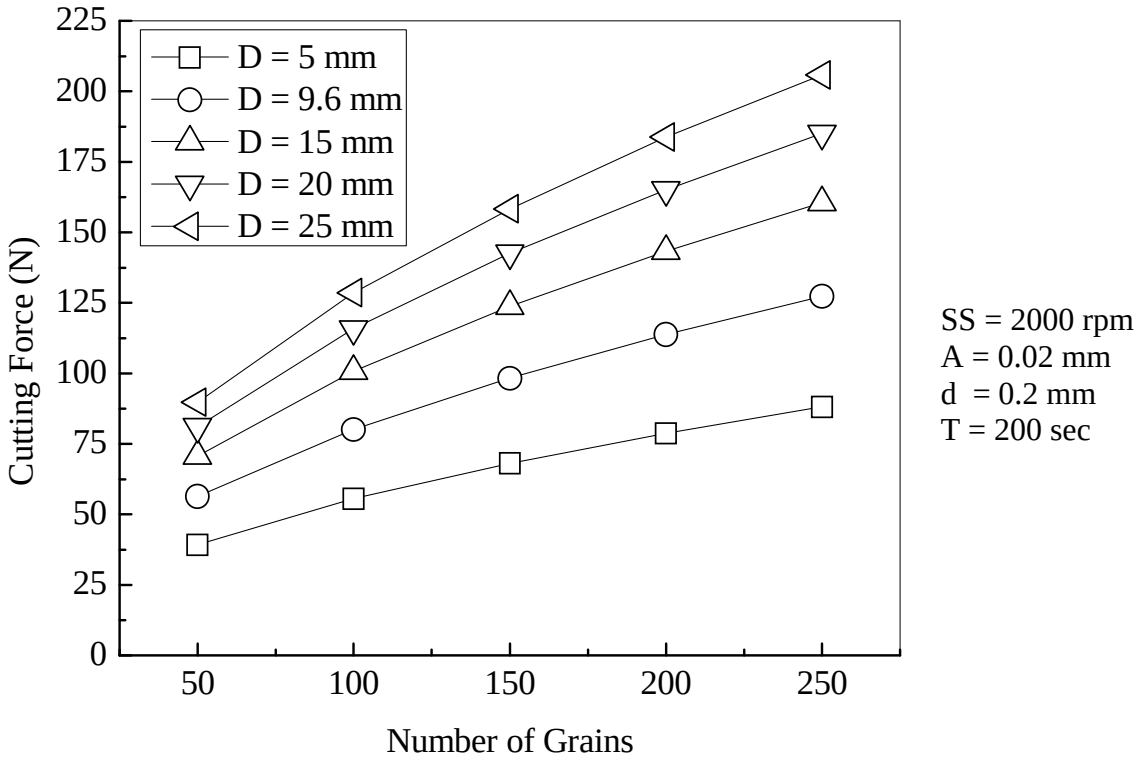

Figure 9.14 Relation between number of grains and cutting force at 5 different levels of tool diameter

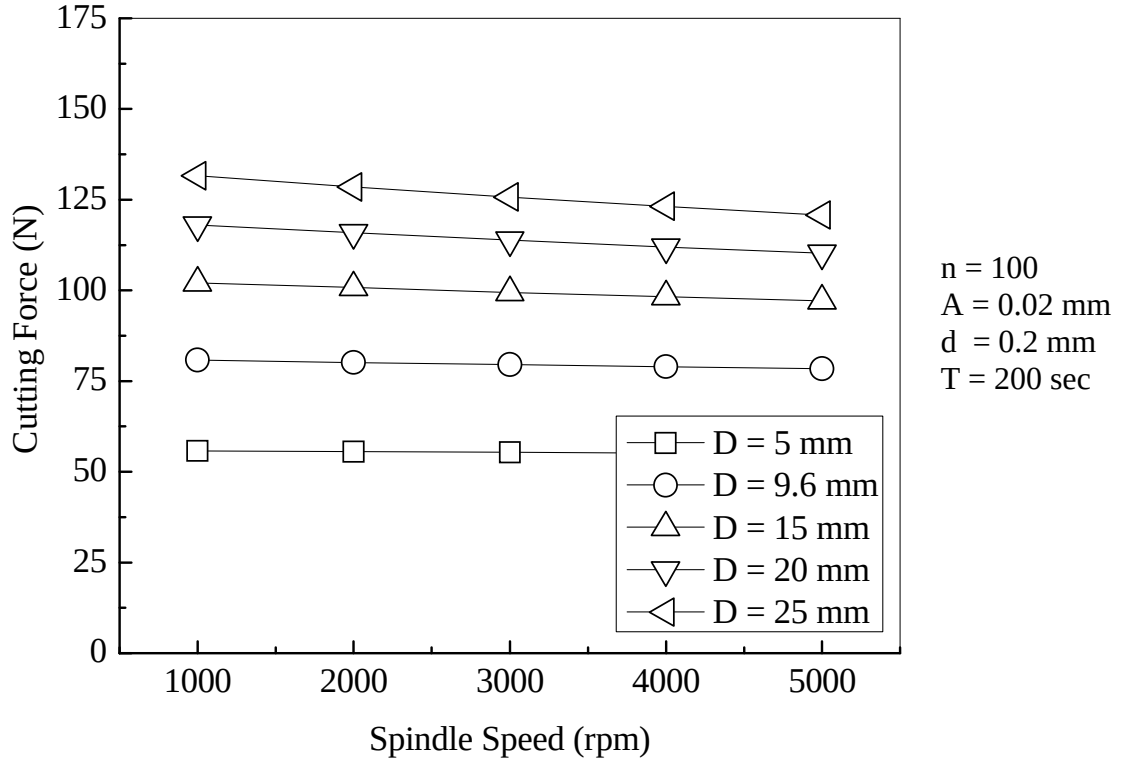

Figure 9.15 Relation between spindle speed and cutting force at 5 different levels of tool diameter

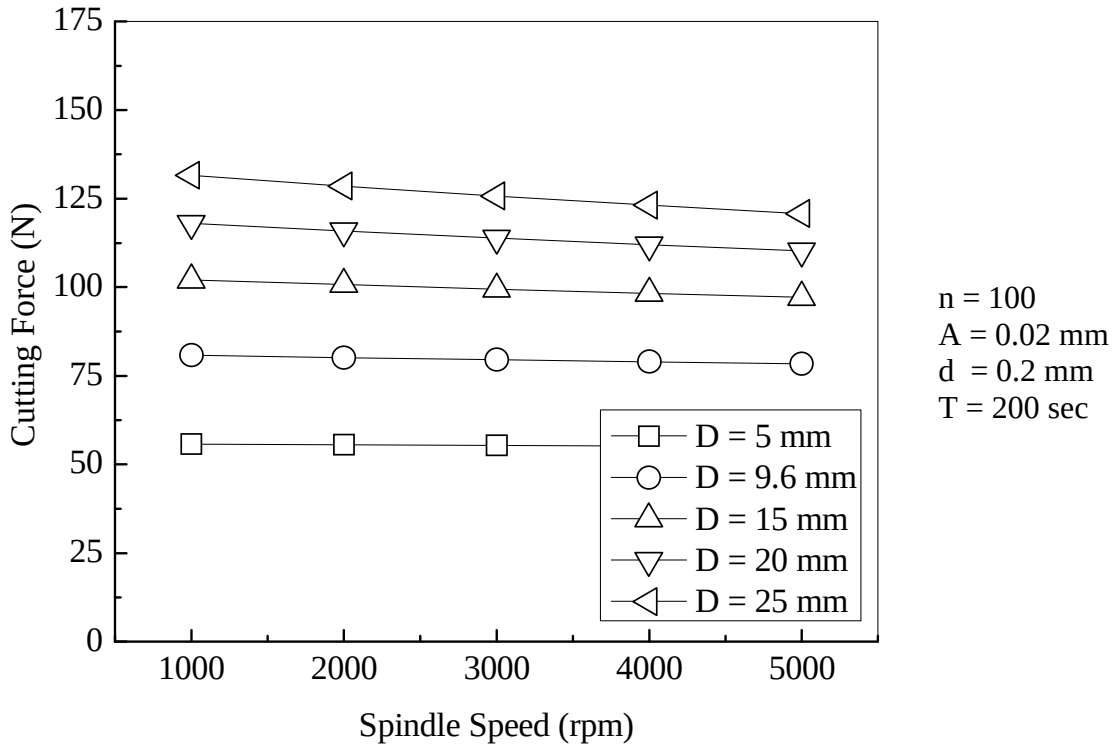

Figure 9.16 Relation between spindle speed and cutting force at 5 different levels of tool diameter

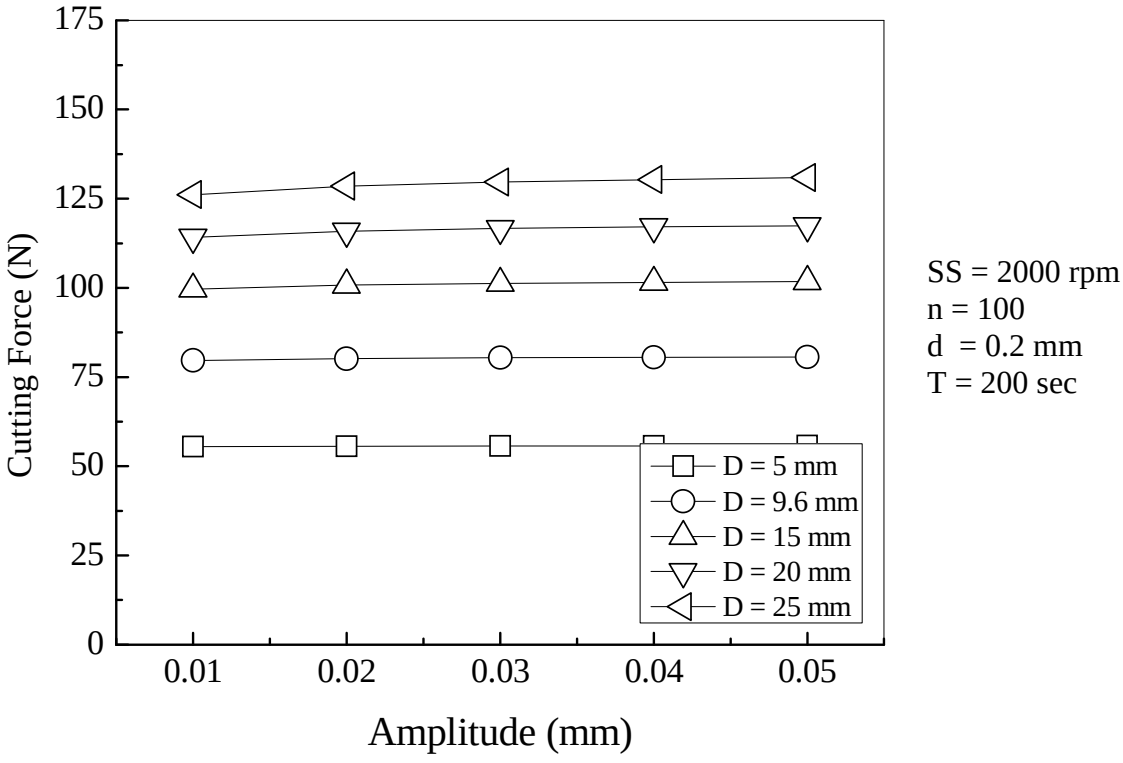

Figure 9.17 Relation between amplitude and cutting force at 5 different levels of tool diameter

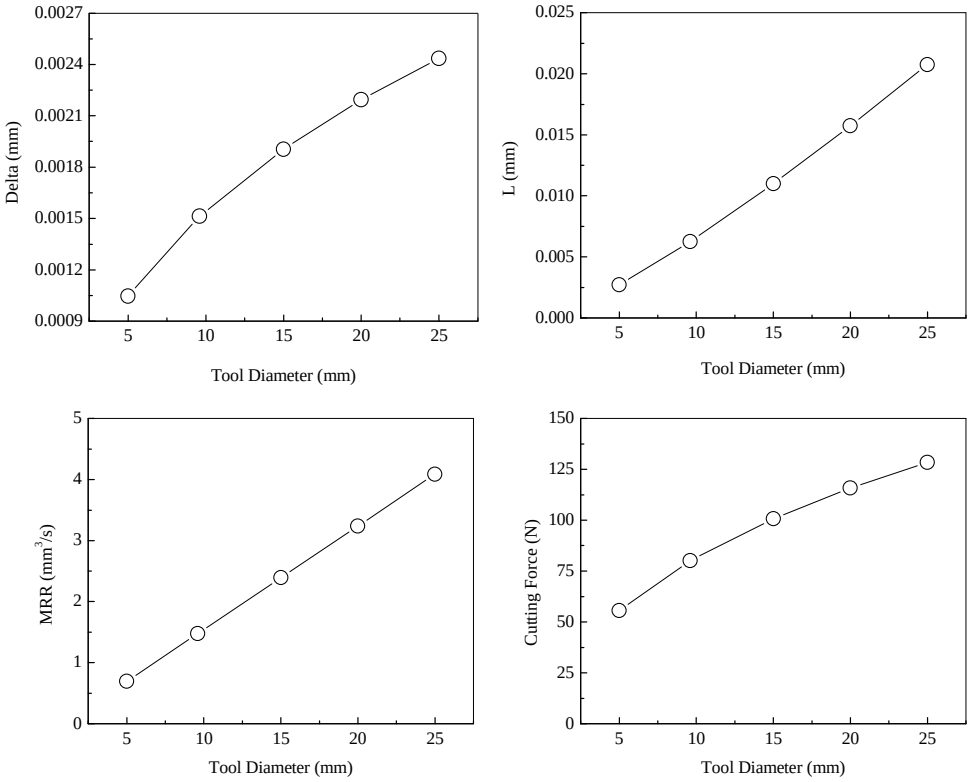

SS = 2000 rpm
n = 100
A = 0.02 mm
d = 0.2 mm
T = 200 sec

Figure 9.18 Influence of tool diameter

9.4.4 NUMBER OF GRAINS

The predicted relation between cutting force at 5 different levels of number of grains are plotted against grit diameter, tool diameter, spindle speed, machining time and amplitude (Fig. 9.19 to 9.23). It is observed that the cutting force steadily increases with increase in grit diameter and tool diameter. It decreases at a very low rate with increase in spindle speed and it has a tendency to decrease at a higher rate with increase in machining time; and it remains fairly constant with increasing amplitude. These trends are consistent with the experimental data presented in Chapter 4. Our analysis says that with the increase in number of grains, the total projected area in contact increases. This leads to increase in cutting force. Figure 9.24 shows the variation of different important components of Equation 1 (the cutting force equation) with variation in number of grains. It is observed that the depth of indentation and length of contact decreases at an increasing rate; and material removal rate remains constant. These effects cause the cutting force to increase with increasing number of grains.

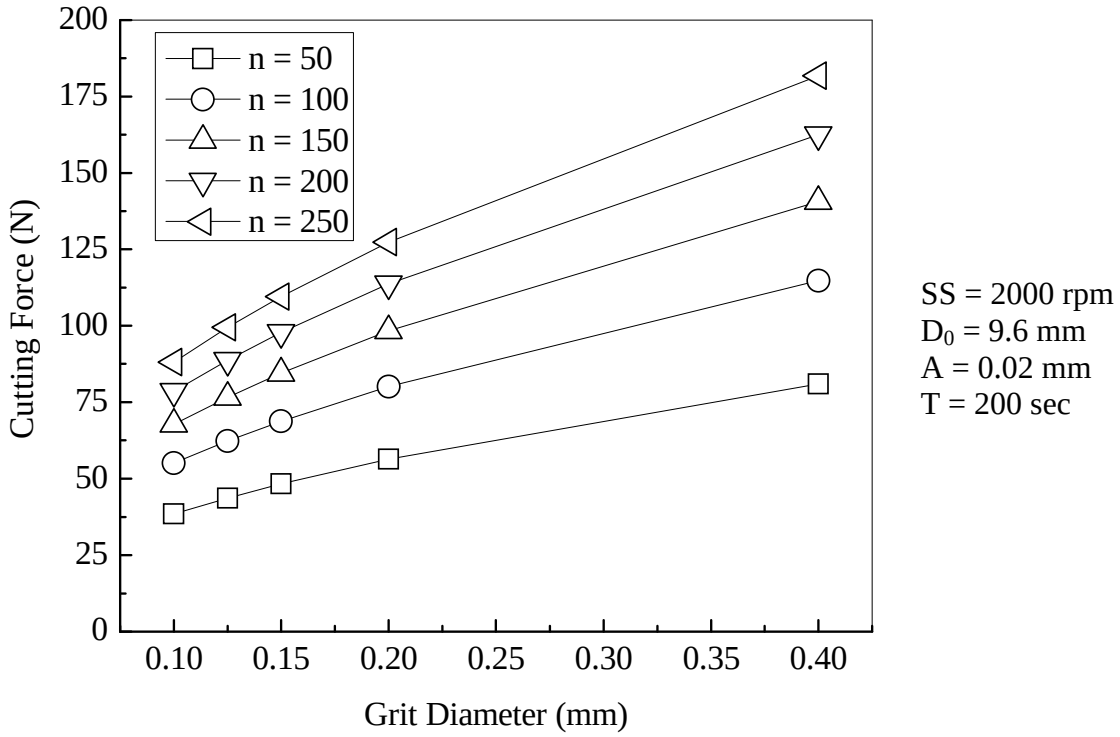

Figure 9.19 Relation between grit diameter and cutting force at 5 different levels of number of grains

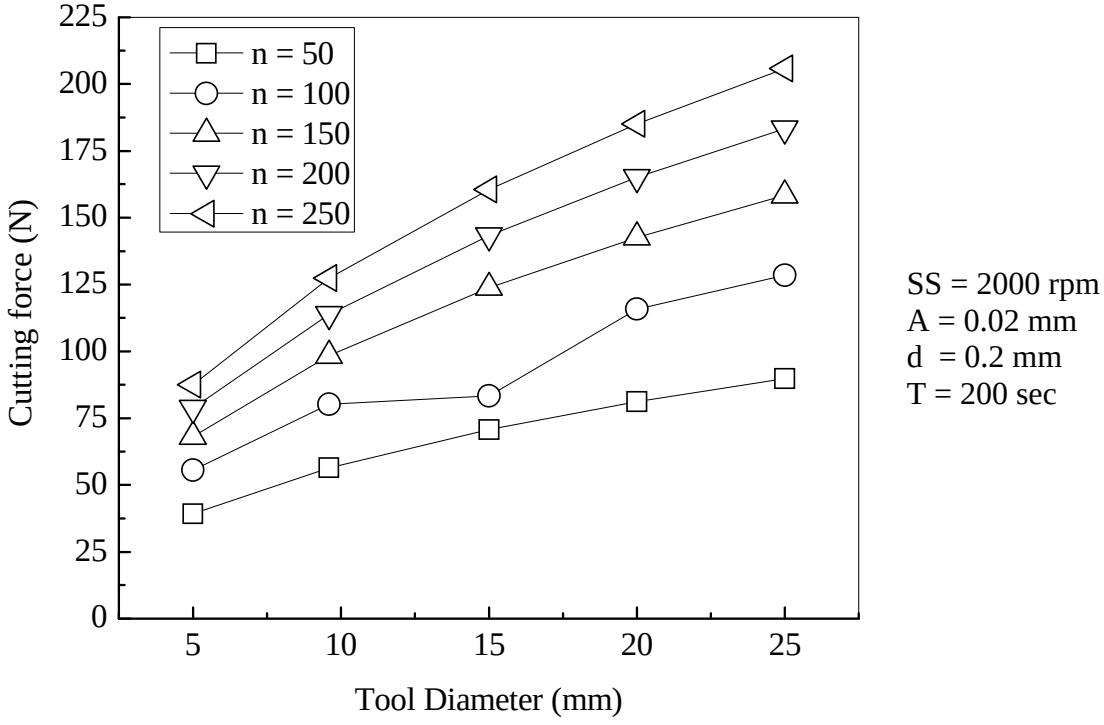

Figure 9.20 Relation between tool diameter and cutting force at 5 different levels of number of grains

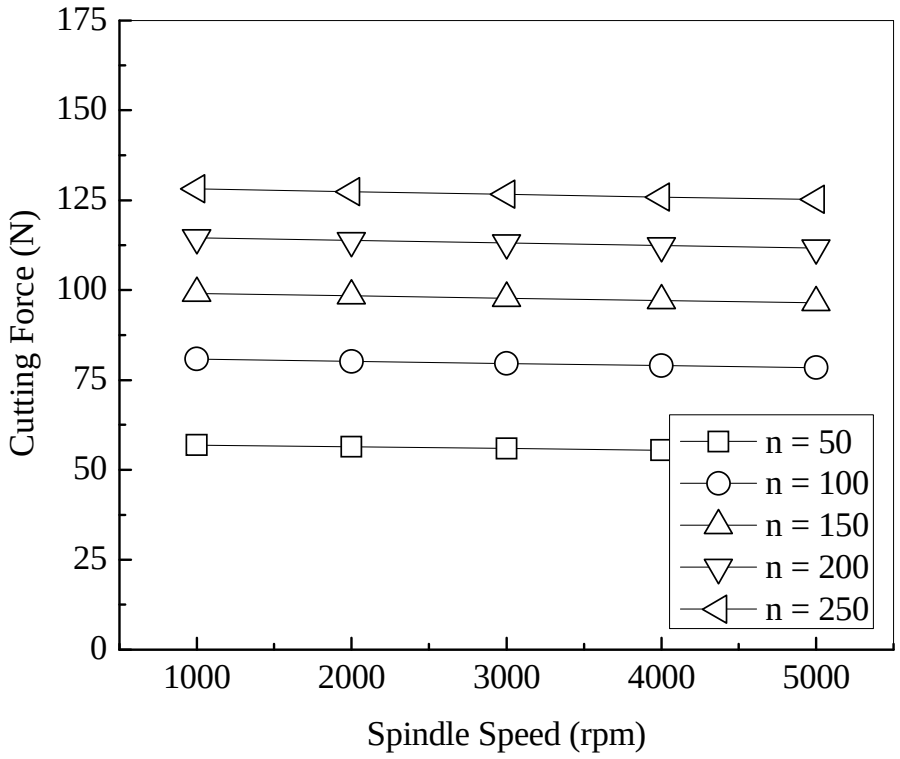

Figure 9.21 Relation between spindle speed and cutting force at 5 different levels of number of grains

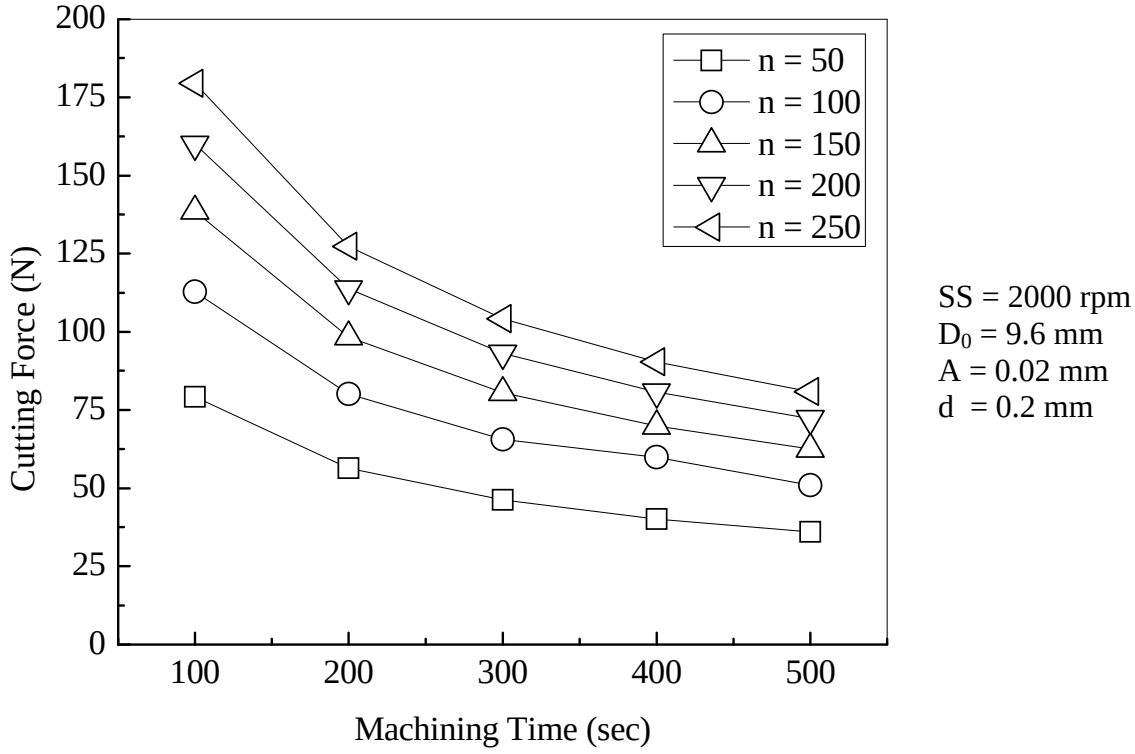

Figure 9.22 Relation between machining time and cutting force at 5 different levels of number of grains

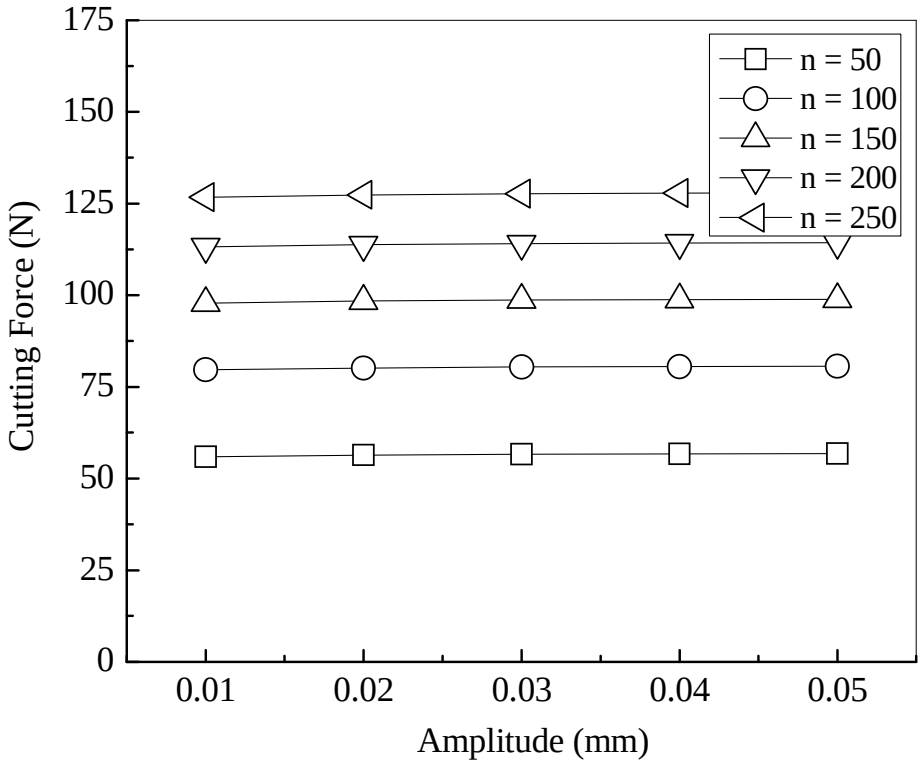

Figure 9.23 Relation between amplitude and cutting force at 5 different levels of number of grains

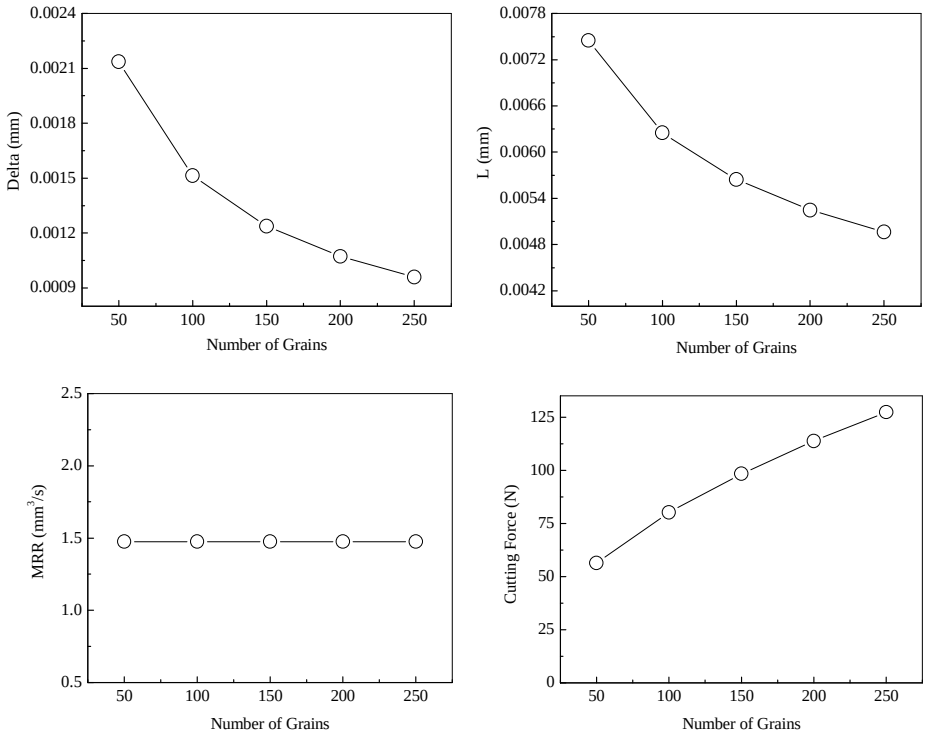

Figure 9.24 Influence of number of grains

9.4.5 SPINDLE SPEED

The predicted relation between cutting force at 5 different levels of spindle speeds are plotted against grit diameter, tool diameter, machining time, amplitude and number of grains (Fig. 9.25 to 9.29). It is observed that the cutting force steadily increases with increase in grit diameter, tool diameter and number of grains. The force decreases at a very low rate with increase in amplitude and it has a tendency to decrease at a higher rate with increase in machining time. The experimental trends reported in Chapter 5 are similar to the model predictions. The only difference is that the cutting force decreases at a higher rate for the data reported in Chapter 5. These observed differences in our model and experiments may be explained by the differences in assumptions and different sets of conditions reported. The trend predicted by our model can be explained with the help of Figure 9.30, which shows the variation of different important components of Equation 1 (the cutting force equation) with variation in spindle speed. Two effects are visible. First, it is observed that the depth of indentation decreases linearly with increase in spindle speed. Second, the length of contact increases at a constant rate with the spindle speed. These two effects cause the cutting force to increase linearly with increasing spindle speed.

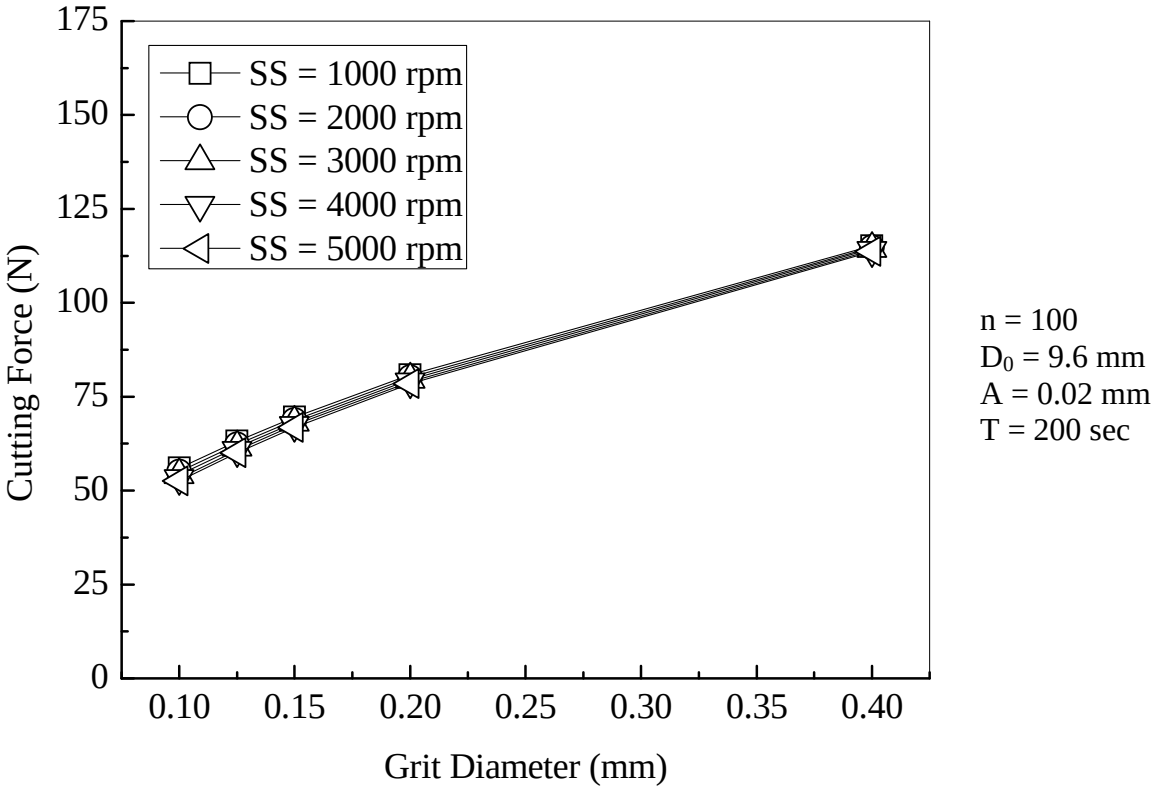

Figure 9.25 Relation between grit diameter and cutting force at 5 different levels of spindle speed

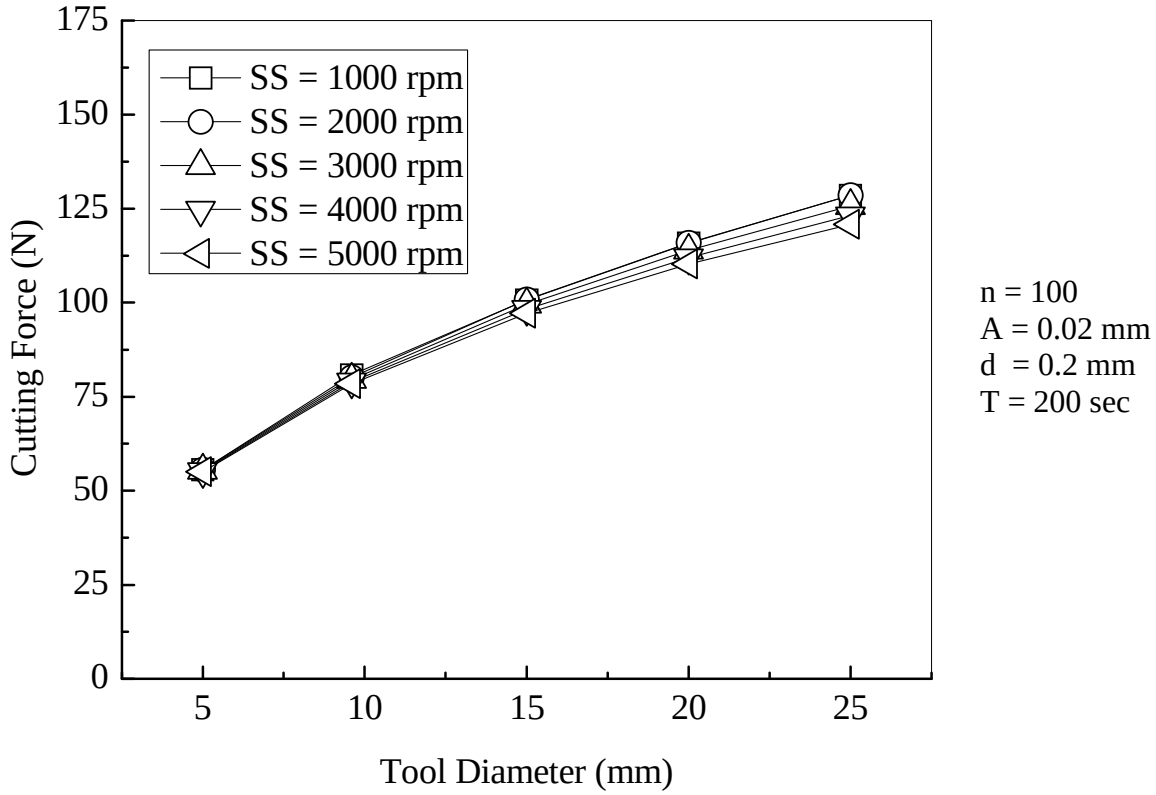

Figure 9.26 Relation between tool diameter and cutting force at 5 different levels of spindle speed

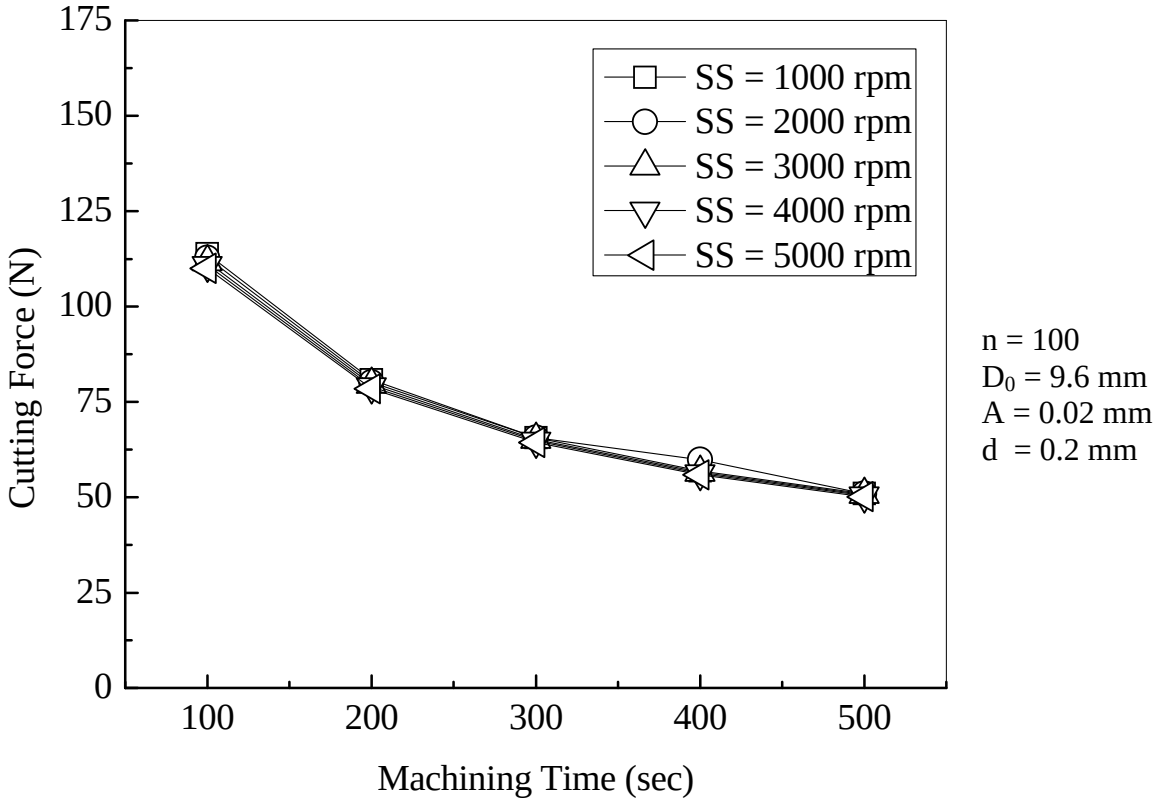

Figure 9.27 Relation between machining time and cutting force at 5 different levels of spindle speed

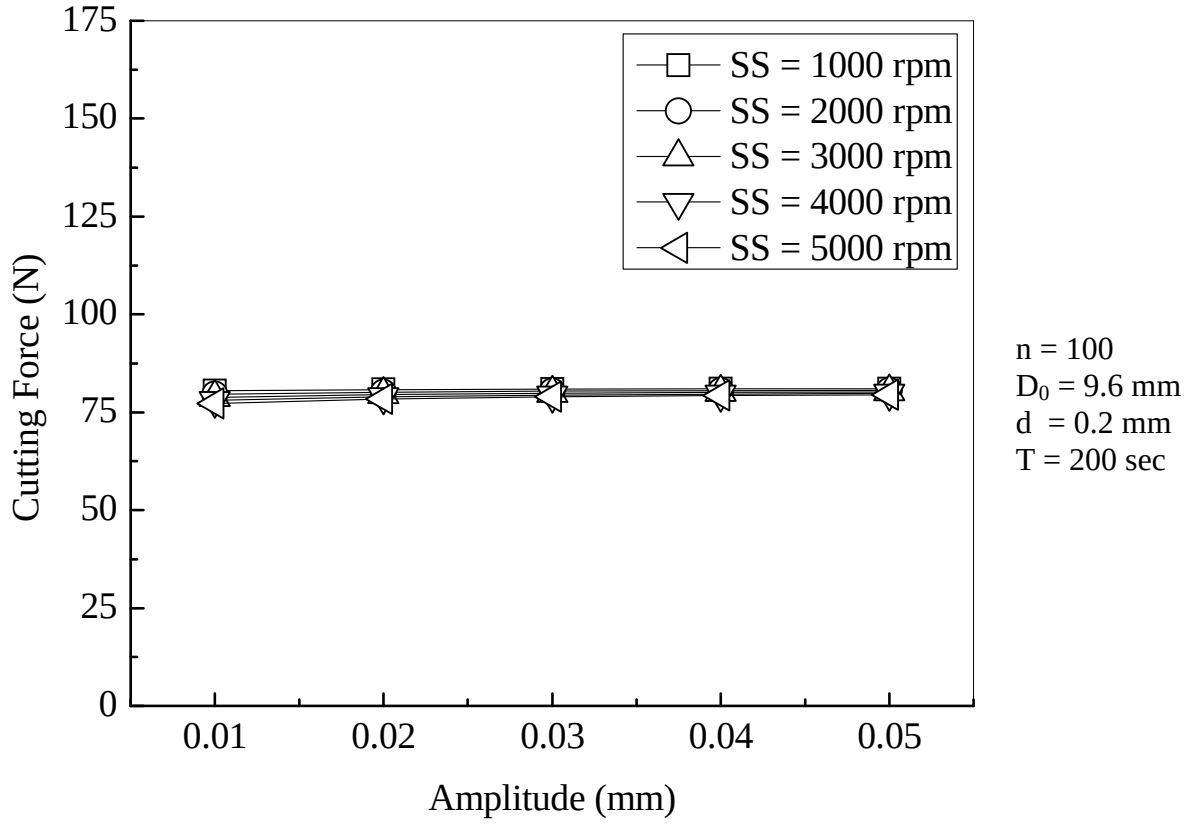

Figure 9.28 Relation between amplitude and cutting force at 5 different levels of spindle speed

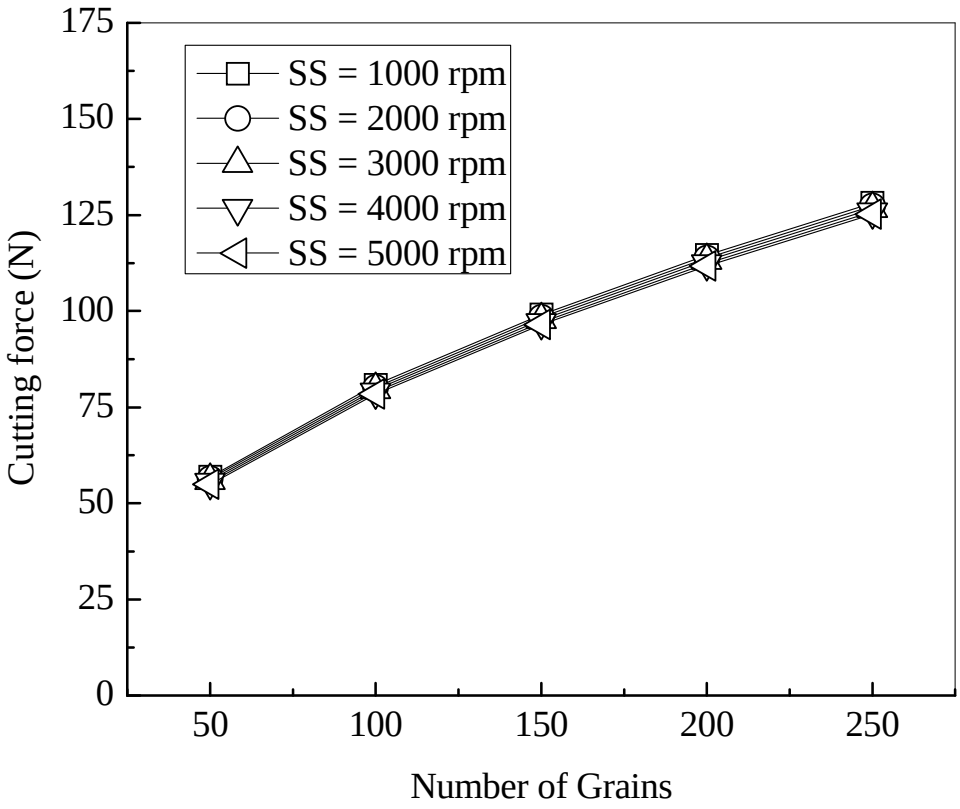

D_0 = 9.6 mm
A = 0.02 mm
d = 0.2 mm
T = 200 sec

Figure 9.29 Relation between number of grains and cutting force at 5 different levels of spindle speed

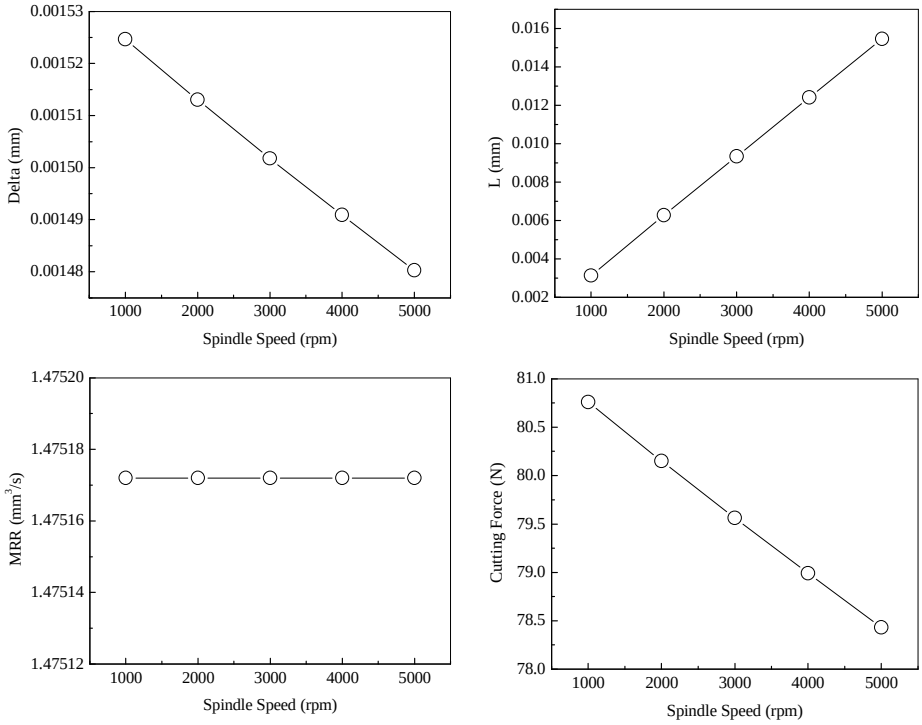

n = 100
D_0 = 9.6 mm
A = 0.02 mm
d = 0.2 mm
T = 200 sec

Figure 9.30 Influence of spindle speed

9.4.6 MACHINING TIME

The predicted relation between cutting force at 5 different levels of machining time are plotted against grit diameter, tool diameter, amplitude, number of grains and spindle speed (Fig. 9.31 to 9.35). It is observed that the cutting force steadily increases with increase in grit diameter, tool diameter and number of grains. The force decreases at a very low rate with increase in amplitude and spindle speed. These predictions are consistent with the data reported in Chapter 5. Figure 9.36 shows the variation of different important components of Equation 1 (the cutting force equation) with variation in spindle speed. It is observed that the depth of indentation, length of contact and material removal. All these factors have direct effect on cutting force.

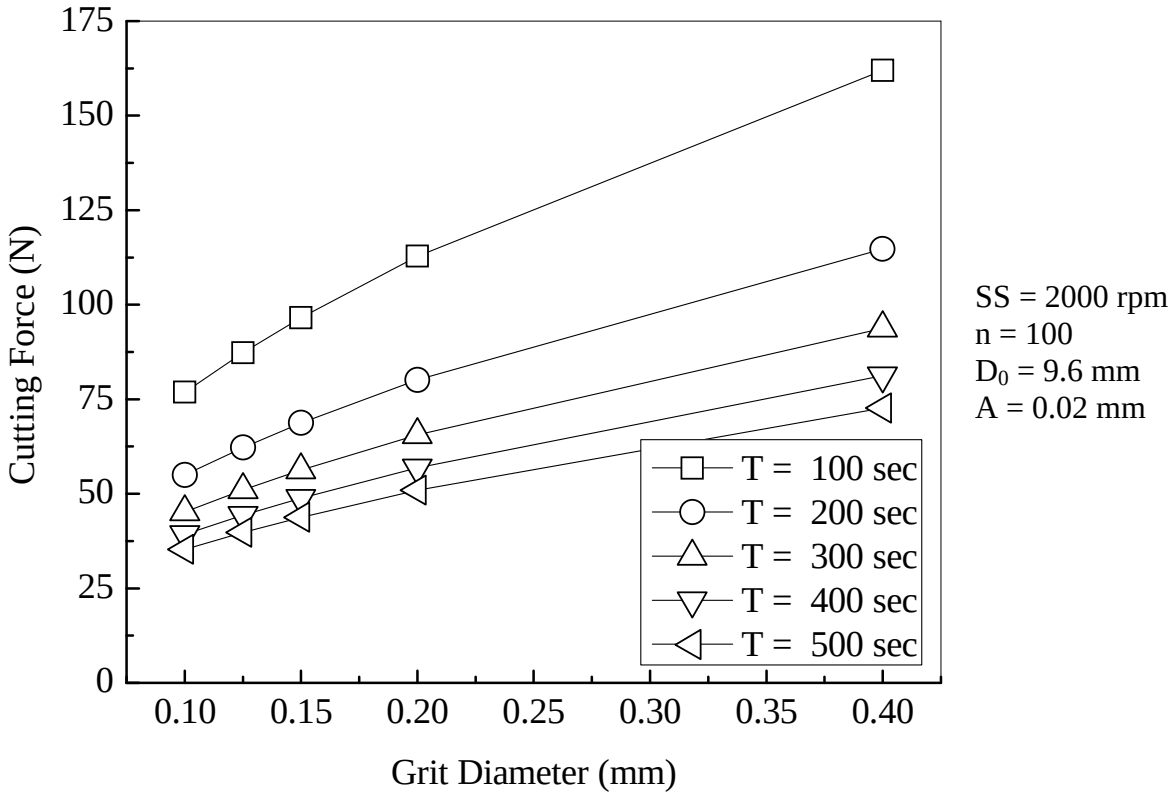

Figure 9.31 Relation between grit diameter and cutting force at 5 different levels of machining time

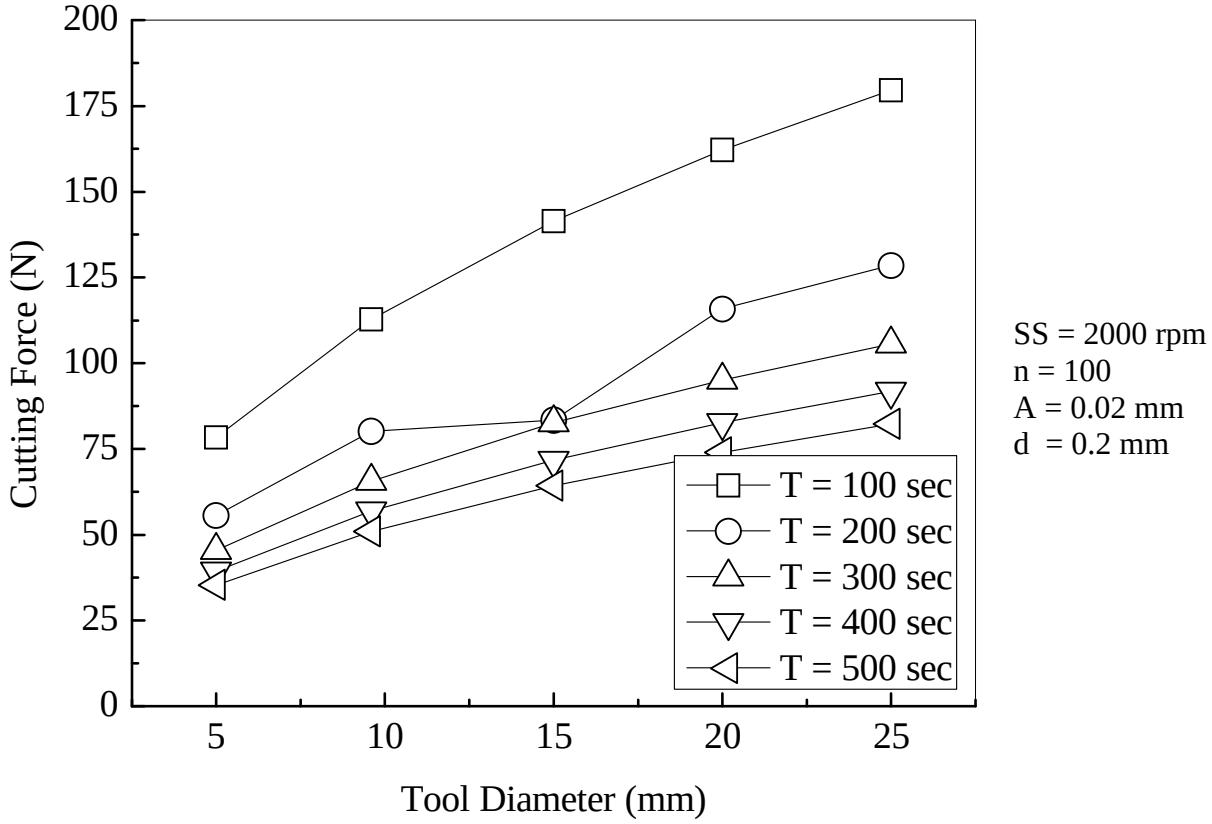

Figure 9.32 Relation between tool diameter and cutting force at 5 different levels of machining time

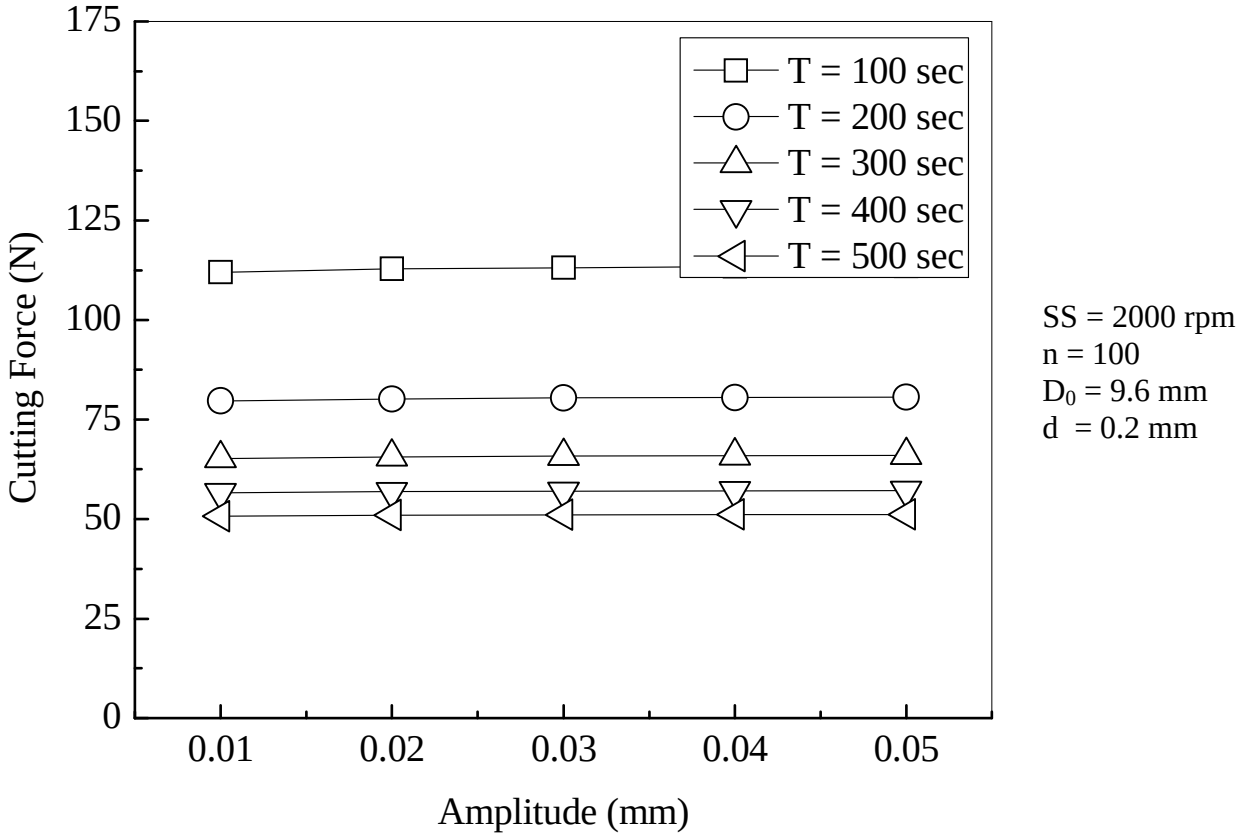

Figure 9.33 Relation between amplitude and cutting force at 5 different levels of machining time

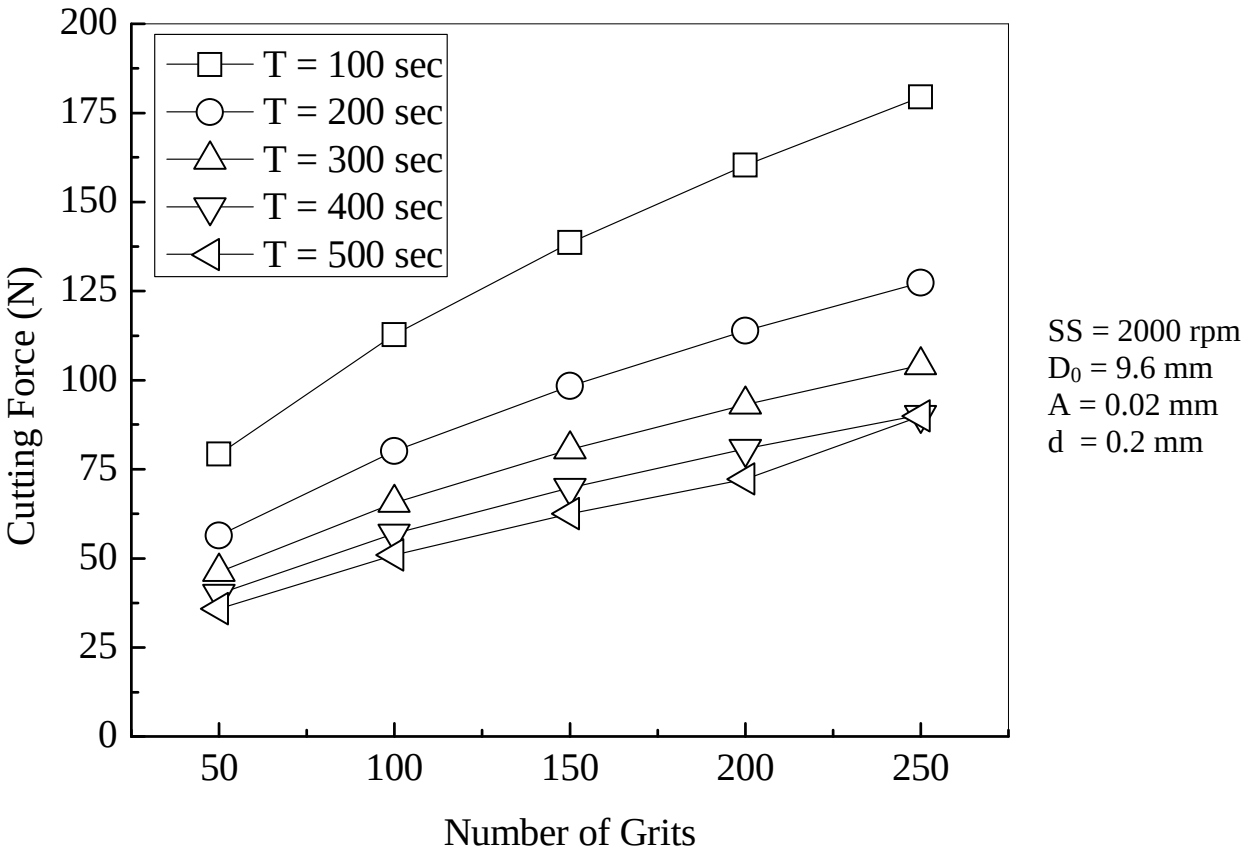

Figure 9.34 Relation between number of grits and cutting force at 5 different levels of machining time

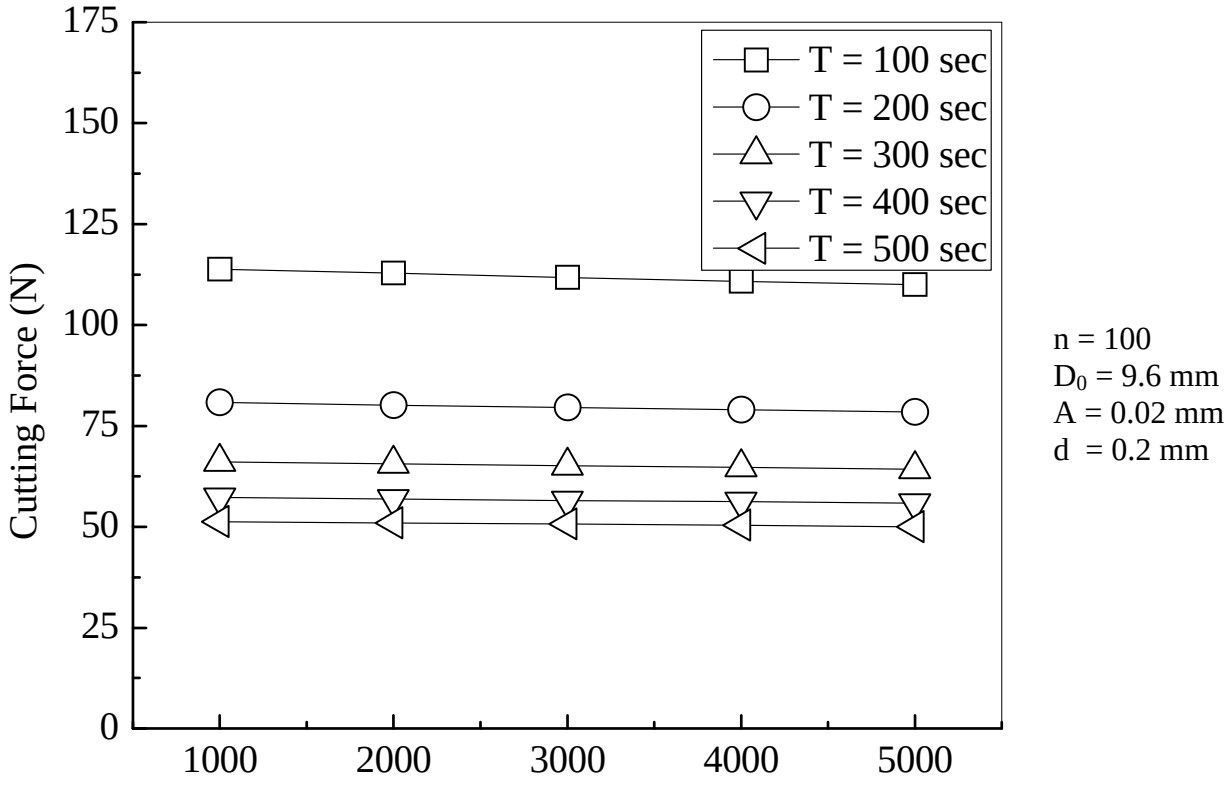

Figure 9.35 Relation between spindle speed and cutting force at 5 different levels of machining time

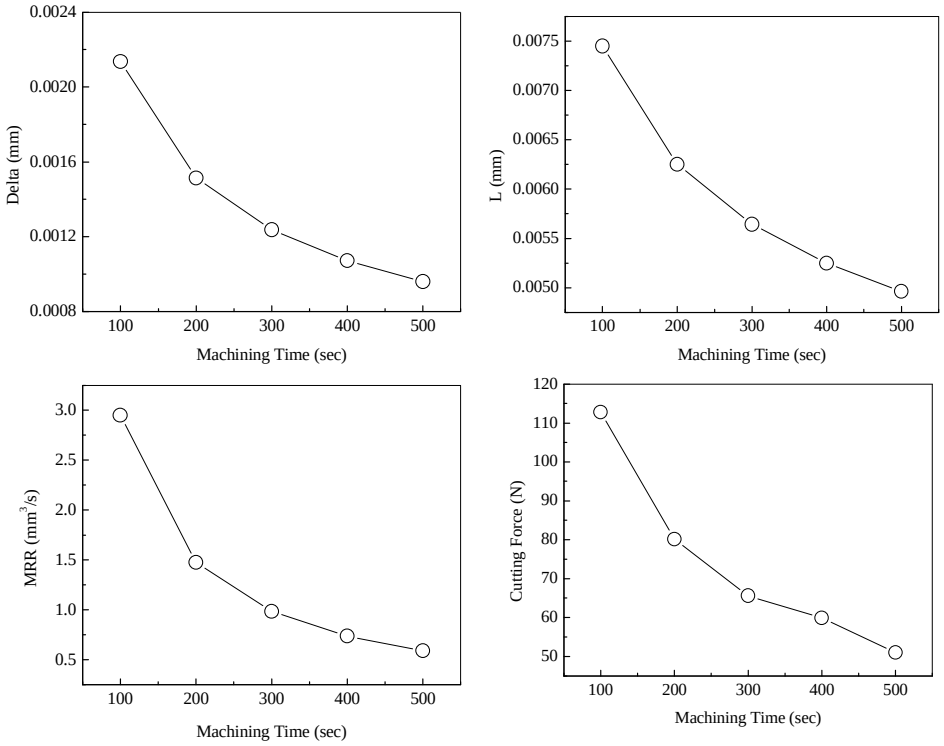

SS = 2000 rpm
n = 100
D_0 = 9.6 mm
A = 0.02 mm
d = 0.2 mm

Figure 9.36 Influence of machining time

9.5 SUMMARY

This chapter reports a theoretical model to predict cutting force for rotary ultrasonic machining of titanium. The model is based on the assumption that the workpiece material is rigid plastic and diamond abrasive grain is rigid material; and the material removal rate is constant.

In order to verify the model, the predicted results were compared to experimental data reported by the authors in different published studies. For all the cases except one, the trends matched for the model and experimental results but there were differences in the estimated values. Our analysis states this might be due to the differences between assumptions and actual conditions.

CHAPTER 10

CONCLUSIONS

10.1 SUMMARIES AND CONCLUSIONS OF THIS DISSERTATION

In this dissertation, rotary ultrasonic machining (RUM) process is used to machine titanium alloy, silicon carbide and dental ceramics. The feasibility of drilling these materials by RUM is studied and the effects of different machining and tool variables are studied on different output variables (cutting force, material removal rate, surface roughness, etc.). The different studies presented in this dissertation are shown in Figure 10.1

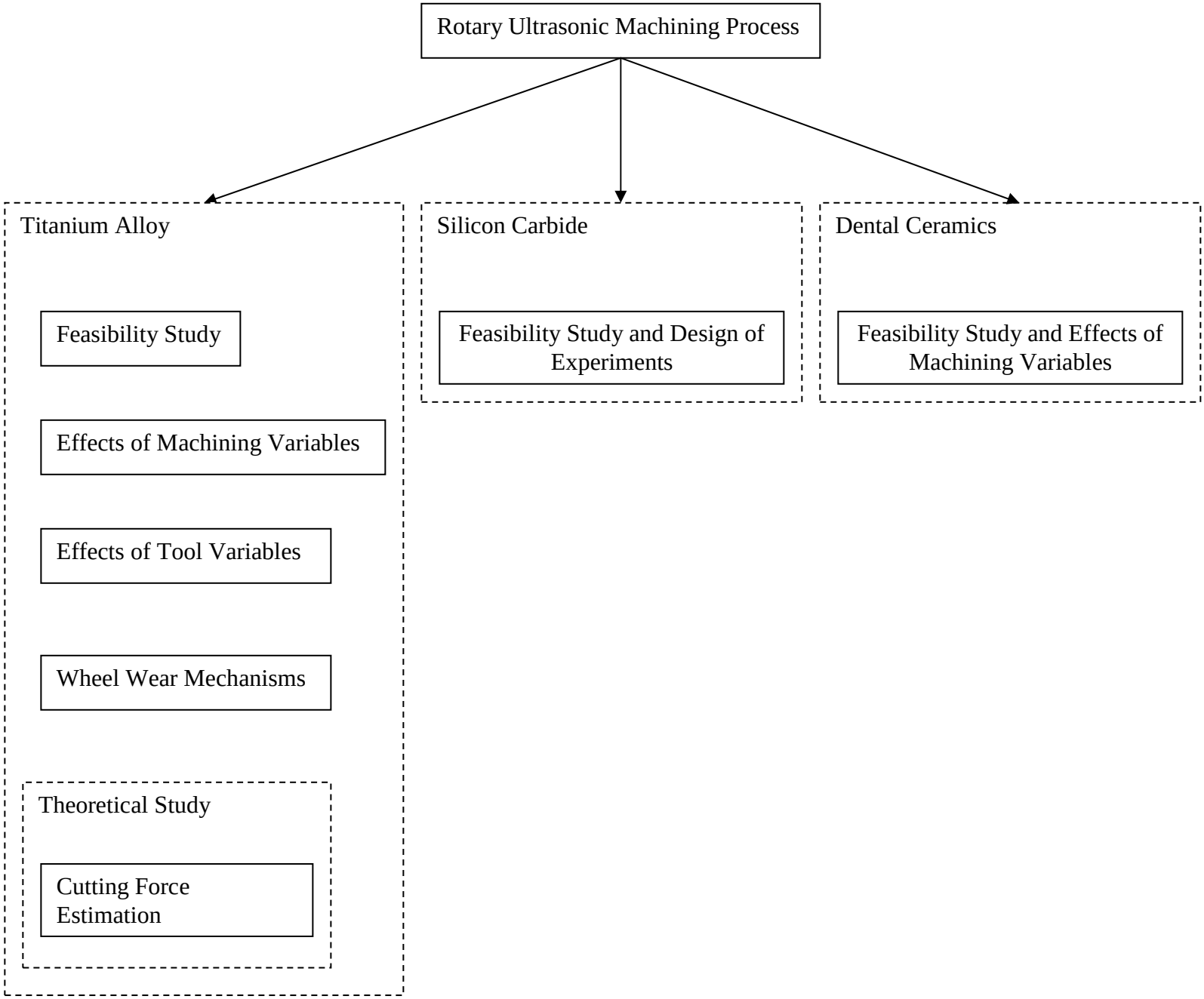

Figure 10.1 Achievements of this dissertation

The conclusions drawn from this dissertation are:

1. The results on RUM of titanium alloys show that it is feasible to machine titanium alloy using RUM. Furthermore, tool wear and cutting force are lower with RUM compared with the diamond drilling process.

- When machining titanium, the RUM tools with higher grit size produces lower tool wear but higher cutting force and surface roughness. Similarly, the RUM tools with lower diamond concentration give lower surface roughness and tool wear but higher cutting force.
- When machining titanium, with the increase in spindle speed, the surface roughness and cutting force decreases significantly. The cutting force decreases initially and then increases as the ultrasonic vibration power increases. The surface roughness shows a steady decrease with increase in ultrasonic vibration power.
- Attritious wear, grain pullout, grain fracture, bond fracture and catastrophic types of failures are the different wheel wear mechanisms observed while RUM of titanium alloys.

2. Results on RUM of on silicon carbide show that spindle speed and feedrate have significant effects on cutting force, surface roughness and chipping size. Additionally, ultrasonic vibration power and grit size also have significant effects on surface roughness and chipping size.
3. Results on RUM of dental ceramics show that the spindle speed, feedrate, and ultrasonic vibration power have variable effects on the cutting force, chipping size, and surface roughness.
4.

10.2 CONTRIBUTIONS OF THIS DISSERTATION

The contributions of this research are:

1. For the first time in the public domain, systematic studies on machining three hard-to-machine materials (titanium alloy, silicon carbide and dental ceramics) have been conducted.
2. The results stated are of practical use in industry for machining these materials cost effectively by reducing the time of machining and improved machined surface quality.
3. The research achievements will have positive impacts on the future machining processes since RUM is a comparatively new machining technology.
4. Since it is proved in this dissertation that it is feasible to machine the three hard-to-machine materials with RUM, a thorough future research focused on improving the machining time and surface quality will be helpful for its successful implementation in the leading industry segments (such as aerospace, automobile, medical, and sporting goods) where these materials are widely used.

References

Abdullin I., Bagautinov A., Ibragimov G., Improving surface finish for titanium alloy medical instruments, Biomedical Engineering 22 (2) (1988) 48-50.

Adithan M., Abrasive wear in ultrasonic drilling, Tribology international, 16 (5) (1983) 253-255.

Adithan M., Tool wear studies in ultrasonic drilling, Wear, 29 (1) (1974) 81-93.

Adithan M., Venkatesh V., Effect of system parameters on tool wear in ultrasonic drilling, Journal of the institution of engineers (India), part mc: mechanical engineering division, 57 (1) (1976) 33-35.

Allen K., Titanium dioxide pigment (and titanium metal), 1997, available at: http://www.chemlink.com.au/titanium.htm#Titanium%20metal

Anantha Ramu B., Krishnamurthy R., Gokularathnam C., Machining performance of toughened zirconia ceramic and cold compact alumina ceramic in ultrasonic drilling, Journal of Mechanical Working Technology 20 (9) (1989) 365-375.

Anonymous, Titanium and environment, 2005, available at: http://www.stainless-steel-world.net/titanium/environment.asp

Anonymous, Report on Titanium, Common Minerals and Their Uses, Mineral Information Institute, Denver, CO, 2004.

Anonymous, New automotive materials, Advanced Materials and Processes 135 (1) (1989) 6.

Anonymous, 2004, Report on Titanium, Common Minerals and Their Uses, Mineral Information Institute, Denver, CO.

Anonymous, Weekly prices, Platt's metal week 70 (44) (1999) 11.

Anonymous, Silicon carbide products, available at http://www.exolon.com/silicon_carbide.html

Anonymous, Dental Products and Materials to 2008, Freedonia Group Inc., Cleveland, OH, 2004, available at: http://www.freedoniagroup.com/Dental-Products-And-Materials.html

Anonymous, Ultrasonic drilling with a diamond impregnated probe, Ultrasonics, 2 (1-3) (1964) 1-4.

Anonymous, "An improved ultrasonic machine tool for glass and ceramics," Industrial Diamond Review, 26 (308) (1966) 274-278.

Anonymous, Drilling deep holes in glass, Ultrasonics, May (1973) 103-106.

Anonymous, Titanium alloy properties, available at: http://64.233.187.104/search?q=cache:cQz17heMf00J:www.roymech.co.uk/Useful_Tables/Matter/Titanium.html+&hl=en

Anonymous, New automotive materials, Advanced Materials and Processes 135 (1) (1989) 6.

Anonymous, Report on Titanium, Common Minerals and Their Uses, Mineral Information Institute, Denver, CO, 2004.

Arola D., McCain M., Kunaporn S., Ramulu M., Waterjet and abrasive waterjet surface treatment of titanium: A comparison of surface texture and residual stress, Wear, 249 (11) (2001) 943-950.

Arzhaou M., Dzhumabekov Z., Konov V., Ral'chenko V., Silenok A., Chapliev N., 1989, Underwater laser cutting and drilling of metals, Physics and Chemistry of Material Treatment, 23 (3) (1989) 136-140.

Boyer R., Overview on the use of titanium in the aerospace industry, Materials Science and Engineering A: Structural Materials: Properties, Microstructure and Processing 213 (2) (1996) 103-114.

Bandopadhyay S., Gokhale H., Sundar J., Sundararajan G., Joshi S., A statistical approach to determine process impact in Nd: YAG laser drilling of IN718 and Ti-6Al-4V sheets, Optics and Lasers in Engineering 43 (2005) 163-182.

Beck T., Bostanjoglo G., Kugler N., Richter K., Weber H., Laser beam drilling applications in novel materials for the aircraft industry, Proceedings of Laser Materials Processing Conference, Laser Institute of America, Orlando, FL, 1997, pp. 93-102.

Bandopadhyay S., Sundar S., Sundarajan G., Joshi S., Geometrical features and metallurgical characteristics of Nd: YAG laser drilled holes in thick IN718 and Ti-6Al-4V sheets, Journal of Materials Processing Technology 127 (2002) 83-95.

Bandopadhyay S., Sundar S., Joshi S., Pulsed CO2 and Nd: YAG laser drilling of CP titanium – a study on process parameter impact on formation of taper, barreling and heat –affected zone, Journal of Materials Processing Technology 83 (2001) 27-36.

Chandler T. Jr., Lari M., Sudarshan T., Damage-free surface modification of hexagonal silicon carbide wafers, International Conference of Silicon Carbide and Related Materials, Research Triangle Park, North Carolina (2000) pp. 845-848.

Claus V., Machinable Glass-Ceramics – A heat-treated material of unusual properties and broad applicability, Industrial Heating 48 (4) (1979) 10-13.

Cleave D., Ultrasonic gets bigger jobs in machining and welding, Iron Age, September (1976) 69-72.

Chechines L., Tikhonov G., Ultrasonic machining with a tool charged with diamond power, Coll. electrophysical and electrochemical methods of machining, MDNTP, 1968.

Cusumano J., Huber J., Marshall K., Ultrasonic drilling of boron fiber composites, Modern Plastics 52 (6) (1974) 88-90.

Chu H., Shah G., Macall T., Titanium Alloys: Ti-6Al-4V, http://www.efunda.com/materials/alloys/titanium/show_titanium.cfm?ID=T18_AB&prop=all&Page_Title=Ti%2D6Al%2D4V

Cho S., Huh Y., Yoon K., Ogawa T., Aspects in grinding of ceramics, Journal of American Ceramic Society 77 (9) (1994) 2443-2444.

Datta M., Chaudhari B., Preparation of nano β-silicon carbide crystalline particles by attrition grinding, International Ceramic Review 52 (6) (2003) 340-343.

Datta M., Bandyopadhyay A., Chaudhari B., Preparation of nano α-silicon carbide crystalline particles by attrition grinding, International Ceramic Review 53 (4) (2004) 242-244.

Dolotov N., Levchuk B., Makarov V., Tairov Y., Tsvetkov V., Effect of machining on the surface structure of single crystals of silicon carbide, Physics and Chemistry of Material Treatment 20 (4) (1986) 340-341.

Dabnun M., Hashmi M., El-Baradie M., Surface roughness prediction model by design of experiments for turning machinable glass ceramic (Macor), Journal of Materials Processing Technology 164-165 (2005) 1289-1293.

Dawe Instruments Ltd., Dawe Type 1138A Ultrasonic Machine Tool, Metalworking Production, 111 (17) (1967) 77-79.

Dam H., "Surface characterization of ultrasonic machined ceramics with diamond impregnated sonotrode," Machining of advanced materials, Ed. S. Jhanmir, NIST Special Publication 847, 1993, pp. 125-133.

Deng G., Li S., Wu S., Yang X., Ultrasonic vibration drilling of small diameter deep holes of difficult-to-machine stainless steel: theoretical analysis and comparative experimental research, American Society of Mechanical Engineers, Production Engineering Division (Publication) PED, Manufacturing Science and Engineering 64, 1993, pp. 835-839.

de Oliveira J., Coelho R., Neto C., Development of an optical scanner to study wear on the working surface of grinding wheels, Machining Science and Technology 3 (2) (1999) 239-253.

Diepold T., Obermeier E., Smoothing of ultrasonically drilled holes in borosilicate glass by wet chemical etching, Journal of Micromechanics and Microengineering, 6 (1) (1996) 29-32.

Egashira K., Mizutani K., Nagao T., Ultrasonic vibration drilling of micro hole in glass, CIRP Annals - Manufacturing Technology 51 (1) (2002) 339-342.

Froes F., Allen P., Niinomi M., Non-aerospace application of titanium: an overview, Proceedings of Minerals, Metals and Materials Meeting, Minerals, Metals and Materials Society, Warrendale, PA, pp. 3-18.

Farthing T., Application of titanium in the chemical industry, Chemical Age of India 30 (2) (1979) 151-166.

Fowler G., Shipway P., Pashby I., A technical note on grit embedment following abrasive water-jet milling of a titanium alloy, Journal of Materials Processing Technology 159 (3) (2005) 356-368.

Froes F., Titanium sport and medical application focus, Materials Technology 17 (1) (2002) 4-7.

Gopal A., Rao P., The optimization of the grinding of silicon carbide with diamond wheels using genetic algorithms, International Journal of Advanced Manufacturing Technology 22 (7-8) (2003) 475-480

Gopal A., Rao P., A new chip-thickness model for performance assessment of silicon carbide grinding, International Journal of Advanced Manufacturing Technology 24 (11-12) (2004) 816-820.

Grossman D., Machining machinable glass ceramics, Glass, 54 (11) (1977) 509-516.

Grossman D, The formation of chips in a machinable glass ceramic, Glass Technology 24 (1) (1983) 11-13.

Goldman R., Ultrasonic technology, Reinhold Publishing Corporation, London, 1962.

Graff K., Ultrasonic machining, Ultrasonic, May (1975) 103-109.

Huber J., Ultrasonic drilling, International Journal for Numerical Methods in Engineering 5 (1973) 28-42.

Hylton K., Carnal C., Jackson J., Egert C, Ion beam milling of silicon carbide optical components, Proceedings of Society of Photo-Optical Instrumentation Engineers - The International Society of Optical Engineering (1993) 16-26, San Diego, CA.

Hards K., Ultrasonic speed diamond machining, Ceramic Age 82 (12) (1966) 34-36.

Hu P., Zhang J., Jiao Y., Pei Z.J., Treadwell C, Experimental investigation on coolant effects in rotary ultrasonic machining, Proceedings of the NSF Workshop on Research Needs in Thermal Aspects of Material Removal Processes, 2003, pp. 340-345.

Hocheng H., Tai N., Liu C., Assessment of ultrasonic drilling of C/SiC composite material, Composite: Part A (31) (2000) 133-142.

Hocheng H., Kuo K., Lin J., Machinability of zirconia ceramics in ultrasonic drilling, Materials and Manufacturing Processes, 14 (5) (1999) 713-724.

Hahin R., Schulze P., Effective applications of ultrasonic machining of glass and ceramics, American Ceramic Society Bulletin, 72 (8) (1993) 102-106.

Hwang T., Evans C., Whitenton E., Malkin S., High speed grinding of silicon nitride with electroplated diamond wheels, I. Wear and wheel life, Manufacturing Science and Engineering 10 (1999) 431-441.

Huang H., Yin L., Zhou L., High speed grinding of silicon nitride with resin bond diamond wheels, Journal of materials Processing Technology 141 (2003) 329-336.

Ilhan R., Satyanarayanan G., Storer R., Phillips R., Study of wheel wear in electrochemical surface grinding, Journal of Engineering for Industry 114 (1) (1992) 82-93.

Johnson W., Peker A., Amorphous alloy surpasses steel and titanium, available at: http://www.liquidmetal.com/news/dsp.news.11x304.asp

Jenkins M., Boeing puts the pedal to the metal, available at: http://www.boeing.com/news/frontiers/archive/2003/november/i_tt.html

Jana J., Satyanarayana A., Production of fine diameter holes on ultrasonic drilling marching, Journal of the Institution of Engineers (India), Part MC: Mechanical Engineering Division, 54 (1) (1973) 36-40.

Jiao Y., Hu P., Pei Z.J., Treadwell C., Rotary ultrasonic machining of ceramics: design of experiments, accepted to appear in International Journal of Manufacturing Technology and Management.

Jahanmir S., Tribology issues in machining, Machining Science and Technology 2 (1) (1998) 137-154.

Kumar K., Grinding titanium, Aerospace Engineering 11 (9) (1991) 17-19.

W. Koenig, Wertheim R., Humbs H., Machining of titanium alloy by the EDM and ECM processes, Journal of the Association of Engineers and Architects in Israel 36 (6) (1976) 39-45.

Kremer D., Lhiaubet C., Moisan A., A study of the effect of synchronizing ultrasonic vibrations with pulse in EDM, Annals of the CIRP 40 (1) (1991) pp. 211-214.

Kudesia S., Solana P., Rodden W., Hand D., Jones J., Appropriate regimes of laser drilling models containing melt eject mechanisms, Journal of Laser Applications 14 (3) (2002) 159-164.

Kibble K., Phelps L., Influence of grinding variables on strength of reaction bonded silicon carbide, British Ceramic Transactions 94 (5) (1995) 209-216.

Kartz N., Advanced Ceramics: Dental Ceramics, 2000, available at: http://www.ceramicindustry.com/CDA/Archives/9074c9fbcb9c7010VgnVCM100000f932a8c0

Kelly J., Giordano R., Pober R., Cima M., Fracture surface analysis of dental ceramics: clinically-failed restoration, International Journal of Prosthodontics 3 (1990) 430-440.

Kohls J., Ultrasonic manufacturing process: ultrasonic machining and ultrasonic impact grinding, Carbide and Tool Journal (9-10) (1984) 12-15.

Kubota M., et al., Ultrasonic machining with a diamond impregnated tool, Bulletin of Japan Society of Precision Engineering 11(3) (1977) 127-132.

Komaraiah M., Reddy P., Rotary ultrasonic machining-A new cutting process and its performance, International Journal of Production research, 29 (11) (1991) 2177-2187.

Khanna N., Pei Z.J., An experimental investigation of rotary ultrasonic grinding of ceramic disks, Technical paper of the North American Manufacturing Research Institute of SME (1995) pp. 67-72.

Ken-ichi I., Hitoshi S., Tetsuhiro N., Michio U., Study on combined vibration drilling by ultrasonic and low-frequency vibrations for hard and brittle materials, Precision Engineering 22 (4) (1998) 196-205.

Keisaku O., Chisato T., Ryoji M., Satosi I., Machining of ceramics (Part 3) - Machining characteristics of ceramics in ultrasonic core-drilling, Journal of Mechanical Engineering Laboratory, Tokyo, Japan, 42 (4) (1988) 159-168.

Karpov V, Stepanov A, Diamond drilling of high strength glass- and boron-reinforced plastics, Soviet Journal of Super-Hard Materials (English translation of Sverkhtverdye Materialy) 8 (2) (1986) 72-77.

Kuriyagawa T., Syoji K., Study on grinding of cermet with hybrid bond diamond wheel: reduction of wheel wear, Bulletin of the Japan Society of Precision Engineering 24 (2) (1990) 118-123.

Lin Y., Yan B., Chang Y., 2000, Machining characteristics of titanium alloy (Ti-6Al-4V) using a combination process of EDM with USM, Journal of Materials Processing Technology 104 (2000) 171-177.

Lerner I., Titanium market recovering on commercial military aircraft, Chemical Market Reporter 266 (18) (2004) 17.

Li E., Johnson W., Evaluation of hybrid titanium composite laminates for room temperature fatigue, Proceedings of American Society for Composites, Lancaster, PA, 1996, pp. 505-514.

Lash J., Gilgenbach R., Copper vapor laser drilling of copper, iron, and titanium in atmospheric pressure air and argon, Review of Scientific Instruments 64 (1993) 3308-3313.

Lash J., Gilgenbach R., Copper vapor laser drilling of copper, iron, and titanium in atmospheric pressure air and argon, Review of Scientific Instruments 64 (1993) 3308-3313.

Luis C., Puertas I., Villa G., Material removal rate and electrode wear study on the EDM of silicon carbide, Journal of Materials Processing Technology 164-165 (2) (2005) 889-896.

Legge P., 1964, Ultrasonic drilling of ceramics, Industrial diamond review 24 (278) (1964) 20-24.

Li Z.C., Jiao Y., Deines T., Pei Z.J., and Treadwell C., 2005, "Development of an innovative coolant system for rotary ultrasonic machining," International Journal of Manufacturing Technology and Management 7 (2–4) (2005) 318–328.

Li Z.C., Cai L., Pei Z.J., Treadwell C., Finite element simulation of rotary ultrasonic machining for advanced ceramics, to appear in CD-ROM Proceedings of the International Mechanical Engineering Congress and Exposition 2004 (IMECE 2004), Anaheim, CA.

Lunzer L., Diamond Drilling in Glass, Proceedings of the 18th Symposium on the Art of Glassblowing, Machine Design (1973) pp. 21-25.

Liu Y., Chen Y., Ultrasonic circular vibration drilling for deep holes, Meitan Xuebao/Journal of China Coal Society 21 (5) (1996) 8-9.

Li Z.C., Jiao Y., Deines T., Pei Z.J., Treadwell C., Experimental study on rotary ultrasonic machining (RUM) of poly crystalline diamond compacts (PDC), CD-ROM Proceedings of the 13th Annual Industrial Engineering Research Conference (IERC-2004).

Liao T., Li K., McSpadden S., O'Rourke L., Wear of diamond wheels in creep-feed grinding of ceramic materials I: mechanisms, Wear 211 (1997) 94-103.

Li K., Liao T., O'Rourke L., McSpadden S., Wear of diamond wheels in creep-feed grinding of ceramic materials II: effects on process responses and strength, Wear 211 (1997) 104-112.

Montgomery J., Wells M., Titanium armor applications in combat vehicles, Journal of Machining 53 (4) (2001) 29-32.

Marshall D., Lawn B., Cook R., Microstructural effects on grinding of alumina and glass-ceramics, Journal of American Ceramic Society 70 (6) (1987) C-139-C-140.

Markov A., Ultrasonic machining of intractable materials (Translated from Russian), Illife Books, London, 1966.

Moore D., Ultrasonic impact grinding, Carbide and Tool Journal (11-12) (1986) 21-23.

Tyrrell W., Rotary ultrasonic machining, SME technical paper MR 70 (1970) 516.

Markov I., "Ultrasonic drilling of deep holes in quartz, with a bonded abrasive-diamond tool," Electrophysical and electrochemical methods of machining, NIIMASH (1969) 5-6.

Markov A., Ustinov I., A study of the ultrasonic diamond drilling of nonmetallic materials, Industrial Diamond Review 3 (1972) 97-99.

Markov A., Ultrasonic drilling and milling of hard non-metallic materials with diamond tools, Machine & Tooling, 48 (9) (1977) 45-47.

McGeough J., Advanced methods of machining, Chapman and Hall Ltd., London, (1988).

Malkin S., Grinding Technology: Theory and Applications of Machining with Abrasives, Society of Manufacturing Engineering, Dearborn, MI, 1996.

Malkin S., Grinding Technology: Theory and Applications of Machining with Abrasives, Ellis Horwood Limited, Chichester, West Sussex, United Kingdom (1989) pp. 197.

Nelson O., Titanium starves of composites, Advanced Materials and Processes 139 (6) (1991) 18-23.

Noort R., Introduction to Dental Materials, Mosby-Wolfe, 2nd edition, London, UK, (2002).

Orr N., Industrial application of titanium in the metallurgical industries, and chemical light metals, Proceedings of Technical Sessions at the 111th American Institute of Mining, Metallurgical and Petroleum Engineers, Annual Meeting, AIME, Warrendale, PA, (1982) pp. 1149-1156.

Peacock D., Aerospace applications for titanium, Sheet Metal Industries 65 (8) (1988) 406-408.

Puertas I., Perez C., Modeling the manufacturing variables in electrical discharge machining of siliconized silicon carbide, Proceedings of the Institution of Mechanical Engineers, Part B, Journal of Engineering Manufacture 217 (6) (2003) 791-803.

Prabhakar D., Machining advanced ceramic materials using rotary ultrasonic marching process, M.S. Thesis, University of Illinois at Urbana-Champaign, 1992.

Petrukha P., Ultrasonic diamond drilling of deep holes in brittle materials, Russian Engineering Journal 50 (10) (1970) 70-74.

Prabhakar D., "An experimental investigation of material removal rates in rotary ultrasonic machining," Transactions of the North American Manufacturing Research Institution of SME (1992) pp. 211-218.

Pei Z.J., Ferreira P., Modeling of ductile-mode material removal in rotary ultrasonic machining, International Journal of Machine Tools and Manufacture 38 (1998) 1399-1418.

Petrukha P., Ultrasonic diamond drilling of deep holes in brittle materials, Russian Engineering Journal 50 (10) (1970) 70-74.

Pei Z.J., Khanna N., Ferreira P., Rotary ultrasonic machining of structural ceramics-A review, Ceramic Engineering Science Proceeding 16 (1) (1995) 259-278.

Prabhakar D., Pei Z.J., Ferreira P., Mechanistic approach to the prediction of material removal rates in rotary ultrasonic machining, Manufacturing Society Engineering, ASME PED 64 (1993) 771-784.

Pecherer E., Malkin S., Grinding steels with cubic boron nitride (CBN), CIRP Annals – Manufacturing technology 33 (1) (1984) 211-216.

Peacock D., Aerospace applications for titanium, Sheet Metal Industries 65 (8) (1988) 406-408.

Pei Z.J., "Rotary Ultrasonic machining of Ceramics," PhD thesis, University of Illinois at Urbana-Champaign, 1995.

Qin G., Oikawa K., Smith G., Hao S., Wire electric discharge machining induced titanium hydride in Ti-46Al-2Cr alloy, Intermetallics 11 (9) (2003) 907-910.

Rozenberg L., Kazantsev V., Makarov L., Yakhimovich D., Ultrasonic cutting (translated from Russian), Consultants Bureau, New York, 1964.

Rodden W., Kudesia S., Hand D., Jones J., Use of "assist" gas in the laser drilling of titanium, Journal of Laser Applications 13 (5) (2001) 204-208.

Rice G., Jones D., Kim K., Girkin J., Jarozynski G., Dawson M., Micromachining of gallium nitride, sapphire and silicon carbide with ultra short pulses, International Conference on Advanced Laser Technologies, Adelboden, Singapore (2002) 299-307.

Rosenthal H., Adams T., A research for new manufacturing processes, Journal of Engineering for Industry, ASME Transactions, Series B 86 (1964) 55-61.

Seddon M., Titanium demand forecast to recover with increasing aircraft orders, 2004, available at: http://www.roskill.com/news/newsCMS/newsItems/170604120648/viewNe wsItem

Shipway P., Fowler G., Pashby I., Characteristics of the surface of a titanium alloy following milling with abrasive waterjets, Wear, 258 (1-4) (2005) 123-132.

Stinson D., Assessment of the state of the art in machining and surface preparation of ceramics, ORNL/TM Report 10791, Oak Ridge National Laboratory, Oak Ridge, TN, November 1988.

Shaw M., Ultrasonic grinding, Microtechnic 10 (6) (1956) 257-265.

Schwartz M., Handbook of structural ceramics, McGraw-Hill, Inc., New York. 1992.

Suzuki K., Recent advanced in the grinding ceramics and hard metals, Hard Material Production 88, London, 1988.

Saha J., Roy-Choudhury P., Lahiri B., Mishra P., Ultrasonic machining of glass ceramics, Thin Solid Films 2 (1977) 100-107.

Shaw M., Principles of Abrasive Processing, Oxford University Press, New York, 1996.

Sathyanarayanan G., Pandit S., Fracture and attritious wear in grinding by data dependent systems, 13th North American Manufacturing Research Conference Proceedings, Manufacturing Engineering Transactions, Berkeley, CA, 1985, pp. 314-320.

Tam S., Loh N., Mah C., Loh N., Electrochemical polishing of biomedical titanium orifice rings, Journal of Materials Processing Technology 35 (1) (1992) 83-91.

Tam S., William R., Yang L., Jana S., Lim L., Lau M., A review of the laser processing of aircraft components, Journal of Material Process and Technology 23 (1) (1990) 177-194.

Thompson J., Anusavice K., Morris H., Fracture surface characterization of clinically failed all-ceramic crowns, Journal of Dental Research 73 (1994) 1824-1832.

Tonshoff H., Karpuschewski B., Hartmann M., Spengler C., Grinding-and-slicing technique as an advanced technology for silicon wafer slicing, Machining Science and Technology 1 (1) (1997) 33-47.

Treadwell C., Pei Z.J., Machining Ceramics with Rotary Ultrasonic Machining, Ceramic Industry 7 (2003) 39-42.

Wang A., Yan B., Li X., Huang F., 2002, Use of micro ultrasonic vibration lapping to enhance the precision of microholes drilled by micro electro-discharge machining, International Journal of Machine Tools and Manufacture 42 (2002) 915-923.

Weber H., Herberger J., Pilz R., Turning of machinable glass ceramic with ultrasonically vibrated tool, Annals of the CIRP 33 (1) (1984) 85-87.

Warkentin A., Bauer R., Analysis of wheel wear using force data in surface grinding, Transactions of Canadian Society of Mechanical Engineering 27 (3) (2003) 193-204.

Xie Z., Moon R., Hoffman M., Munroe P., Cheng Y., Role of microstructure in the grinding and polishing of α-sialon ceramics, Journal of European Ceramic Society 23 (13) (2003) 2351-2360.

Yamashita Y., Takayama I., Fujii H., Yamazaki T., Applications and features of titanium for automotive industry, Nippon Steel Technical Report 85 (2002) 11-14.

Yang X., Liu R., Machining titanium and its alloys, Machining Science and Technology 3 (1) (1999) 107-139.

Yan B., Shieh F., Electrical discharge machining characteristics of Ti-6Al-4V alloy, Journal of Japan Institute of Light Metals 42 (11) (1992) 644-649.

Yan B., Chen M., Effect of ultrasonic vibration on electrical discharge machining characteristics of Ti-6Al-4V alloy, Journal of Japan Institute of Light Metals 44 (5) (1994) 281-285.

Yishuang H., The effect of ultrasonic vibration to EDM, Metals and Machines Overseas 4 (1990) 1-5.

Yilbas B., Parametric study to improve laser hole drilling process, Journal of Materials Processing Technology 70 (1997) 264-273.

Yilbas B., Davis R., Yilbas Z., Begh F., 1990, Study into the measurement and prediction of penetration time during CO2 laser cutting process, Journal of Laser Applications 204 (5) (1990) 105-113.

Yilbas B., Yilbas Z., 1988, Investigation into drilling speed during laser drilling of metals, Optimization of Laser Technology 20 (1) (1988) 29-32.

Yin L., Vancoille E., Lee L., Huang H., Ramesh K., Liu X., High-quality grinding of polycrystalline silicon carbide spherical surfaces, Wear 256 (1-2) (2004) 197-207.

Ya G., Qin H., Yang S., Xu Y., Analysis of the rotary ultrasonic machining mechanism, Journal of Material Processing Technology 129 (1-3) (2002) 182-185.

Ya G., Qin H., Xu Y., Zhang Y., An experimental investigation on rotary ultrasonic machining, Key Engineering Materials 202-203 (2001) 277-280.

Yoshikawa H., Sata T., Study on wear of grinding wheels, Journal of Engineering for Industry 85 (1) (1963) 39-43.

Yoshikawa H., Fracture wear of grinding wheels, ASME Production Engineering Research Conference (1963), pp. 209-217.

Yoshikawa H., Criterion of grinding wheel tool life, Bulletin Japan Society of Grinding Engineers 3 (1963) 29-32.

Yamashita Y., Takayama I., Fujii H., Yamazaki T., Applications and features of titanium for automotive industry, Nippon Steel Technical Report 85 (2002) 11-14.

Yang X., Liu R., Machining titanium and its alloys, Machining Science and Technology 3 (1) (1999) 107-139.

Zhao W., Wang Z., Di S., Chi G., Wei H., 2002, Ultrasonic and electric discharge machining to deep and small hole on titanium alloy, Journal of Materials Processing Technology 120 (2002) 101-106.

Zeng W., Li Z.C., Pei Z.J., Treadwell C., Experimental investigation into rotary ultrasonic machining of alumina, to appear in CD-ROM Proceedings of the International Mechanical Engineering Congress and Exposition 2004 (IMECE 2004) Anaheim, CA.

Zhang Q., Wu C., Sun J., Jia Z., Mechanism of material removal in ultrasonic drilling of engineering ceramics, Proceedings of the Institution of Mechanical Engineers, Part-B: Journal of Engineering Manufacture 214 (9) (2000) 805-810.

Zhang Q., Zhang J., Jia Z., Ai X., Fracture at the exit of the hole during the ultrasonic drilling of engineering ceramics, Journal of Materials Processing Technology 84 (1-3) (1998) 20-24.

Zeng W., Li Z.C., Pei Z.J., Treadwell C., Experimental observation of tool wear in rotary ultrasonic machining of advanced ceramics, International Journal of Machine Tool and Manufacture 45 (12-13) (2005) 1468-1473.

LIST OF PUBLICATIONS FROM THIS RESEARCH

[1] Churi, N.J., Pei, Z.J., and Treadwell, C., 2006, "Rotary ultrasonic machining of titanium alloy: effects of machining variables," Machining Science and Technology, Vol. 10, No. 3, pp. 301–321.

[2] Churi, N.J., Pei, Z.J., and Treadwell, C., 2007, "Rotary ultrasonic machining of titanium alloy (Ti-6Al-4V): effects of tool variables," International Journal of Precision Technology, Vol. 1, No. 1, pp. 85–96.

[3] Churi, N.J., Pei, Z.J., Treadwell, C., and Shorter, D., 2007, "Rotary ultrasonic machining of silicon carbide: designed experiments," International Journal of Manufacturing Technology and Management, Vol. 12, No. 1/2/3, pp. 284–298.

[4] Churi, N.J., Pei, Z.J., Treadwell, C., and Shorter, D., 2009, "Rotary ultrasonic machining of dental ceramics," International Journal of Machining and Machinability of Materials, Vol. 6, No. 3-4, pp. 270-284.

[5] Churi, N.J., and Pei, Z.J., 2004, "Experimental investigations into jig grinding," Proceedings of the Seventh International Conference on Progress of Machining Technology, ICPMT'2004, Suzhou, China, December 8–11, pp. 219–224.

[6] Churi, N.J., Li, Z.C., Pei, Z.J., and Treadwell, C., 2005, "Rotary ultrasonic machining of titanium alloy: a feasibility study," Proceedings of the 2005 ASME International Mechanical Engineering Congress and Exposition (IMECE 2005), Orlando, FL, November 5–11, Vol. 16–2, pp. 885–892.

[7] Churi, N.J., Pei, Z.J., and Treadwell, C., 2007, "Wheel wear mechanisms in rotary ultrasonic machining of titanium," Proceedings of the 2007 ASME International

Mechanical Engineering Congress and Exposition (IMECE 2007), Seattle, WA, November 11–15, Vol. 3, pp. 399–407.

[8] Churi, N.J., Pei, Z.J., and Treadwell, C., 2007, "Experimental investigations on rotary ultrasonic machining of hard-to-machine materials," Materials Processing under the Influence of External Fields, Proceedings of the 2007 TMS Annual Meeting & Exhibition, Orlando, FL, February 25 – March 1, edited by Q.Y. Han, G. Ludtka, Q.J. Zhai, the Minerals, Metals & Materials Society, pp. 139–144.

[9] Zhang, P.F., Churi, N.J., Pei, Z.J., and Treadwell C., 2008, "Mechanical drilling processes for titanium alloys: a literature review," Machining Science and Technology, Vol. 130, No. 4, pp. 417-444.

[10] Wang, Q.G., Pei, Z.J., Gao, H., Churi, N., and Kang, R.K., 2008, "Experimental investigation on diamond drilling of potassium di-hydrogen phosphate (KDP) crystal," CD-ROM Proceedings of the 2008 International Manufacturing Science & Engineering Conference (MSEC), MSEC 2008, October 7–10, 2008, Evanston, IL, USA.

[11] Wang, Q.G., Pei, Z.J., Gao, H., Churi, N., and Kang, R.K., 2009, "Rotary ultrasonic machining of potassium dihydrogen phosphate (KDP) crystal: an experimental investigation," International Journal of Mechatronics and Manufacturing Systems, Vol. 2, No. 4, pp. 414-426.

[12] Cong W.L., Pei, Z.J., Churi, N., and Wang, Q.G., 2009, "Rotary ultrasonic machining of stainless steel: design of experiments," Transactions of the North American Manufacturing Research Institution of SME, Vol. 37, pp. 261–268.